Diffusion of Alkane Mixtures in Zeolites: Validating the Maxwell−Stefan Formulation Using MD Simulations

R. Krishna* and J. M. van Baten

Van 't Hoff Institute for Molecular Sciences, University of Amsterdam, Nieuwe Achtergracht 166, 1018 WV Amsterdam, The Netherlands

Received: December 17, 2004; In Final Form: February 4, 2005

Molecular dynamics (MD) simulations have been carried out for pure components, binary, ternary, and quaternary mixtures containing methane, ethane, propane, and *n*-butane in FAU zeolite at 300 K for a range of molecular loadings Θ, approaching saturation limits. The *n*-dimensional matrix of Maxwell−Stefan (M−S) diffusivities $[\Delta]$, defined by $(\mathbf{N}) = -\rho[\Delta][\Gamma](\nabla\Theta)$, was determined along with the *self*-diffusivities, $D_{i,\text{self}}$. Additionally, configurational-bias Monte Carlo (CBMC) simulations were carried out to obtain the pure component sorption isotherms and the saturation capacities $\Theta_{i,\text{sat}}$. From the information on Δ_{ij}, $D_{i,\text{self}}$, and $\Theta_{i,\text{sat}}$, the various M−S diffusivities were determined: (1) component $Đ_i$, reflecting the interactions of the species *i* with the zeolite, *self*-exchange $Đ_{ii}$, and (2) *binary* exchange $Đ_{ij}$. The obtained data underline the major advantage of the M−S formulation that at a given occupancy, $\theta = \sum_{i=1}^{n}\Theta_i/\Theta_{i,\text{sat}}$ within the zeolite, the $Đ_i$ has nearly the same value for species *i* whether this species is present on its own or in a mixture with other species. The same advantage holds, too, for the self-exchange $Đ_{ii}$; the value at a given occupancy, θ, is the same whether determined from pure component, binary, or ternary mixture data. For all binary and ternary mixtures studied, it was verified that the binary exchange coefficient $Đ_{ij}$ can be interpolated from the corresponding values of the self-exchange parameters $Đ_{ii}$ and $Đ_{jj}$ using a generalization of the interpolation formula developed earlier (Skoulidas et al., *Langmuir,* **2003,** *19*, 7977). We also demonstrate that if the occupancy dependence of the *pure* component parameters $Đ_i$ and $Đ_{ii}$ are modeled properly, this information is sufficient to provide very good estimates of the matrix $[\Delta]$ for mixtures with 2, 3, or 4 components over the entire range of loadings. Simulations of mixture diffusion of alkanes in MFI and LTA confirm that the above-mentioned advantages of the M−S formulation also hold for these zeolite topologies.

1. Introduction

Zeolites are widely used as catalysts and adsorbents in a variety of applications in the chemical process industries,[1] and the reliable estimation of the intracrystalline diffusion coefficients remains a challenging task.[2,3] There are two types of zeolite diffusivites: *self* diffusivities and *transport* diffusivities; the latter are also referred to as "corrected" or Maxwell−Stefan (M−S) diffusivities. From a practical viewpoint, the M−S diffusivities are the ones that are required, for example, for calculating breakthrough curves in adsorbers or permeation fluxes across membranes.[4−7] Several publications in recent years have used molecular dynamics (MD) simulations to determine transport diffusivities of pure components and binary mixtures in a variety of zeolite topologies.[7−15] For pure component diffusion, MD simulations have been shown to be in reasonably good agreement with experimental data.[16−20] MD simulations[11,12] have also demonstrated the ability of the M−S diffusion formulation[5,11,12,21]

$$-\rho\frac{\Theta_i}{k_B T}\nabla\mu_i = \sum_{\substack{j=1\\ j\neq i}}^{n}\frac{\Theta_j\mathbf{N}_i - \Theta_i\mathbf{N}_j}{\Theta_{j,\text{sat}}Đ_{ij}} + \frac{\mathbf{N}_i}{\Theta_{i,\text{sat}}Đ_i}; \quad i = 1,...n \quad (1)$$

for predicting *mixture* diffusion on the basis of information on the *pure* component M−S diffusivities. In eq 1, $\mathbf{N}_i$ is the flux of species *i* expressed in molecules per square meter per second, ρ is the zeolite density expressed as the number of unit cells per cubic meter, Θ_i is the loading in molecules per unit cell, $\Theta_{i,\text{sat}}$ represents the saturation loading of species *i*, *n* is the total number of diffusing species, and k_B is the Boltzmann constant. Equation 1 *defines* two types of M−S diffusivities: $Đ_i$ and $Đ_{ij}$. If we have only a single sorbed component, then only one $Đ_i$ is needed, and in this case, $Đ_i$ is equivalent to the single component "corrected" diffusivity.[22] The binary exchange coefficients $Đ_{ij}$ reflect *correlation* effects in mixture diffusion.[23] For mixture diffusion, the $Đ_{ij}$ tends to slow the more mobile species and speed up the relatively sluggish ones. A lower value of the exchange coefficient $Đ_{ij}$ implies a *stronger* correlation effect. When $Đ_{ij} \rightarrow \infty$, correlation effects vanish. For two-component mixtures, a logarithmic interpolation formula has been suggested:[11]

$$\Theta_{2,\text{sat}}Đ_{12} = [\Theta_{2,\text{sat}}Đ_{11}]^{\Theta_1/(\Theta_1+\Theta_2)}[\Theta_{1,\text{sat}}Đ_{22}]^{\Theta_2/(\Theta_1+\Theta_2)} \quad (2)$$

for estimating the binary exchange parameter $Đ_{12}$ from information on the pure component *self*-exchange coefficients $Đ_{11}$ and $Đ_{22}$. The self-exchange diffusivities $Đ_{ii}$ are determined from information on transport *and* self diffusivities.[11] Equation 2 has been validated for binary mixtures of CH_4 and CF_4 in MFI[11] and for mixtures of light alkanes and CF_4 in FAU.[12]

* Author to whom correspondence should be addressed. E-mail: r.krishna@uva.nl. Fax: +31 20 5255604.

10.1021/jp044257l CCC: $30.25
Published on Web 03/11/2005

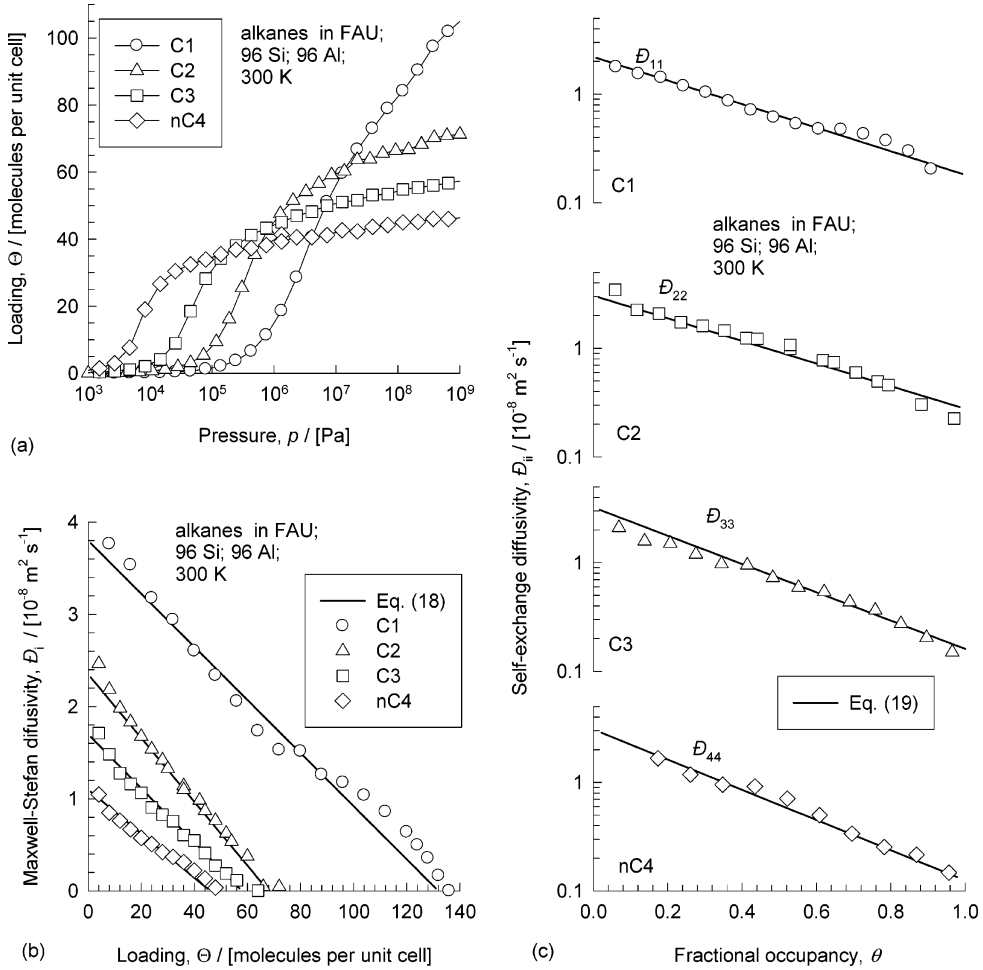

Figure 1. Sorption and diffusion data for pure alkanes in FAU at 300 K. (a) CBMC simulation data on pure component isotherms. (b) MD Simulation results for M−S diffusivities $Đ_i$ (symbols) compared with the calculations following eq 18. (c) MD simulation results for self-exchange $Đ_{ii}$ (symbols) compared with the calculations following eq 19.

In the process industries, we often encounter mixtures with three or more species. Ternary diffusion is described by three pure component M−S diffusivities $Đ_1$, $Đ_2$, and $Đ_3$, and three binary pair exchange diffusivities $Đ_{12}$, $Đ_{13}$, and $Đ_{23}$. Formally, the logarithmic interpolation formula 2 can be generalized as follows

$$\Theta_{j,\mathrm{sat}} Đ_{ij} = [\Theta_{j,\mathrm{sat}} Đ_{ii}]^{\Theta_i/(\Theta_i+\Theta_j)} [\Theta_{i,\mathrm{sat}} Đ_{jj}]^{\Theta_j/(\Theta_i+\Theta_j)}; \quad i, j = 1, 2, \ldots n \quad (3)$$

to allow estimation of the three-pair $Đ_{ij}$ from the three self-exchange $Đ_{ii}$. However, the applicability of eq 3 has never been tested against MD simulations for mixtures containing three or more species.

The current paper has three main objectives. First, we extend the work of Chempath et al.[12] for diffusion of binary mixtures in FAU to mixtures containing *three* light alkanes to examine whether the advantages of the M−S formulation extend to ternary systems as well. Ternary mixtures provide a much more stringent test of the M−S formulation and its ability to predict multicomponent diffusion from pure component data alone. We report MD simulations for diffusion of ternary mixtures containing methane (C1), ethane (C2), and propane (C3) in FAU zeolite at 300 K. Additionally, we have carried out MD simulations of diffusion of the constituent pure components C1, C2, and C3 in FAU, along with the three binary mixtures C1−C2, C1−C3, and C2−C3 (in 75−25, 50−50 and 25−75 mole percentages, respectively). We aim to show that diffusion in the ternary, and constituent binary pairs, can all be described using only pure component data. In contrast to earlier studies,[11,12] we have determined all *three* sets of M−S diffusivities $Đ_i$, $Đ_{ii}$, and $Đ_{ij}$ from the mixture simulations. A further distinguishing feature of the MD simulations presented here is that in all cases the diffusion was studied for a range of loadings approaching saturation conditions. We also aim to show, for example, that the pure component diffusivity of methane in FAU $Đ_1$, and its self-exchange coefficient, $Đ_{11}$, have nearly the same values whether these are obtained from single component data, from binary mixtures with either C2 *or* C3, or from data in a ternary mixture with C2 *and* C3, provided the comparisons are made at the same total occupancy $\theta = \sum_{i=1}^{n} \Theta_i/\Theta_{i,\mathrm{sat}}$. To stress this point even further, we perform MD simulations with the binary mixture of C1 and *n*-butane (*n*C4) to demonstrate the independence of $Đ_1$ and $Đ_{11}$ on its partner(s) in the mixture. We also test the predictive capability of the M−S formulation for a four-component mixture in FAU.

The second objective of this paper is to test the validity of the interpolation formula 3 as applied to a ternary mixture. The final objective is to test the predictive capability of the M−S formulations for diffusion of alkane mixtures in zeolite topologies other than FAU, namely MFI and LTA. There are no published MD investigations on mixture diffusion in LTA, and for MFI, only transport diffusivities in *binary* mixtures of CH_4 with CF_4 or He have been investigated.[7,11]

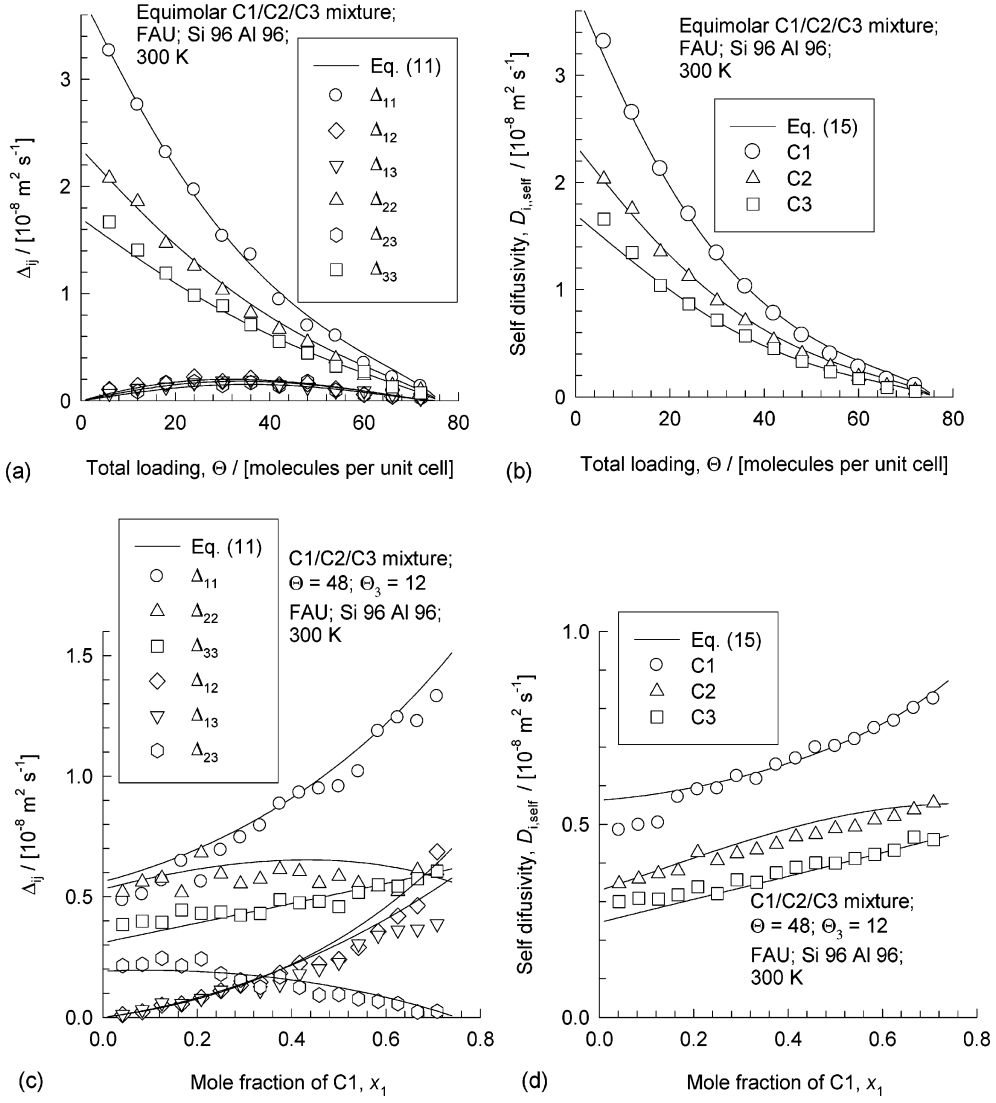

Figure 2. Diffusion data for ternary mixture of C1, C2, and C3 in FAU at 300 K. Elements of (a) Δ_{ij} and (b) $D_{i,\mathrm{self}}$ for equimolar ternary mixture at various loadings. Elements of (c) Δ_{ij} and (d) $D_{i,\mathrm{self}}$ for varying C1/C2 compositions at constant total loading $\Theta = 48$ and loading of C3 also kept constant at $\Theta_3 = 12$. The MD simulation results (open symbols) are compared with the calculations following eqs 11 and 15, indicated by the continuous solid line. Parameter values are given in Table 2.

2. CBMC and MD Simulations

Simulations have been carried out for diffusion and adsorption of alkane mixtures in three different zeolite topologies: FAU (96 Si, 96 Al), MFI (all silica silicalite-1), and LTA (5A zeolite, 96 Si, 96 Al); the crystallographic data are available elsewhere.[24,25] For both adsorption and diffusion simulations, we used the united atom model. We considered the CH_x groups as single, chargeless interaction centers with their own effective potentials. The beads in the chain are connected by harmonic bonding potentials. A harmonic cosine bending potential models the bond bending between three neighboring beads, and a Ryckaert−Bellemans potential controls the torsion angle. The beads in a chain separated by more than three bonds interact with each other through a Lennard−Jones potential. The Lennard−Jones potentials are shifted and cut at 12 Å. Pure component adsorption isotherms for alkanes were determined using configurational-bias Monte Carlo (CBMC) simulations. The CBMC simulation details, along with the force fields, have been given in detail in other publications.[26−28] For FAU and LTA, the influence of cations were not taken into consideration either for adsorption or diffusion. The simulation boxes for FAU and LTA consisted of $1 \times 1 \times 1$ unit cells, and for MFI, $2 \times 2 \times 2$ unit cells.

Diffusion in a system of N molecules is simulated using Newton's equations of motion until the system properties, on average, no longer change in time. The Verlet algorithm is used for time integration. The energy drift of the entire system is monitored to ensure that the time steps taken were not too large. A time step of 1 fs was used in all simulations. For each simulation, *initializing* CBMC moves are used to place the molecules in the domain, minimizing the energy. Next, an *equilibration* stage follows. Like the initialization stage, this consists of CBMC moves, but now using velocity scaling; at each cycle, all adsorbent pseudo-atom velocities are scaled to match the specified temperature. After a fixed number of initialization and equilibrium steps, the MD simulation *production* cycles start. For every cycle, the statistics for determining the mean-square displacements (MSDs) are updated. The MSDs are determined for time intervals ranging from 2 fs to 1 ns. To do this, an order-N algorithm, as detailed in Chapter 4 of Frenkel and Smit[29] is implemented. The Nosé−Hoover thermostat is used to maintain constant temperature conditions.

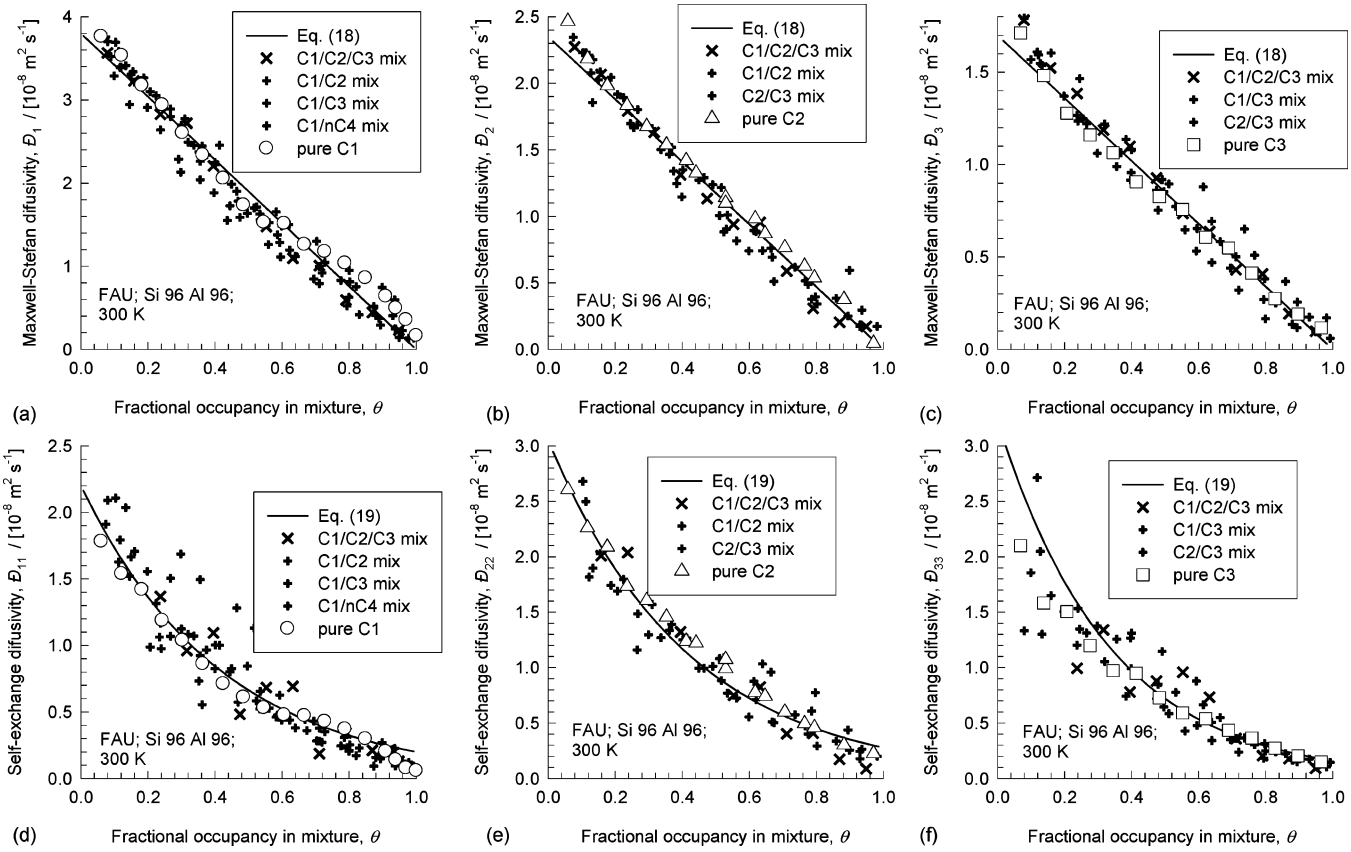

Figure 3. M−S diffusivities $Đ_i$ (symbols) for (a) C1, (b) C2, and (c) C3 in FAU at 300 K compared with the calculations following eq 18. MD simulation results for self-exchange $Đ_{ii}$ (symbols) for (d) C1, (e) C2, and (f) C3 compared with the calculations following eq 19. Parameter values are given in Table 2.

In the earlier publications of Sanborn and Snurr[6,15] and Skoulidas et al.,[10] the Onsager matrix $[L]$, defined by $(\mathbf{N}) = -[L](\nabla\mu)$ were determined from the MSDs. From the viewpoint of determination of the M−S diffusivities, we find it much more convenient to define a matrix $[\Delta]$:

$$(\mathbf{N}) = -\rho\frac{[\Delta]}{k_B T}\begin{bmatrix}\Theta_1 & 0 & 0 & 0 & 0\\ 0 & \Theta_2 & 0 & 0 & 0\\ 0 & 0 & \ddots & 0 & 0\\ 0 & 0 & 0 & \ddots & 0\\ 0 & 0 & 0 & 0 & \Theta_n\end{bmatrix}(\nabla\mu) \qquad (4)$$

and determine the elements of this matrix from

$$\Delta_{ij} = \frac{1}{6}\lim_{\Delta t\to\infty}\frac{1}{N_i}\frac{1}{\Delta t}\langle(\sum_{l=1}^{N_i}(\mathbf{r}_{l,i}(t+\Delta t) - \mathbf{r}_{l,i}(t)))\cdot (\sum_{k=1}^{N_j}(\mathbf{r}_{k,j}(t+\Delta t) - \mathbf{r}_{k,j}(t)))\rangle \qquad (5)$$

In this expression, N_i and N_j represent the number of molecules of species i and j, respectively, and $\mathbf{r}_{l,i}(t)$ is the position of molecule l of species i at any time t. From the definition $\Theta_i = N_i/\rho V$, where V is the volume of the simulation box, we see that $\rho\Theta_i\Delta_{ij} = L_{ij}k_BT$ and, therefore, the Onsager reciprocal relations $L_{ij} = L_{ji}$ yields

$$\Theta_i\Delta_{ij} = \Theta_j\Delta_{ji} \qquad (6)$$

Detailed derivations are available in Appendix B of the Supporting Information. For single component diffusion, $n = 1$, Δ_{11} can be identified with the M−S, or "corrected" diffusivity $Đ_1$. Defining an n-dimensional square matrix $[B]$ with elements

$$B_{ii} = \frac{1}{Đ_i} + \sum_{j=1;j\neq i}^{n}\frac{\theta_j}{Đ_{ij}}; \quad B_{ij} = -\frac{\Theta_{i,\mathrm{sat}}}{\Theta_{j,\mathrm{sat}}}\frac{\theta_i}{Đ_{ij}}; \quad i,j = 1,2,...n \qquad (7)$$

with the fractional occupancies θ_i defined by

$$\theta_i \equiv \Theta_i/\Theta_{i,\mathrm{sat}} \quad i = 1,2,...n \qquad (8)$$

allows us to recast eq 1 into n-dimensional matrix notation as

$$(\mathbf{N}) = -\rho[B]^{-1}[\Gamma](\nabla\Theta) \qquad (9)$$

The matrix of thermodynamic correction factors $[\Gamma]$ are defined by

$$\frac{\Theta_i}{k_BT}\nabla\mu_i \equiv \sum_{j=1}^{n}\Gamma_{ij}\nabla\Theta_j; \quad \Gamma_{ij} = \frac{\Theta_i}{\Theta_j}\frac{\partial\ln p_i}{\partial\ln\Theta_j}; \quad i,j = 1,...n \qquad (10)$$

where p_i represents the partial pressure (or, more strictly, the fugacity) of component i in the bulk fluid phase. The Γ_{ij} can be calculated from knowledge of the multicomponent sorption isotherms.[5,11] From eqs 4, 9, and 10, we note that

$$[\Delta] = [B]^{-1} \qquad (11)$$

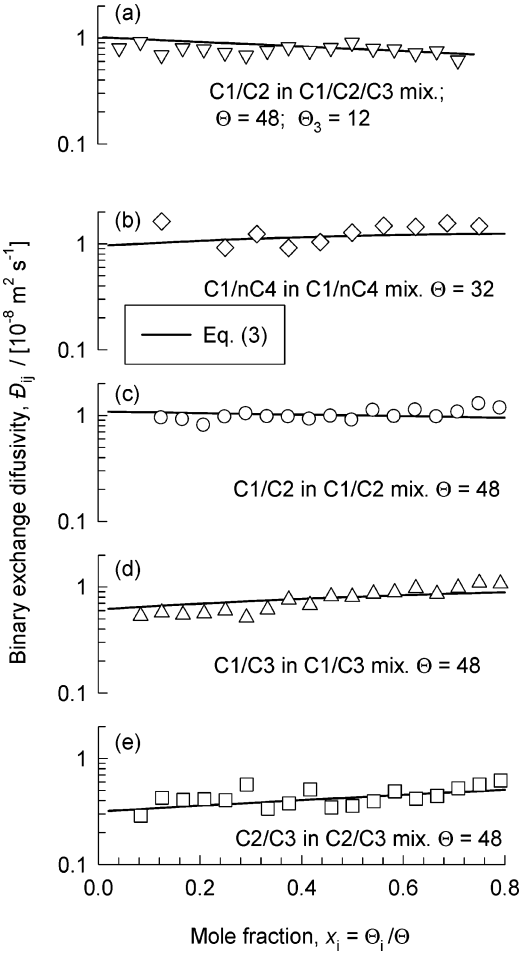

Figure 4. Binary self-exchange coefficients $Đ_{ij}$ for binary and ternary mixture diffusion in FAU at 300 K. MD simulation results (symbols) compared with calculations following eq 3. Parameter values are given in Table 2.

and so the elements of [*B*] can be obtained by matrix inversion of the MD simulated [Δ]. The binary exchange diffusivities $Đ_{ij}$ can be determined from

$$Đ_{ij} = -\frac{\Theta_{i,\mathrm{sat}}}{\Theta_{j,\mathrm{sat}}}\frac{\theta_i}{B_{ij}}; \quad i,j = 1, 2,...n \tag{12}$$

The M−S diffusivities $Đ_i$ can then be calculated from

$$Đ_i = \frac{1}{B_{ii} - \sum_{\substack{j=1 \\ j\neq i}}^{n}\frac{\theta_j}{Đ_{ij}}}; \quad i = 1, 2,...n \tag{13}$$

The self-diffusivities, $D_{i,\mathrm{self}}$, in single-component, binary, ternary, and quaternary mixtures were computed by analyzing the mean-square displacement of each component in the usual manner

$$D_{i,\mathrm{self}} = \frac{1}{6N_i}\lim_{\Delta t\to\infty}\frac{1}{\Delta t}\langle(\sum_{l=1}^{N_i}(\mathbf{r}_{l,i}(t+\Delta t) - \mathbf{r}_{l,i}(t))^2)\rangle \tag{14}$$

TABLE 1: MD Simulation Campaigns with Various Alkanes in Various Zeolite Topologies

zeolite	*n*	components	composition
FAU, 300 K	1	C1, C3, C3, *n*C4, *i*C4	pure, varying Θ
	2	C1/C2, C1/C3, C2/C3, C1/*n*C4, *n*C4/*i*C4	75−25, 50−50, 25−75 mixtures, varying Θ
	2	C1/C2, C1/C3, C2/C3, C1/*n*C4, *n*C4/*i*C4	varying x_i, keeping Θ constant
	3	C1/C2/C3	equimolar, varying Θ
	3	C1/C2/C3	varying x_i, keeping Θ constant
	4	C1/C2/C3/*n*C4	equimolar
MFI, 300 K	1	C1, C3, C3	pure, varying Θ
	2	C1/C2, C1/C3, C2/C3	75−25, 50−50, 25−75 mixtures, varying Θ
	2	C1/C2, C1/C3, C2/C3	varying x_i, keeping Θ constant
	3	C1/C2/C3	equimolar, varying Θ
MFI, 373 K	1	C1, *n*C4	pure, varying Θ
	2	C1/*n*C4	75−25, 50−50, 25−75 mixtures, varying Θ
	2	C1/*n*C4	varying x_i, keeping Θ constant
LTA, 750 K	1	C1, C2, C3	pure, varying Θ
	2	C1/C2	75−25, 50−50, 25−75 mixtures, varying Θ
	2	C1/ C2	varying x_i, keeping Θ constant
	3	C1/C2/C3	equimolar, varying Θ

The M−S formulation leads to the following expression for the self-diffusivity of component *i* in a multicomponent mixture:[11]

$$\frac{1}{D_{i,\mathrm{self}}} = \frac{1}{Đ_i} + \sum_{j=1}^{n}\frac{\theta_j}{Đ_{ij}} = \frac{1}{Đ_i} + \frac{\theta_i}{Đ_{ii}} + \sum_{\substack{j=1 \\ j\neq i}}^{n}\frac{\theta_j}{Đ_{ij}} \tag{15}$$

Using the definition of B_{ii} from eq 7 allows us to recast eq 15 in the form

$$Đ_{ii} = \frac{\theta_i}{\frac{1}{D_{i,\mathrm{self}}} - B_{ii}}; \quad i = 1, 2,...n \tag{16}$$

in which the expression allows the calculation of the *self*-exchange coefficients $Đ_{ii}$ in *n*-component mixtures.

The simulation campaigns are summarized in Table 1. In each case, both the $Δ_{ij}$ and $D_{i,\mathrm{self}}$ were determined from simulations for various loadings $\Theta = \Theta_1 + \Theta_2 + \cdots\Theta_n$ at a fixed mixture composition or varying mixture composition for a fixed loading Θ. CBMC simulations of the pure component isotherms were used to estimate the saturation capacities $\Theta_{i,\mathrm{sat}}$; with this information, the fractional occupancies θ_i and also the total occupancy:

$$\theta = \sum_{i=1}^{n}\theta_i = \sum_{i=1}^{n}\frac{\Theta_i}{\Theta_{i,\mathrm{sat}}} \tag{17}$$

were determined. Equations 12, 13, and 16 then allowed calculation of the M−S diffusivities $Đ_i$, $Đ_{ii}$, and $Đ_{ij}$. In most cases, where the CBMC simulations were run to high enough pressures so that component loadings reached a stable plateau value (see, e.g., Figure 1a), this plateau value was taken to be $\Theta_{i,\mathrm{sat}}$. In all cases, the saturation loading $\Theta_{i,\mathrm{sat}}$ also corresponds with the loading for which the M−S diffusivity of a component reaches near-zero values as seen for example in Figure 1b; this provides an independent check of the value of $\Theta_{i,\mathrm{sat}}$. The complete set of data on $Δ_{ij}$, $D_{i,\mathrm{self}}$, $Đ_i$, $Đ_{ii}$, and $Đ_{ij}$ for each

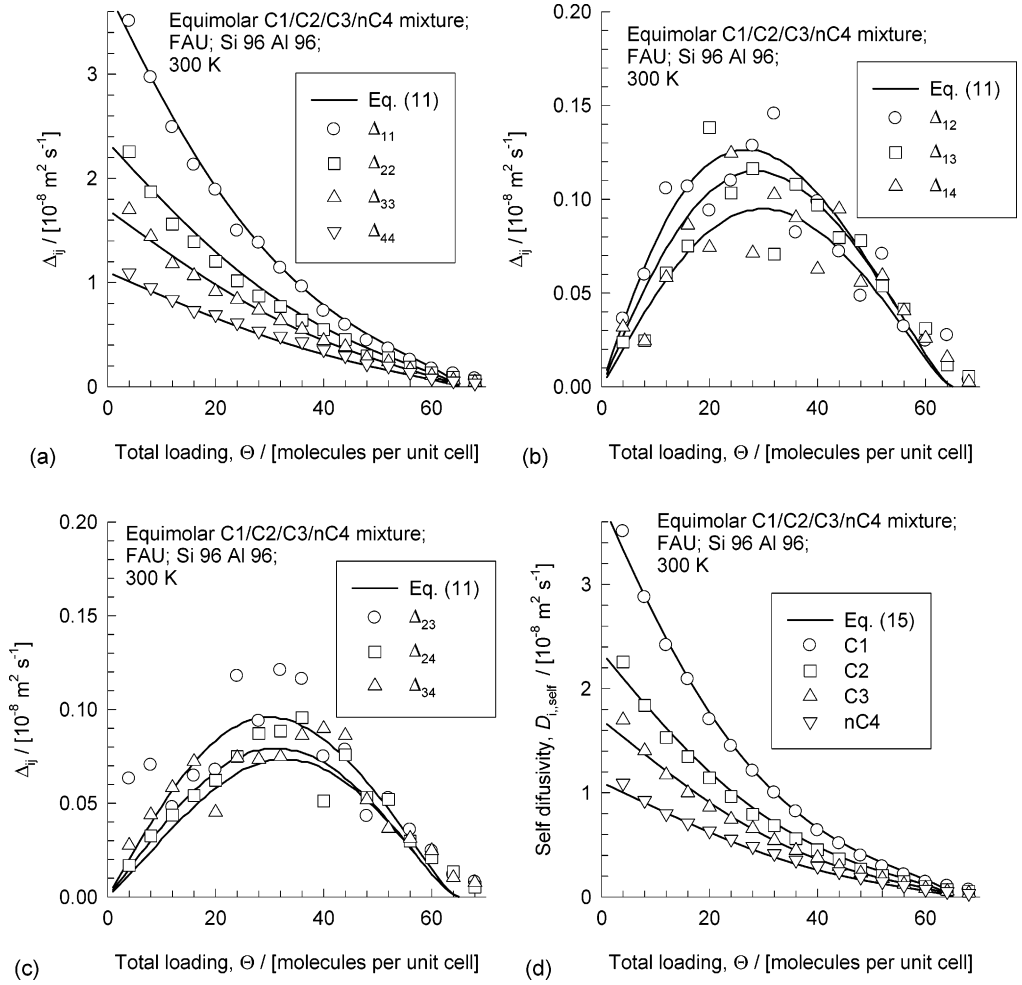

Figure 5. Diffusion data for an equimolar quaternary mixture of C1, C2, C3, and *n*C4 in FAU at 300 K. Elements of (a), (b), (c) Δ_{ij}, and (d) $D_{i,\text{self}}$ at various loadings. The MD simulation results (open symbols) are compared with the calculations following eqs 11 and 15 with parameter values in Table 2, indicated by the continuous solid lines.

campaign have been presented separately in graphical form in Appendix A of the Supporting information accompanying this publication. Below, we present a representative selection of the major results with the objective of drawing important conclusions regarding the applicability of the M−S formulation to describe multicomponent diffusion in zeolites.

3. Simulation Results and Discussion

Consider first diffusion in FAU that consists of cages separated from one another by large windows. Figure 1 shows the sorption and diffusion data for pure components C1, C2, C3, and *n*C4 in FAU at 300 K. From the pure component sorption isotherms, the saturation capacities were estimated and these are summarized in Table 2. The loading dependence of the pure component M−S diffusivities $Đ_i$ can be approximated by

$$Đ_i = Đ_i(0)(1 - \theta_i) = Đ_i(0)\left(1 - \frac{\Theta_i}{\Theta_{i,\text{sat}}}\right) \qquad (18)$$

with the zero-loading diffusivity values as given in Table 2; see Figure 1b. We note that the $Đ_i$ of C1 exhibits a slight inflection at a loading $\Theta = 72$; the reasons for this are explained in an earlier publication.[30] For the purposes of the current investigation, we ignore the slight inflection characteristic and adopt the simple scenario described by eq 18. The data presented in Figure 1b for $Đ_i$ of light alkanes are in reasonably good agreement with the corresponding data for all-silica FAU reported by Chempath et al.;[12] small differences can be attributed to two factors: (1) we use 96 Si, 96 Al FAU topology, and (2) our force fields are also slightly different. An important difference in the simulation work of Chempath et al.[12] and that reported here is that in all cases we have determined $Đ_i$ for loadings up to saturation limits.

In the work of Skoulidas et al.,[9,11] the self-exchange coefficient was fitted in the form $Đ_{ii}/Đ_i = a_i \exp(-b_i\theta_i)$. For the molecule−zeolite systems considered in this paper, the M−S diffusivity $Đ_i$ reduces to zero at saturation loading (see Figure 1b), and consequently, the self-exchange coefficient $Đ_{ii}$ is also predicted to reduce to zero by their correlation. However, the simulated data show that $Đ_{ii}$ do not reduce to zero; rather, they

TABLE 2: Pure Component Data for Alkanes in FAU at 300 K

component	saturation capacity, $\Theta_{i,\text{sat}}$ / [molecules per unit cell]	$Đ_i(0)$/ [10^{-8} m^2 s^{-1}]	parameters describing self-exchange, defined by eq 19	
			a_i	b_i
methane (C1)	132	3.8	0.58	2.4
ethane (C2)	68	2.35	1.3	2.4
propane (C3)	58	1.7	1.9	3
n-butane (*n*C4)	46	1.1	2.8	3.2
i-butane (*i*C4)	46	1.4	1.8	3.2

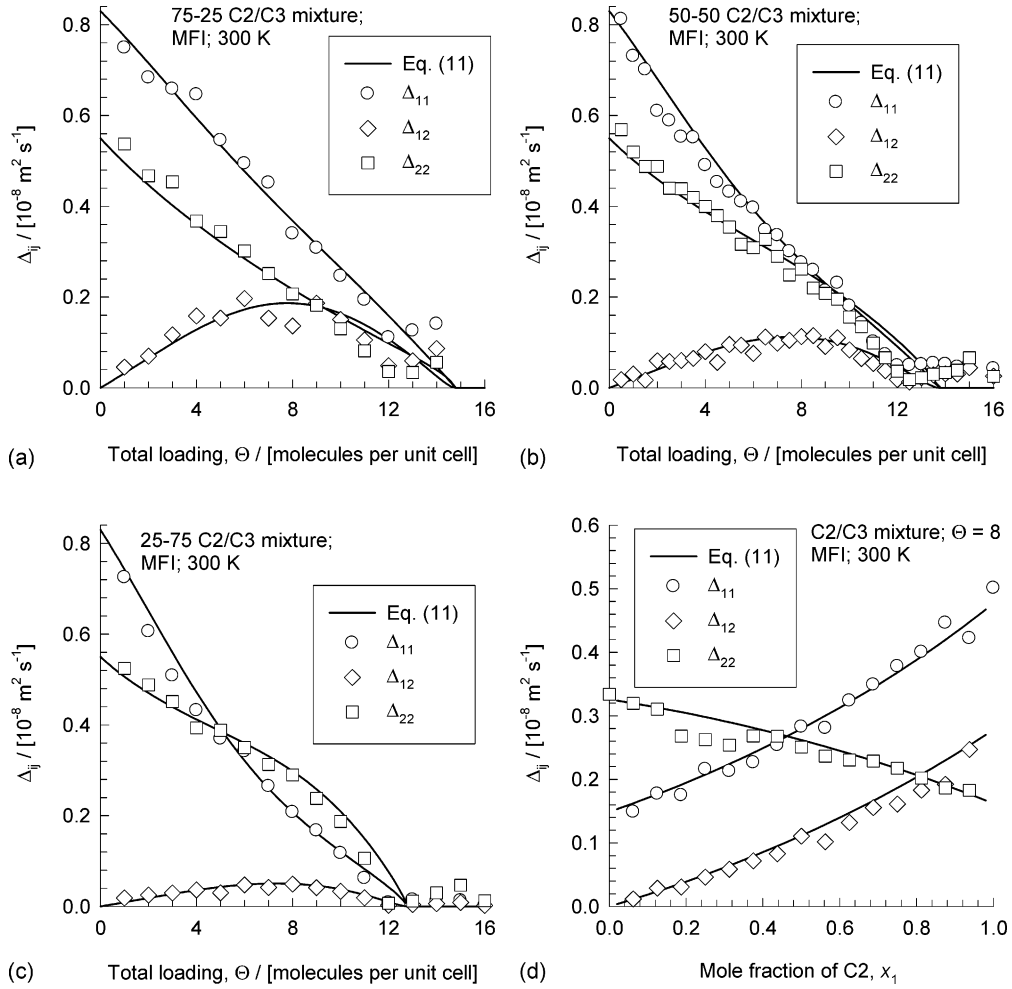

Figure 6. MD simulation data (open symbols) for Δ_{ij} (a) 75−25, (b) 50−50, and (c) 25−75 mixtures of ethane (C2) and propane (C3) mixtures in MFI at 300 K. (d) MD simulation data (open symbols) for Δ_{ij} as a function of the mole fraction of C2 in a mixture at a total loading $\Theta = 8$ molecules per unit cell. The continuous lines in (a), (b), (c), and (d) are estimations of Δ_{ij} using eq 11, with pure component data as listed in Table 3.

decay exponentially with θ and have a small but finite value at $\theta = 1$; this is shown for example in Figure 1c. For this reason we chose to correlate the $Đ_{ii}$ in following the manner

$$\frac{Đ_{ii}}{Đ_i(0)} = a_i \exp(-b_i\theta_i) \tag{19}$$

with the values of the a_i and b_i as given in Table 2. This refinement of earlier works[9,11,12] has come to light because we have carried out all the simulations up to saturation loadings.

Consider ternary diffusion in a C1/C2/C3 equimolar mixture in FAU at various loadings; the open symbols in Figure 2a and b show the MD simulated values of Δ_{ij} and $D_{i,\text{self}}$. The data on the M−S diffusivities $Đ_i$, backed out from the ternary simulations, are shown by the crosses in Figure 3a, b, and c for C1, C2, and C3, respectively, are plotted against the total occupancy θ in the mixture. The pluses represent the M−S diffusivities $Đ_i$ backed out of the various *binary* mixture simulation campaigns listed in Table 1. The M−S diffusivity of any component is seen to have nearly the same value whether the component diffuses on its own or in the company of one or more components. Equation 18, with pure component parameters listed in Table 2, provides a good estimation of $Đ_i$ at any given occupancy. Figure 3d, e, and f show the data on the self-exchange $Đ_{ii}$, backed out of the various binary (pluses) and ternary mixtures (crosses). Again, we note that the self-exchange in any mixture has nearly the same value as for pure component diffusion, provided we compare these at the same total occupancy θ. The scatter in the $Đ_{ii}$ can be explained as follows. The $Đ_{ii}$ is determined from *differences* between the inverse of the self-diffusivity of species i and the B_{ii} coefficient; see eq 16. Consequently, the errors in the $Đ_{ii}$ are larger than the errors in determination of the $D_{i,\text{self}}$ and Δ_{ij} alone. Equation 19, with parameters listed in Table 2, provides a reasonable representation of $Đ_{ii}$ for mixture diffusion.

The next important step is to verify the interpolation formula 3 for *ternary* mixtures. For this purpose, simulations were carried out with the C1/C2/C3 mixture in FAU wherein the total mixture and C3 loadings are held constant at $\Theta = 48$ and $\Theta_3 = 12$, respectively, and the proportions of C1 and C2 are varied; the results for Δ_{ij} and $D_{i,\text{self}}$ are shown by open symbols in Figure 2c and d. The coefficient for exchange between C1 and C2, $Đ_{12}$, backed out from the Δ_{ij} data using eq 12, are shown in Figure 4a as a function of the mole fraction of C1 in the ternary mixture $x_i = \Theta_i/\Theta$. The continuous lines in Figure 4a represent calculations following the interpolation formula 3 with the self-exchange coefficients estimated using eq 19 and parameter values in Table 2. Similar good agreement between the estimations following eq 3 for *all* binary mixture diffusion campaigns carried out at constant total loading Θ and varying

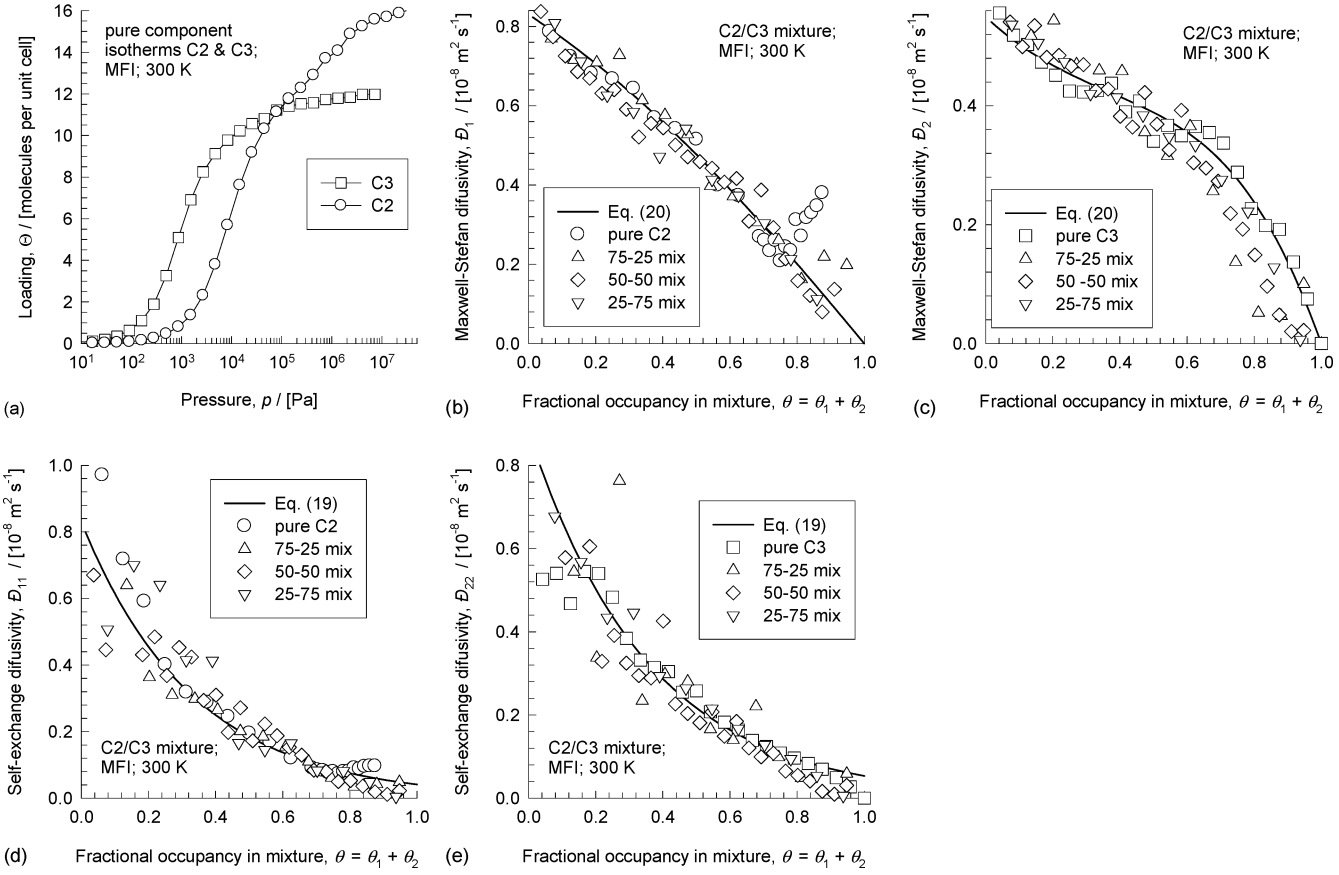

Figure 7. (a) CBMC simulation data on pure component isotherms for C2 and C3. (b, c) M−S diffusivities $Đ_i$ (symbols) for C2 and C3 compared with the calculations of the Reed−Ehrlich model 20, with parameters as specified in Table 3. (d, e) MD simulation results for self-exchange $Đ_{ii}$ (symbols) for C2 and C3 compared with the calculations following eq 19.

mixture compositions; see Figure 4b, c, d, and e. It should be emphasized that eq 3 is not the only way to generalize the binary interpolation formula 2 because, for a binary mixture, $\Theta_i + \Theta_j = \Theta$, and therefore, the powers in eq 2 are the corresponding mole fractions x_i and x_j. By contrast, for a ternary mixture $\Theta_i/(\Theta_i + \Theta_j) \neq x_i$. We verified that eq 3 is the only interpolation formula that matches the ternary simulations; other variants were not as successful.

Having validated the interpolation formula 3, the Δ_{ij} and $D_{i,\text{self}}$ for ternary diffusion can be estimated using eqs 11 and 15, respectively, with inputs of the *pure* component data in Table 2; these calculations are shown by the continuous lines in Figure 2a, b, c, and d. The estimations can be considered very good for the entire range of loadings and mixture compositions. The agreement between the MD simulated self diffusivities and the calculations using eq 15 is particularly heartening because the proper estimation of the self diffusivity of any one component depends on accurate modeling of the loading dependence of not only the $Đ_i$, but additionally the self-exchange $Đ_{ii}$ and binary exchange diffusivities $Đ_{ij}$. Put another way, *all* correlation effects appear to be properly captured by the estimates on the basis of pure component data. Similar good agreement was obtained for all the binary mixture campaigns in FAU, listed in Table 1.

With the pure component data listed in Table 2, we can predict the Δ_{ij} and $D_{i,\text{self}}$ for an equimolar *quaternary* mixture containing C1, C2, C3, and *n*C4 for a variety of loadings. These predictions (continuous solid lines) are in good agreement with the MD simulated values (open symbols); see Figure 5.

We now consider diffusion of binary mixtures of ethane (C2) and propane (C3) in MFI at 300 K. The topology of MFI consists of intersecting straight and zigzag channels. The MD simulated data for the Δ_{ij} are shown in Figure 6a, b, and c for 75−25, 50−50, and 25−75 mixtures at various loadings. From the sorption isotherms determined from CBMC simulations (see Figure 7a), we estimate the saturation capacities as 16 and 12 molecules per unit cell, respectively, for C2 and C3. The component M−S diffusivities $Đ_i$ do not precisely follow the scenario described by eq 18; see Figure 7b and c. It is interesting to note that the $Đ_i$ for C2 exhibits a distinct inflection at a loading $\Theta = 12$, corresponding to the inflection in the isotherm in agreement with the MD simulation results of Shang-Shan et al.[18] The reasons behind this inflection behavior of $Đ_i$ has been discussed in our earlier publication.[30] To describe the loading dependence more precisely, we need to take account of the reduction in the energy barrier for diffusion with increased loading. We ignore the inflection in the C2 diffusivity and proceed further with the model due to Reed and Ehrlich.[31,32] In the Reed−Ehrlich model, the presence of neighboring molecules on a lattice is assumed to influence the jump frequencies of species i by a factor $f_i = \exp(\delta E_i/RT)$, where where δE_i represents the reduction in the energy barrier for diffusion. This model leads to the following expression for the M−S diffusivity as a function of the fractional occupancy,

$$Đ_i = Đ_i(0)\frac{(1+\epsilon_i)^{z-1}}{(1+\epsilon_i/f_i)^z} \tag{20}$$

where z is the coordination number, representing the maximum

TABLE 3: Pure Component Data for Alkanes in MFI and LTA. the Self-exchange Coefficient for Pure C3 in LTA Could Not Be Determined Because $D_{i,self}$ and $Đ_i$ Were Too Close to Each Other

component and zeolite	saturation capacity, $\Theta_{i,sat}$/ [molecules per unit cell]	$Đ_i(0)$/ $[10^{-8}$ m^2 s$^{-1}]$	parameters describing self-exchange, defined by eq 19		Reed−Ehrlich model parameters in eq 20 and 21	
			a_i	b_i	z	f
C1 in MFI, 300 K	23	1.65	0.43	1.9	2.5	1.0 exp(1.1θ)
C2 in MFI, 300 K	16	0.83	1	3	2.5	1.15
C3 in MFI, 300 K	12	0.55	1.6	2.8	2.5	1.0 exp(0.7θ)
C1 in MFI, 373 K	23	2.2	0.45	2	2.5	0.9 exp(1.25θ)
*n*C4 in MFI, 373 K	10	0.6	1.6	2.4	2.5	1.0 exp(0.8θ)
C1 in LTA, 750 K	132	0.12	80	4	9	2.2 exp(−0.3θ)
C2 in LTA, 750 K	88	0.01	700	3.5	9	1.3 exp(0.6θ)
C3 in LTA, 750 K	70	0.0002	-	-	9	1.3 exp(0.87θ)

number of nearest neighbors. The other parameters are defined as (see Krishna et al.[32] for more detailed discussions and derivations)

$$\epsilon_i = \frac{(\beta - 1 + 2\theta_i)f_i}{2(1-\theta_i)}; \quad \beta = \sqrt{1 - 4\theta_i(1-\theta_i)(1-1/f_i)} \quad (21)$$

In the limiting case where there are no interactions between neighboring molecules, i.e., $\delta E_i = 0$, we get $f_i = 1$, $\beta_i = 1$, $\epsilon_i = \theta_i/(1-\theta_i)$, and eq 20 reduces to yield eq 18. For estimation of the number of nearest numbers z, we reason as follows. Of the total of 16 ($= \Theta_{1,sat}$) C2 molecules, 4 molecules are located at the intersections, and the remaining 12 lie within the straight and zigzag channels. Each molecule at the intersection "sees" 4 neighbors. Each molecule within the channels "sees" only 2 neighbors. The *average* number of nearest neighbors is, therefore, $z = (12 \times 2 + 4 \times 4)/16 = 2.5$. We assume this coordination number to hold for C2/C3 mixtures and also for pure C3. The parameters f_i for C2 and C3 can then be "fitted" to match the observed occupancy dependence of $Đ_i$; the fitted values are specified in Table 3. The self-exchange diffusivities $Đ_{ii}$ have practically the same values in mixtures as for the pure components and, as in the case of alkanes diffusion in FAU, eq 19 provides a good representation of the data; see Figure 7d and e.

The continuous lines in Figure 6a, b, and c are calculations of Δ_{ij} from eq 11, wherein the elements of B_{ij} are estimated from pure component data listed in Table 3, after invoking the interpolation formula 3. The agreement with the MD simulated Δ_{ij} is good for all mixture compositions for the whole range of loadings studied. A more stringent test of the interpolation formula 3 is provided in Figure 6d that presents the MD simulated data (open symbols), showing the variation of Δ_{ij} with mixture composition for a fixed loading $\Theta = 8$. The calculations using eq 11, along with the Reed−Ehrlich estimation of pure component $Đ_i$, are shown by the continuous solid lines. The M−S model does a very good job of reproducing the correct variation of Δ_{ij} with x_i at a fixed loading.

Additionally, we carried out MD simulations with C1/C2, C1/C3, C1/*n*C4, and C1/C2/C3 mixtures in MFI. In all these cases, too, the Reed−Ehrlich model, along with the M−S approach, is found to be in good agreement with the MD simulated values of Δ_{ij} and $D_{i,self}$; see Appendix A of the Supporting Information.

Next, we consider diffusion of C1 and C2 mixtures in LTA (5A zeolite) that consists of cages separated from one another by narrow windows. The simulations for C1 and C2 in LTA were carried out at 750 K because the diffusion is too slow at lower temperatures to provide good MSD data for analyses. Zeolite LTA is, however, not stable at 750 K and so any comparison with experimental data will require extrapolation to lower temperatures. Figure 8a and b shows the $Đ_i$, backed out from both mixture and pure component simulations, are close to one another and show the same dependence on the occupancy. The initial sharp increase in the $Đ_i$ with occupancy is due to the reduction in the energy barrier for diffusion with increased loading as explained by Beerdsen et al.[33] The loading dependence of $Đ_i$ is quite different from that observed in FAU; this is because the windows in LTA are much smaller than in FAU, and the presence of neighboring molecules within a cage has a significant influence on the jump rates between cages.[33] To describe the loading dependence of $Đ_i$, we use the Reed−Ehrlich model[31,32] with the parameters as specified in Table 3. The choice of the number of nearest neighbors, $z = 9$, is on the basis of a comparison of MD simulations with kinetic Monte Carlo simulations using a lattice model.[34] The calculations of Δ_{ij} using eq 11 compare very well with the MD simulated values for all mixture simulations; one representative example for the 75−25 mixture is shown in Figure 8c. Another point to note is that for LTA, the cross-coefficient Δ_{12} is practically zero at loadings below 60 molecules per unit cell, suggesting that correlation effects are practically nonexistent. This means that a good *approximation* for diffusion in LTA, for occupancies below say, 0.5, is that the two species diffuse independently and that the binary exchange coefficient follows the facile exchange scenario, i.e., $Đ_{12} \rightarrow \infty$. This is equivalent to the Habgood model for diffusion in binary mixtures.[35] It is interesting to note that Krishna and Baur[5] in their reanalysis of the uptake experiments of Habgood[35] involving binary mixtures of CH_4 and N_2 in LTA (4A zeolite) reached the conclusion that these experiments could best be described using the Maxwell−Stefan formulation employing the facile exchange scenario. The MD simulations reported here provide a firmer justification for this assumption.

We also carried out MD simulations with an equimolar ternary mixture of C1, C2, and C3 in LTA at 750 K. The M−S diffusivities $Đ_i$ of the individual species, backed out of the ternary MD simulations and denoted by the crosses in Figure 8a, b, and d, are in very good agreement with the pure component and the binary mixture data.

4. Conclusions

Using an extensive database of MD simulations for single components, binary, ternary, and quaternary mixtures containing alkanes with 1−4 carbon atoms in three different zeolite topologies, FAU, MFI, and LTA, we have provided stringent tests of the various facets of the Maxwell−Stefan formulation for diffusion in zeolites of differing topologies. The following major conclusions can be drawn from this study.

(1) The M−S diffusivities $Đ_i$ have nearly the *same* value for species i, whether this species is present on its own or in a mixture with one or more species, when compared at the same occupancy $\theta = \sum_{i=1}^{n} \Theta_i/\Theta_{i,sat}$. This definition of occupancy allows us to consider mixtures with even widely different saturation capacities. This is the major advantage of the M−S formulation and forms the basis of the prediction of mixture

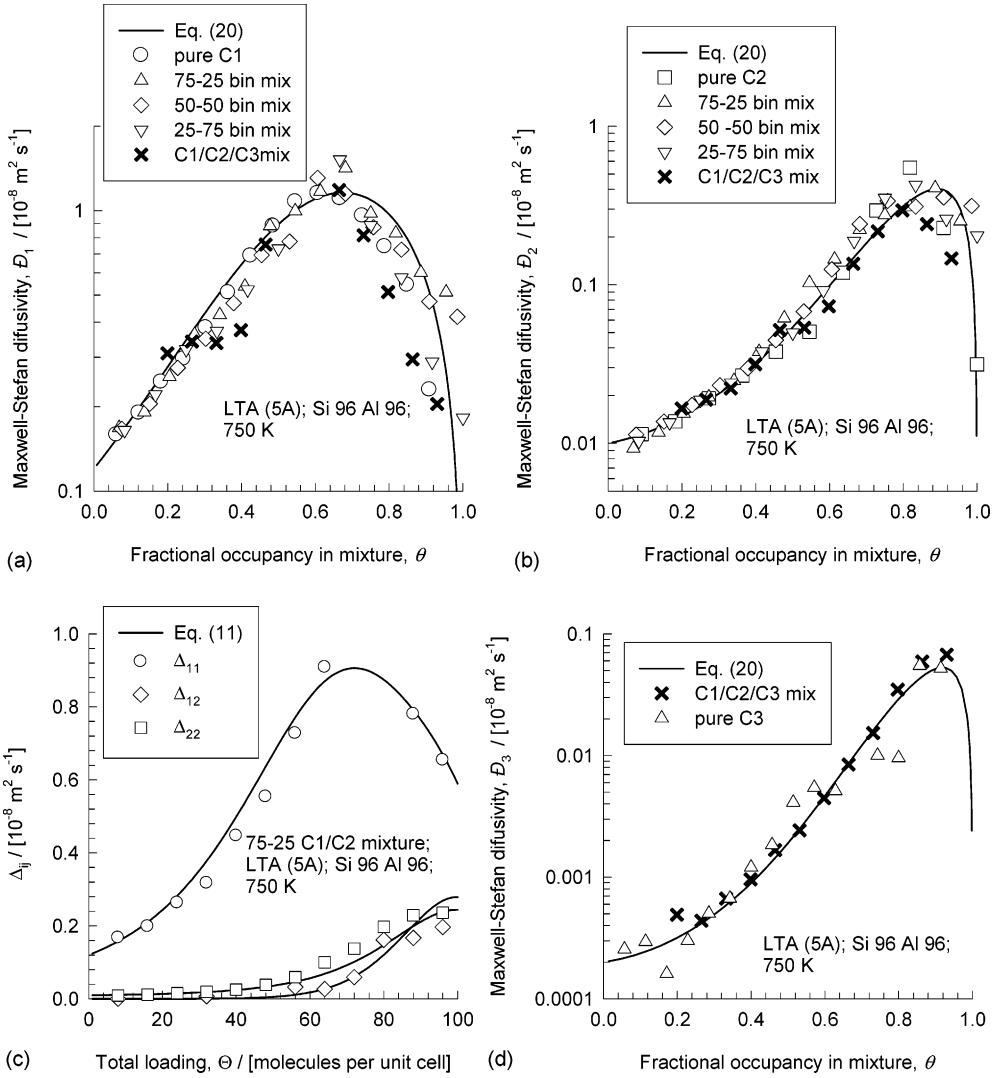

Figure 8. Diffusion data for methane (C1), ethane (C2), and propane (C3) in LTA (5A) at 750 K. M−S diffusivities $Đ_i$ for (a) C1 and (b) C2 obtained from pure component and binary mixture simulations (open symbols) compared with the calculations of the Reed−Ehrlich model 20, with parameters as specified in Table 3. (c) MD simulation results of 75−25 binary mixture of C1 and C2 in LTA at various loadings. (d) Comparison of pure component $Đ_i$ for C3 with values backed out of MD simulations with ternary mixture of C1/C2/C3 (indicated by crosses).

diffusion from pure component parameter values. An essential aspect is the proper description of the dependence of the pure component $Đ_i$ on the occupancy θ. The loading dependence for a given alkane molecule varies according to the zeolite topology. In this study, we have shown that the Reed−Ehrlich model 20 is able to capture the loading dependence in the MFI and in LTA with reasonable success. However, the determination of the number of nearest neighbors z requires careful attention.

(2) The self-exchange diffusivities $Đ_{ii}$, at a given occupancy θ, is the same whether determined from pure component, binary, or ternary mixture data. This is the second major advantage of the M−S formulation.

(3) For all binary and ternary mixtures investigated, in all three zeolite topologies, it was verified that the binary exchange coefficient $Đ_{ij}$ can be interpolated from the corresponding values of the self-exchange parameters $Đ_{ii}$ and $Đ_{jj}$ using the interpolation formula 3.

(4) For all alkane mixtures in all three zeolite topologies, the elements of the matrix $[\Delta]$ can be predicted with good accuracy for a wide range of loadings and mixture compositions using only pure component data. Multiplication of the matrix $[\Delta]$ with the matrix of thermodynamic factors $[\Gamma]$ yields the Fick diffusivity matrix $[D] \equiv [\Delta][\Gamma]$ that is required in the solution of practical problems involving multicomponent diffusion.[5,36]

Further research on multicomponent diffusion will be required to be carried out with molecules other than light alkanes in various zeolite topologies to see whether the advantages of the M−S formulation hold more generally. This is the next goal of our continuing research.

Acknowledgment. R.K. acknowledges two grants: *Programmasubsidie* and TOP subsidy from The Netherlands Foundation for Fundamental Research (NWO-CW) for the development of novel concepts in reactive separations technology and for intensification of reactors. We gratefully acknowledge D. Dubbeldam, S. Calero, T.J.H. Vlugt, E. Beerdsen, and B. Smit for providing the CBMC and MD simulation codes. We acknowledge NWO/NCF for provision of high-performance computing resources in terms of PC clusters running on LINUX.

Supporting Information Available: Diffusion of alkane mixtures in zeolites; validating the Maxwell−Stefan formulation using MD simulations (Supplementary Information); Appendix A contains the complete set of data on Δ_{ij}, $D_{i,\mathrm{self}}$, $Đ_i$, $Đ_{ii}$, and $Đ_{ij}$ for each campaign listed in Table 1, in graphic form;

Appendix B compares the M−S and Onsager formulations; Appendix C contains a list of symbols used in this work. This material is available free of charge via the Internet at http://pubs.acs.org.

References and Notes

(1) Kärger, J.; Ruthven, D. M. *Diffusion in Zeolites and Other Microporous Solids*; John Wiley: New York, 1992.
(2) Ruthven, D. M. *Ind. Eng. Chem. Res.* **2000**, *39*, 2127.
(3) Kärger, J. *Ind. Eng. Chem. Res.* **2002**, *41*, 3335.
(4) Krishna, R.; Paschek, D. *Sep. Purif. Technol.* **2000**, *21*, 111.
(5) Krishna, R.; Baur, R. *Sep. Purif. Technol.* **2003**, *33*, 213.
(6) Sanborn, M. J.; Snurr, R. Q. *AIChE J.* **2001**, *47*, 2032.
(7) Skoulidas, A. I.; Sholl, D. S. *AIChE J.* **2005**, *51*, 867.
(8) Maginn, E. J.; Bell, A. T.; Theodorou, D. N. *J. Phys. Chem.* **1993**, *97*, 4173.
(9) Skoulidas, A. I.; Sholl, D. S. *J. Phys. Chem. A* **2003**, *107*, 10132.
(10) Skoulidas, A. I.; Bowen, T. C.; Doelling, C. M.; Falconer, J. L.; Noble, R. D.; Sholl, D. S. *J. Membr. Sci.* **2003**, *227*, 123.
(11) Skoulidas, A. I.; Sholl, D. S.; Krishna, R. *Langmuir* **2003**, *19*, 7977.
(12) Chempath, S.; Krishna, R.; Snurr, R. Q. *J. Phys. Chem. B* **2004**, *108*, 13481.
(13) Ramanan, H.; Auerbach, S. M.; Tsapatsis, M. *J. Phys. Chem. B* **2004**, *108*, 17171.
(14) Ramanan, H.; Auerbach, S. M.; Tsapatsis, M. *J. Phys. Chem. B* **2004**, *108*, 17179.
(15) Sanborn, M. J.; Snurr, R. Q. *Sep. Purif. Technol.* **2000**, *20*, 1.
(16) Jobic, H.; Skoulidas, A. I.; Sholl, D. S. *J. Phys. Chem. B* **2004**, *108*, 10613.
(17) Papadopoulos, G. K.; Jobic, H.; Theodorou, D. N. *J. Phys. Chem. B* **2004**, *108*, 12748.
(18) Shang-Shan, C.; Jobic, H.; Plazanet, M.; Sholl, D. S. *Chem. Phys. Lett.* **2005**, In press.
(19) Dubbeldam, D.; Calero, S.; Maesen, T. L. M.; Smit, B. *Angew. Chem., Int. Ed.* **2003**, *42*, 3624.
(20) Dubbeldam, D.; Smit, B. *J. Phys. Chem. B* **2003**, *107*, 12138.
(21) Kapteijn, F.; Moulijn, J. A.; Krishna, R. *Chem. Eng. Sci.* **2000**, *55*, 2923.
(22) Skoulidas, A. I.; Sholl, D. S. *J. Phys. Chem. B* **2001**, *105*, 3151.
(23) Kärger, J.; Vasenkov, S.; Auerbach, S. M. Diffusion in Zeolites. In *Handbook of Zeolite Science and Technology*; Auerbach, S. M., Carrado, K. A., Dutta, P. K., Eds.; Marcel Dekker: New York, 2003; Chapter 10, p 341.
(24) Baerlocher, C.; McCusker, L. B. Database of Zeolite Structures. http://www.iza-structure.org/databases/ (accessed October 12, 2004).
(25) van Baten, J. M.; Krishna, R. MD Simulations of Diffusion in Zeolites; University of Amsterdam. http://ct-cr4.chem.uva.nl/md/ (accessed November 1, 2004).
(26) Dubbeldam, D.; Calero, S.; Vlugt, T. J. H.; Krishna, R.; Maesen, T. L. M.; Beerdsen, E.; Smit, B. *Phys. Rev. Lett.* **2004**, *93*(8), No. 088302.
(27) Dubbeldam, D.; Calero, S.; Vlugt, T. J. H.; Krishna, R.; Maesen, T. L. M.; Smit, B. *J. Phys. Chem. B* **2004**, *108*, 12301.
(28) Calero, S.; Dubbeldam, D.; Krishna, R.; Smit, B.; Vlugt, T. J. H.; Denayer, J. F. M.; Martens, J. A.; Maesen, T. L. M. *J. Am. Chem. Soc.* **2004**, *126*, 11377.
(29) Frenkel, D.; Smit, B. *Understanding Molecular Simulations: From Algorithms to Applications*, 2nd ed.; Academic Press: San Diego, 2002.
(30) Krishna, R.; van Baten, J. M.; Dubbeldam, D. *J. Phys. Chem. B* **2004**, *108*, 14820.
(31) Reed, D. A.; Ehrlich, G. *Surf. Sci.* **1981**, *102*, 588.
(32) Krishna, R.; Paschek, D.; Baur, R. *Microporous Mesoporous Mater.* **2004**, *76*, 233.
(33) Beerdsen, E.; Dubbeldam, D.; Smit, B. *Phys. Rev. Lett.* **2005**, *93*(24), No. 248301.
(34) Krishna, R.; van Baten, J. M. *Chem. Eng. Technol.* **2005**, *28*, 160.
(35) Habgood, H. W. *Can. J. Chem.* **1958**, *36*, 1384.
(36) Keil, F. J.; Krishna, R.; Coppens, M. O. *Rev. Chem. Eng.* **2000**, *16*, 71.

Supporting information to accompany:

Diffusion of alkane mixtures in zeolites. Validating the Maxwell-Stefan formulation using MD simulations.

R. Krishna and J.M. van Baten*

Van 't Hoff Institute for Molecular Sciences, University of Amsterdam, Nieuwe Achtergracht 166,

1018 WV Amsterdam, The Netherlands.

Contents:

Appendix A

- Contains data on Δ_{ij}, $D_{i,self}$, $Đ_i$, $Đ_{ii}$ for all the campaigns listed in Table 1 of the manuscript
- The symbols represent the MD simulated data, or data derived from the MD data using Eqs (12), (13) and (16)
- The continuous solid lines represent calculations based on fits of the pure component parameters listed in Tables 2 and 3.
- The Equation numbers in the graphs refer to the equations in the manuscript of the main paper

FAU; 300 K; pure component data; C1, C2, C3 and nC4

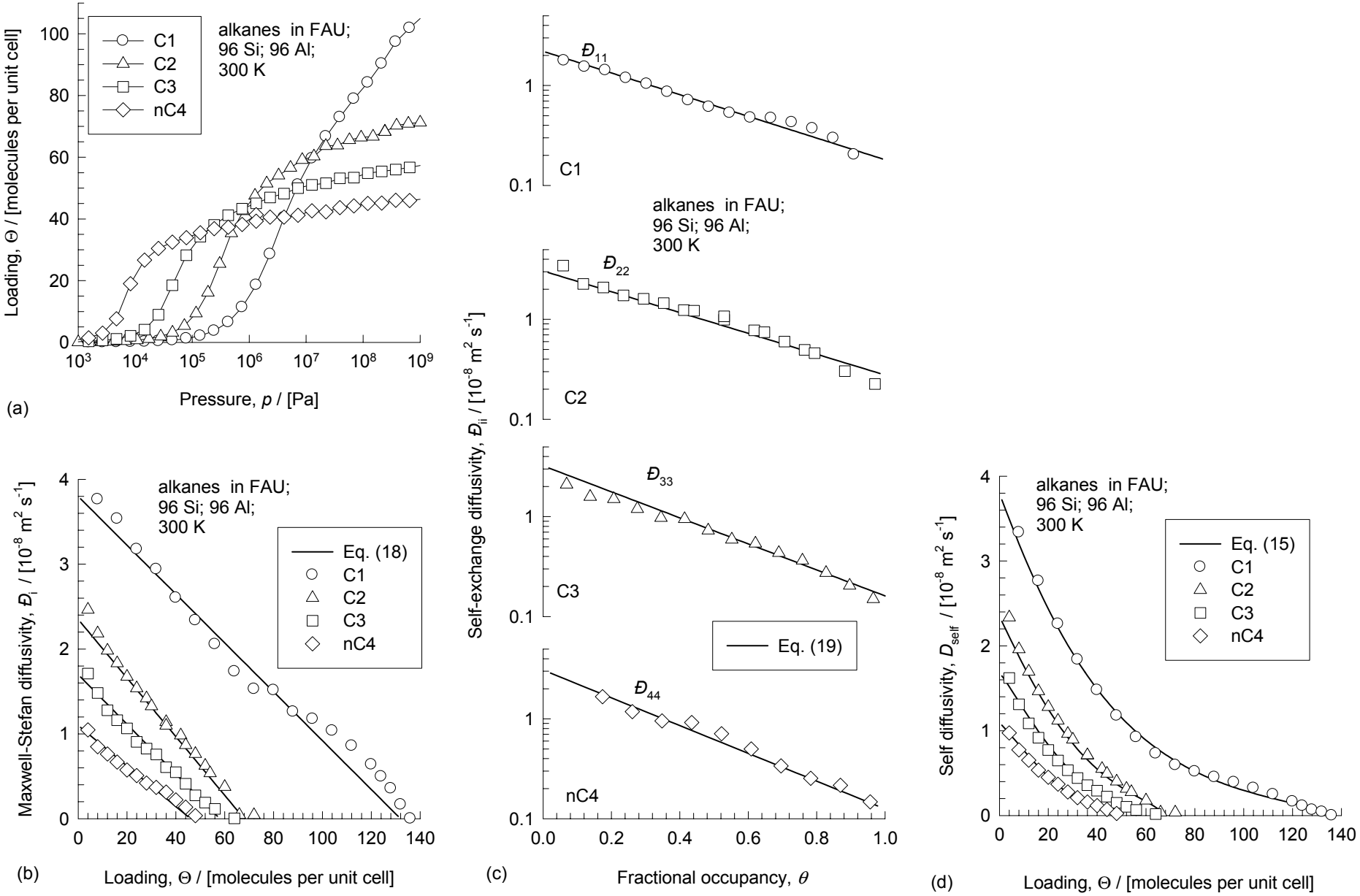

FAU; 300 K; C1/C2 75-25, 50-50, 25-75 mix; varying loadings

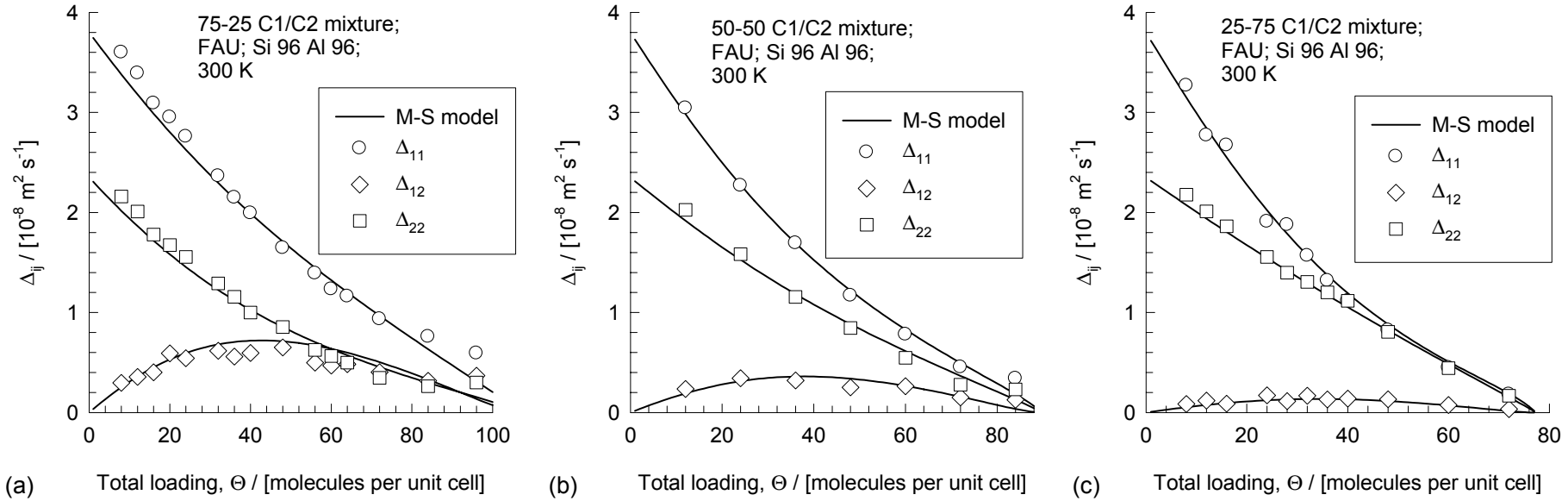

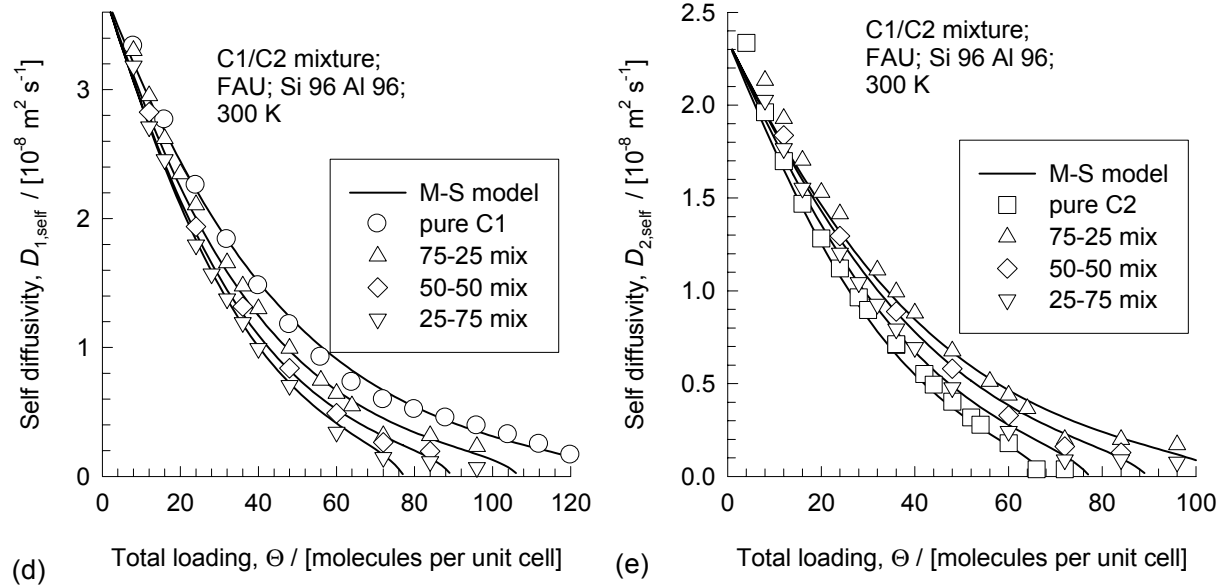

FAU; 300 K; C1/C2 binary; Θ = 48; varying compositions

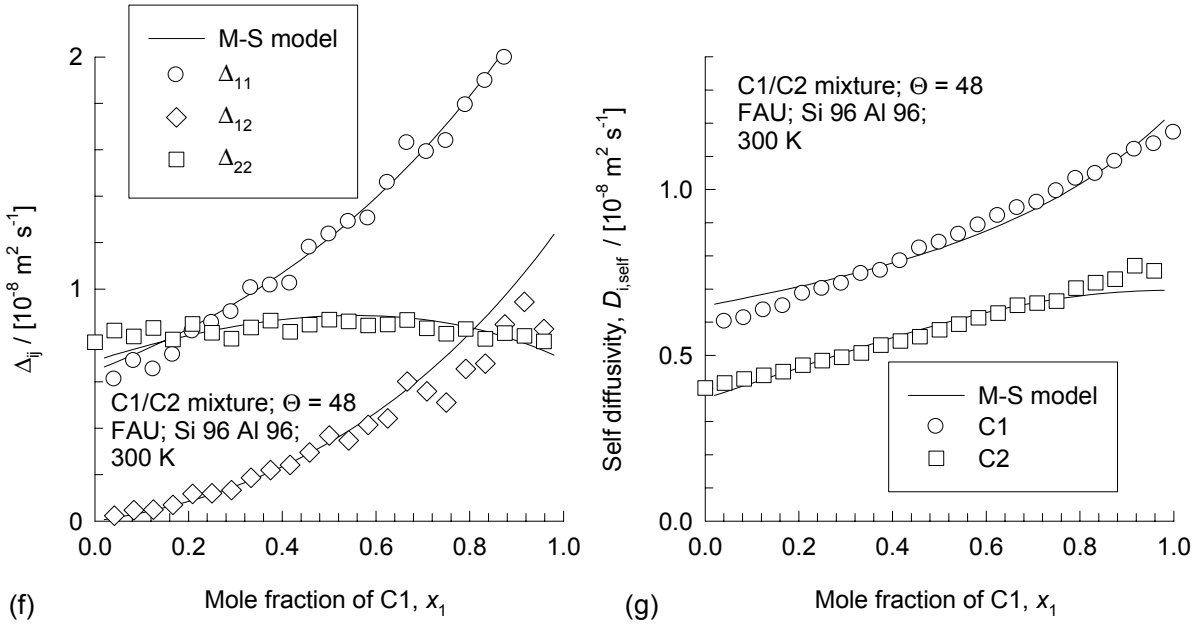

FAU; 300 K; C1/C2 75-25, 50-50, 25-75 binary mixtures; Data on $Đ_i$ and $Đ_{ii}$ backed out from MD simulations

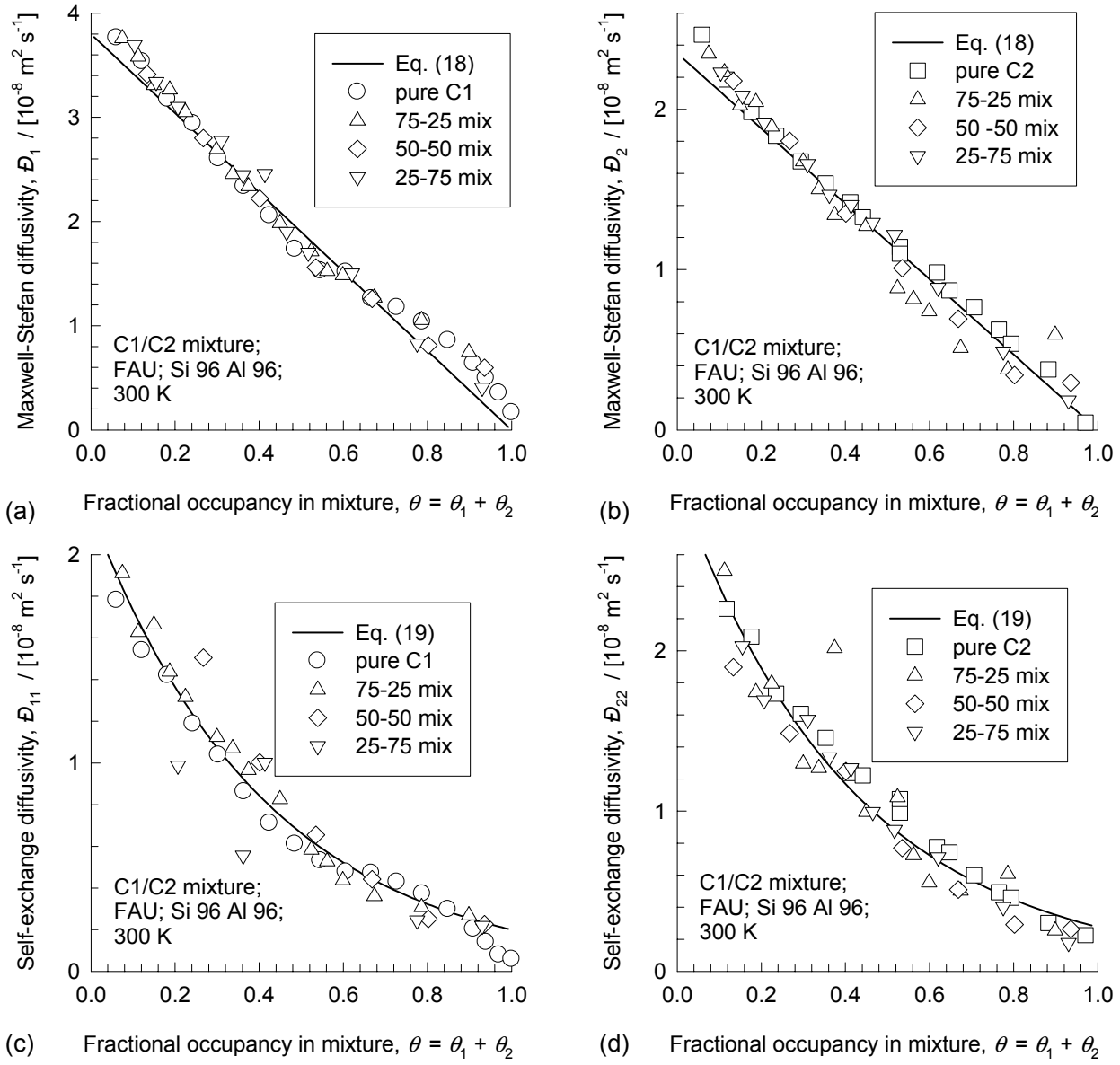

FAU; 300 K; C1/C3 75-25, 50-50, 25-75 mix; varying loadings

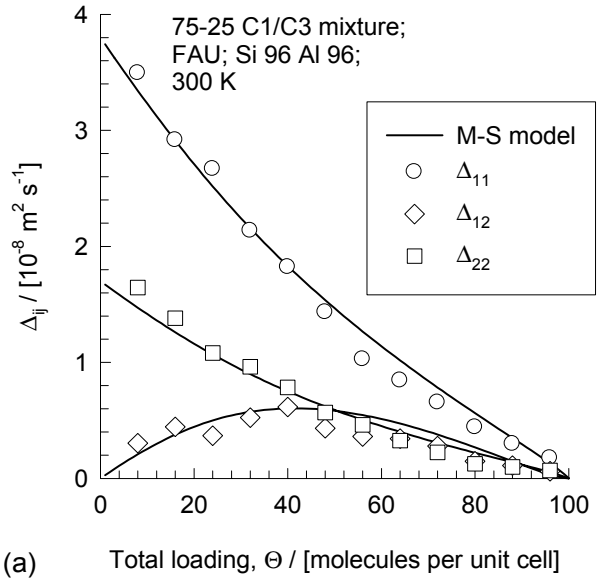

(a)

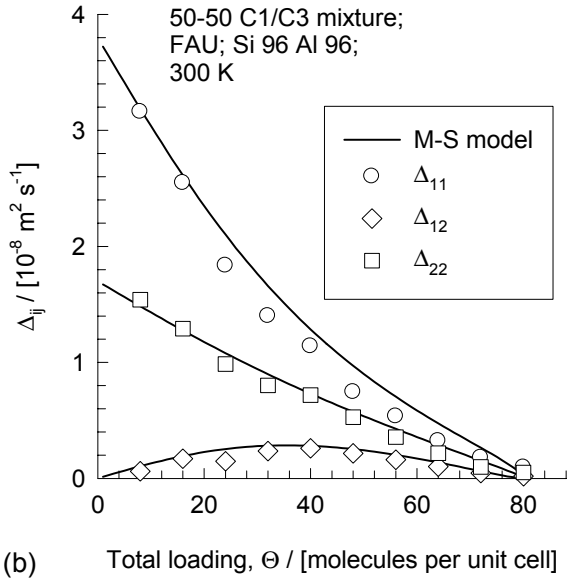

(b)

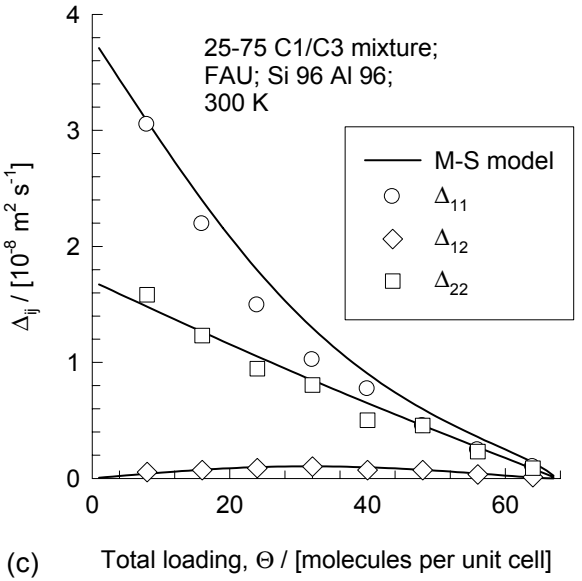

(c)

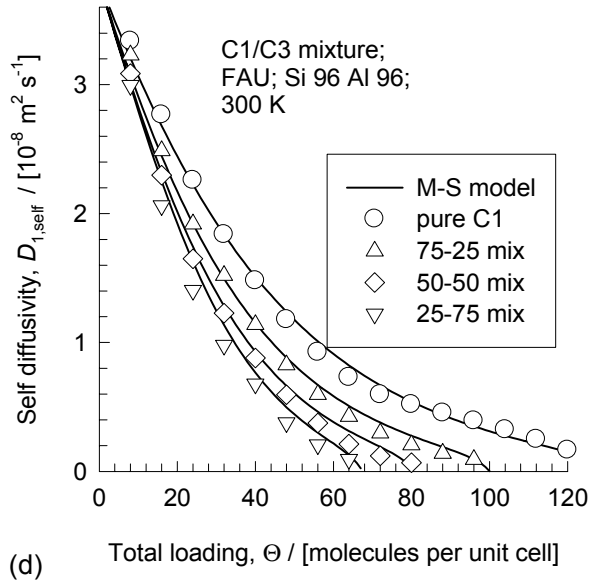

(d)

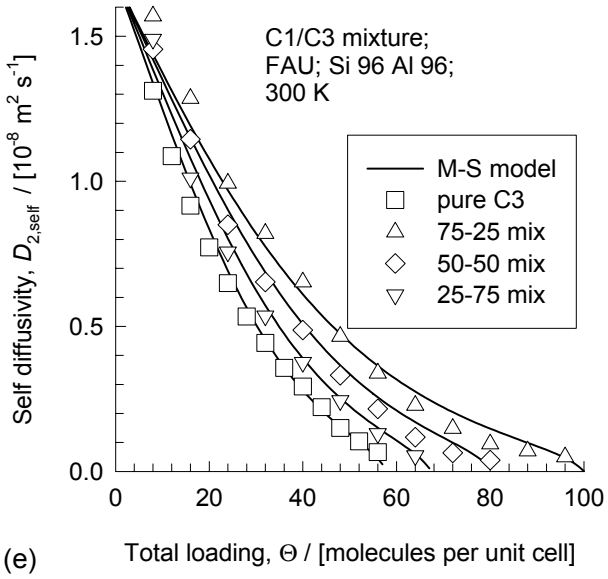

(e)

FAU; 300 K; C1/C3 binary; Θ = 48; varying compositions

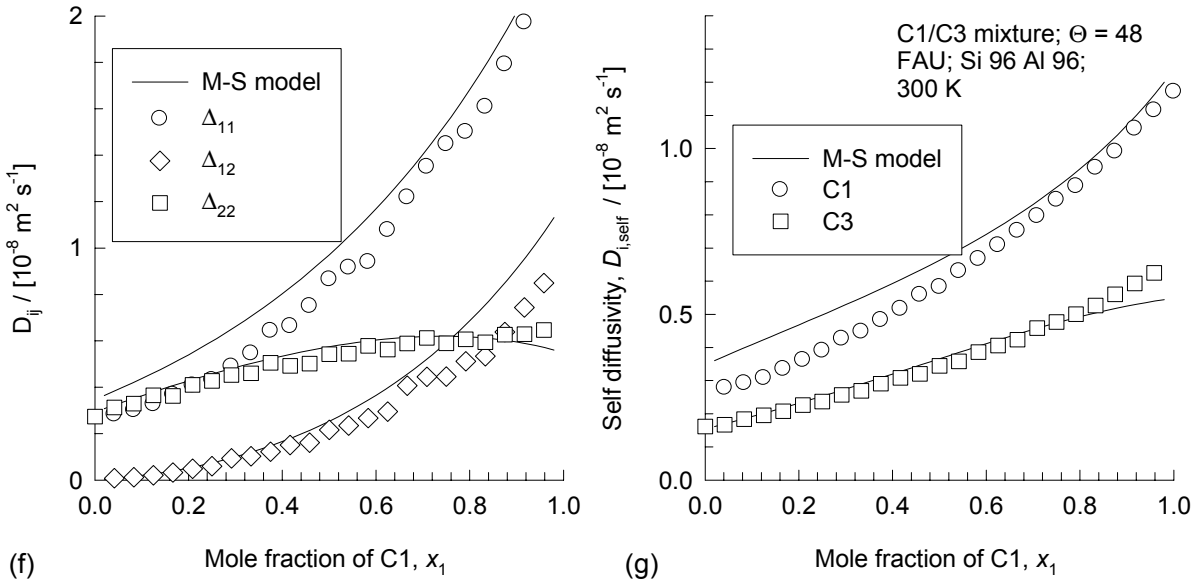

FAU; 300 K; C1/C3 75-25, 50-50, 25-75 binary mixtures; Data on $Đ_i$ and $Đ_{ii}$ backed out from MD simulations

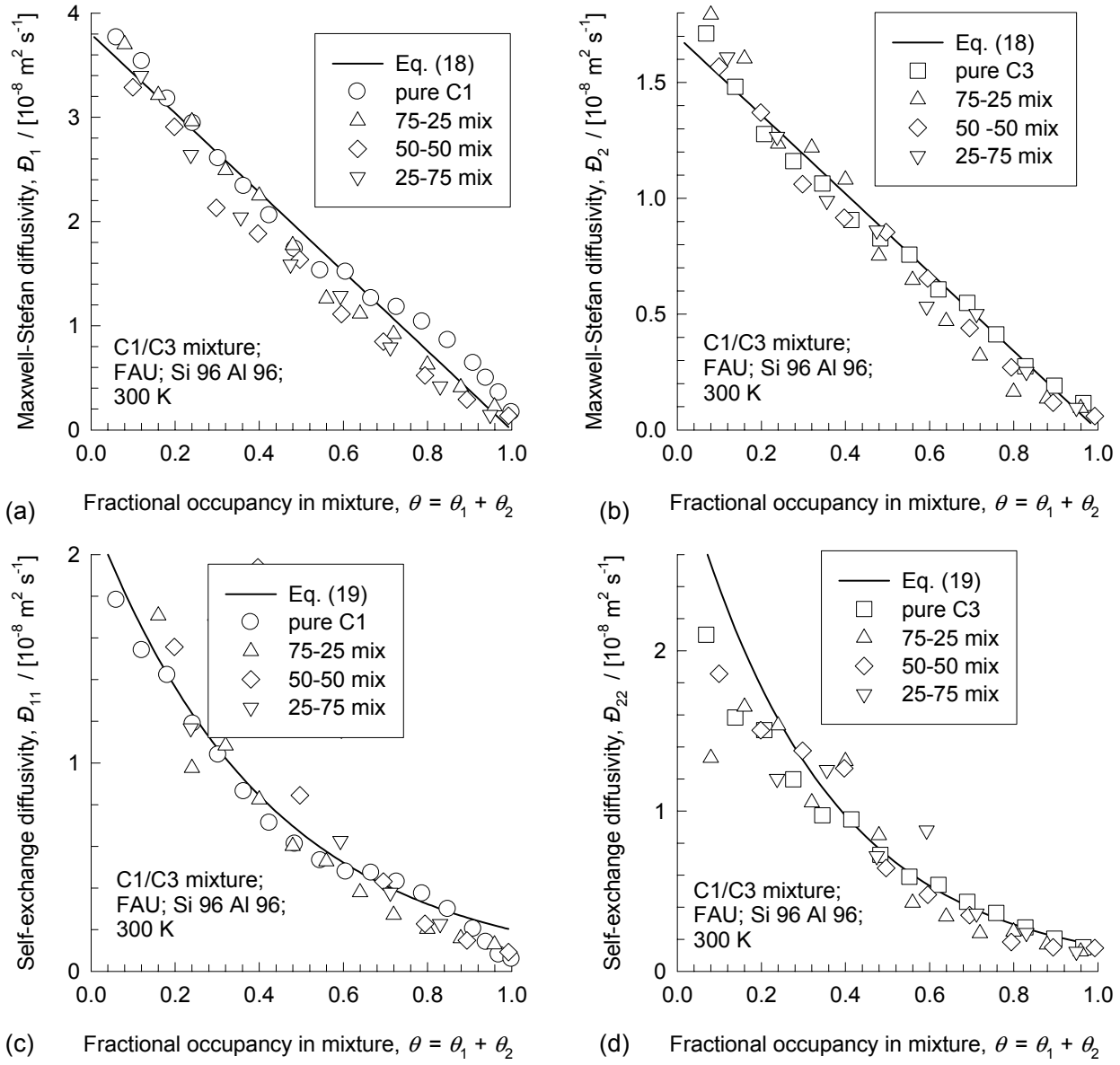

FAU; 300 K; C2/C3 75-25, 50-50, 25-75 mix; varying loadings

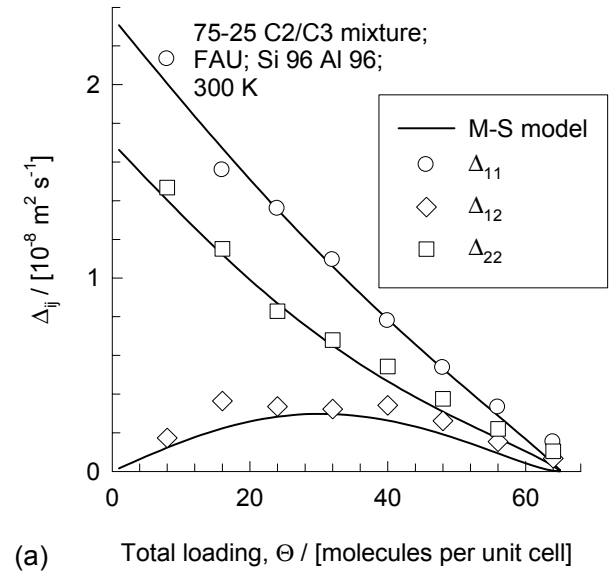

(a)

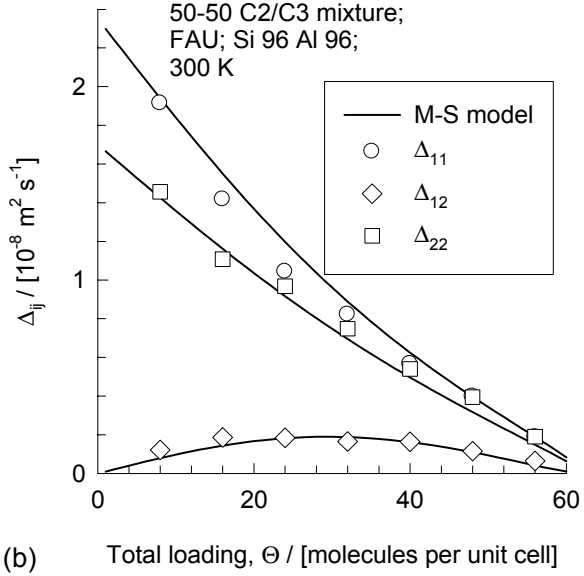

(b)

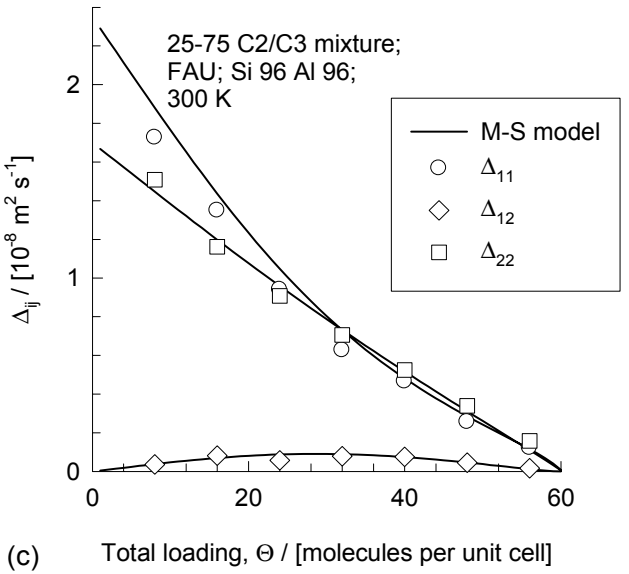

(c)

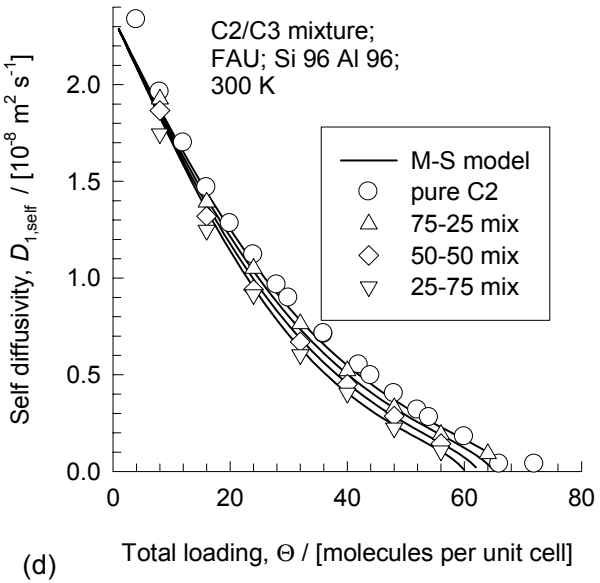

(d)

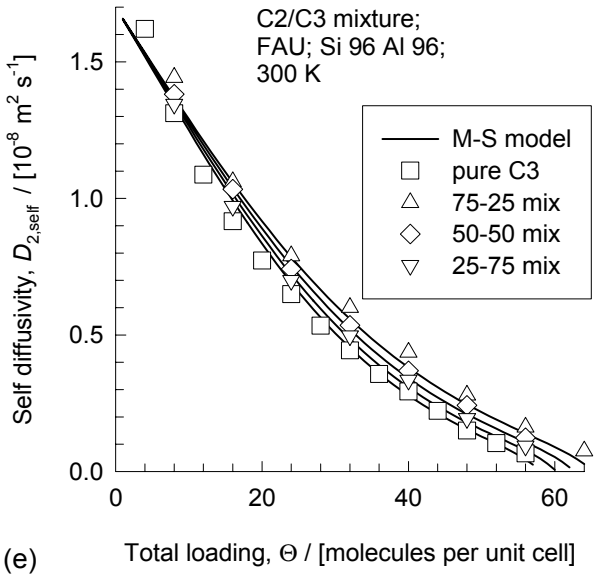

(e)

FAU; 300 K; C2/C3 binary; Θ = 48; varying compositions

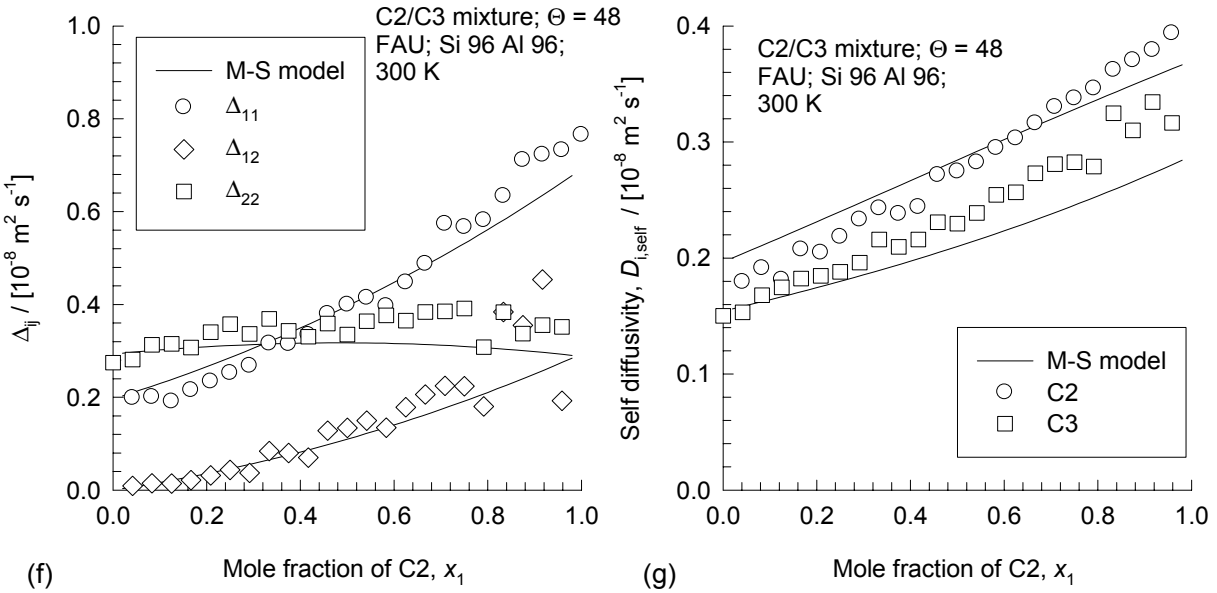

FAU; 300 K; C2/C3 75-25, 50-50, 25-75 binary mixtures; Data on $Đ_i$ and $Đ_{ii}$ backed out from MD simulations

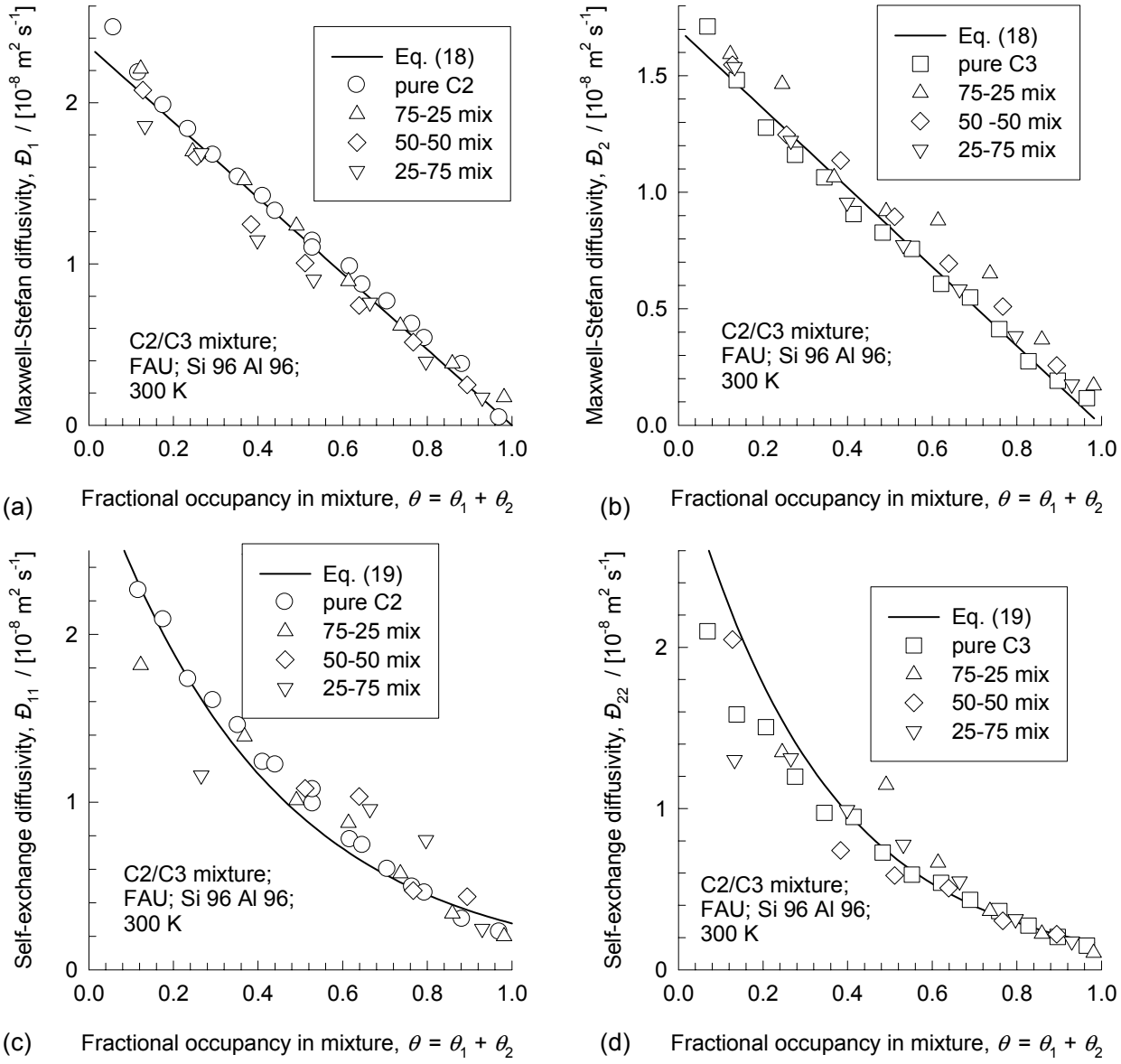

FAU; 300 K; C1/nC4 75-25, 50-50, 25,75 mix; varying loadings

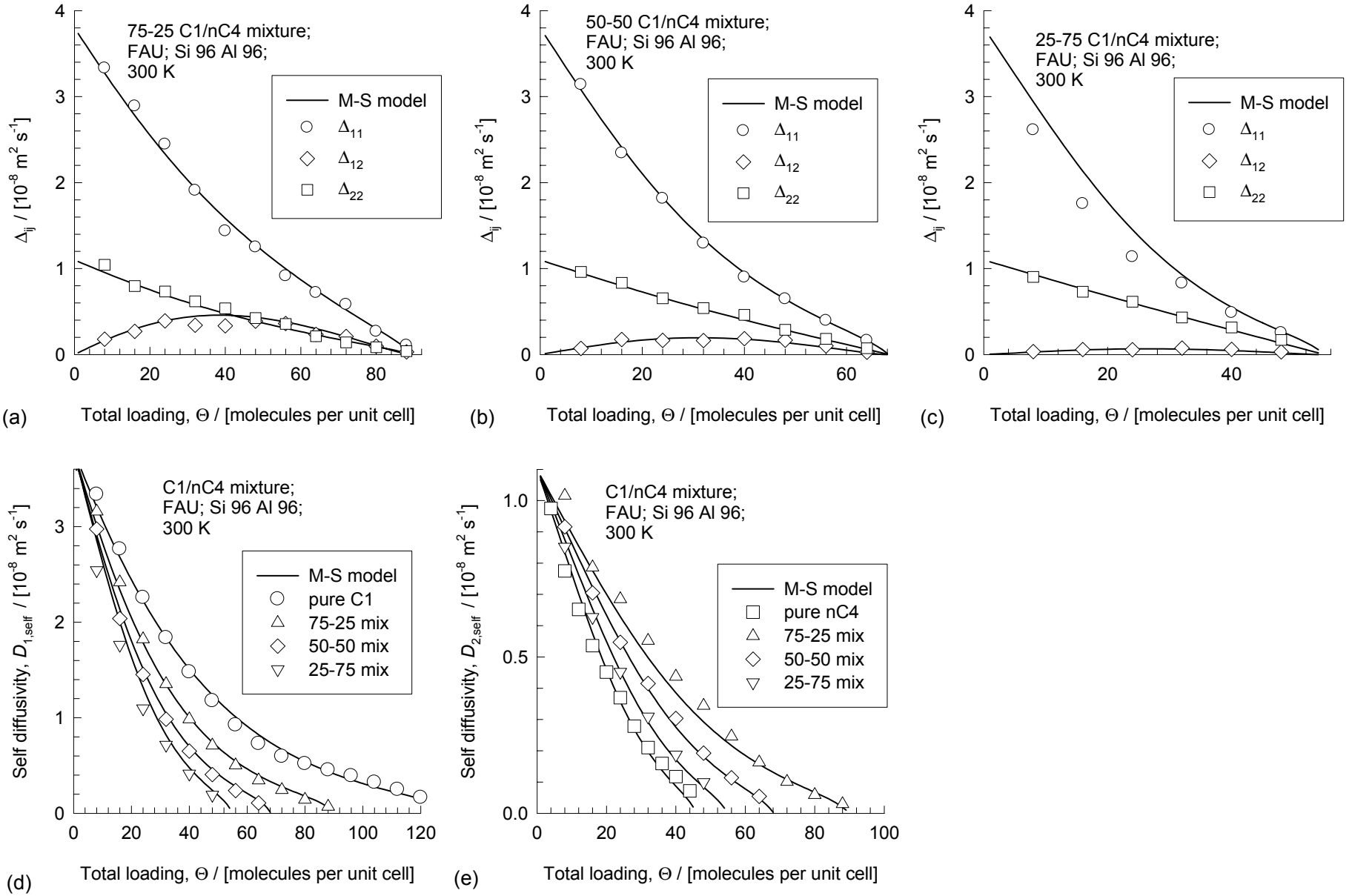

FAU; 300 K; C1/nC4 binary; Θ = 32; varying compositions

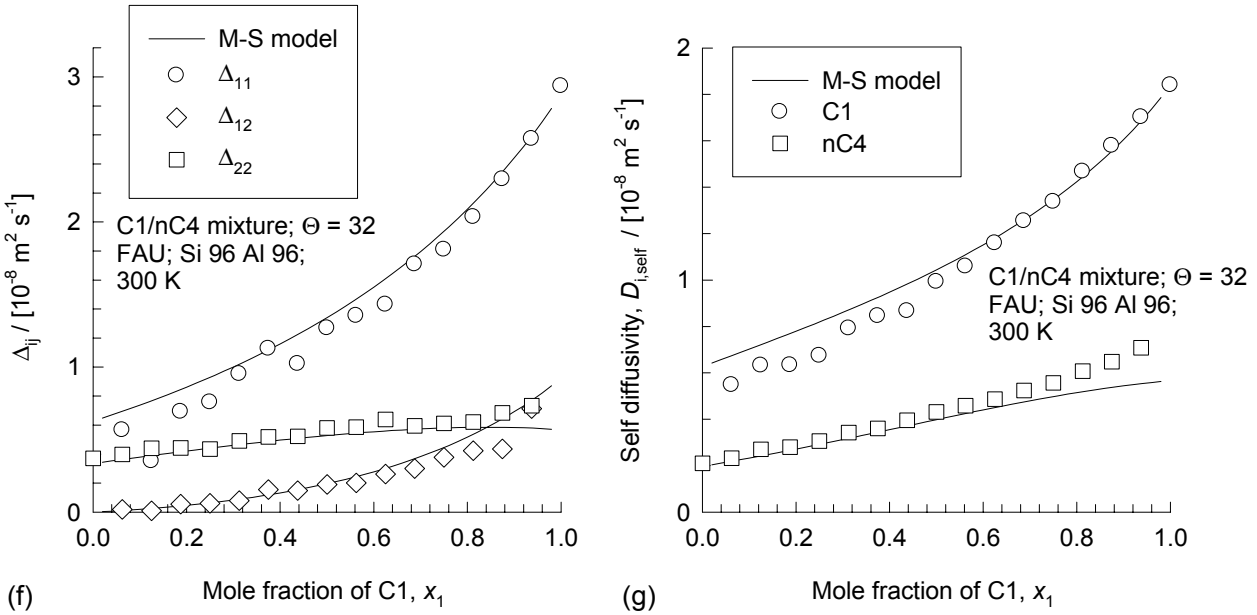

FAU; 300 K; C1/nC4 75-25, 50-50, 25-75 binary mixtures; Data on $Đ_i$ and $Đ_{ii}$ backed out from MD simulations

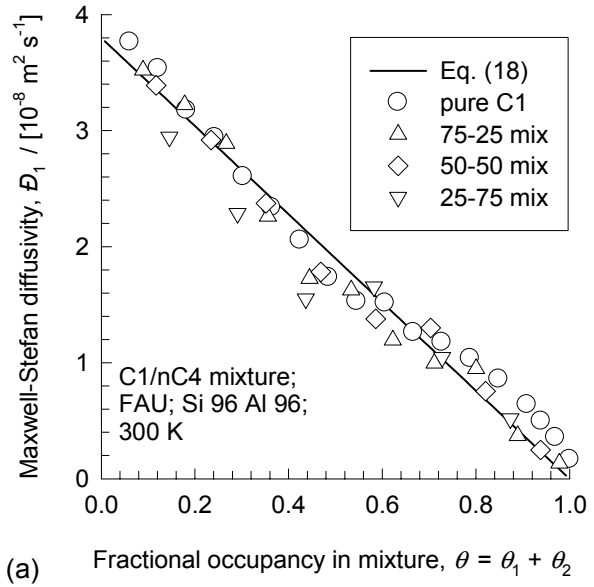

(a)

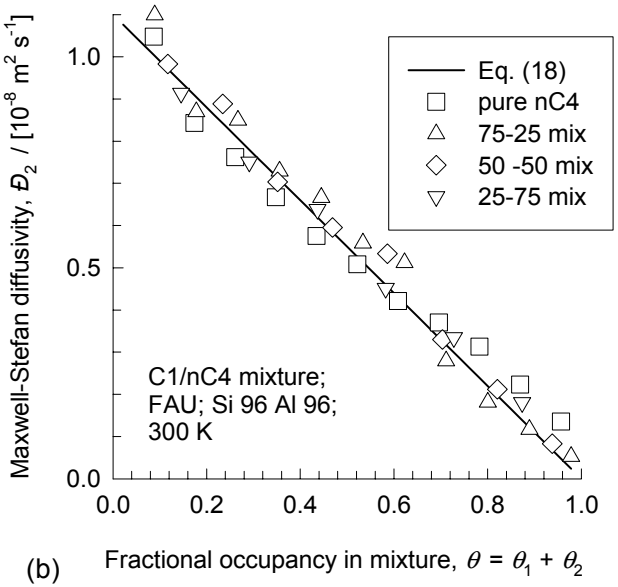

(b)

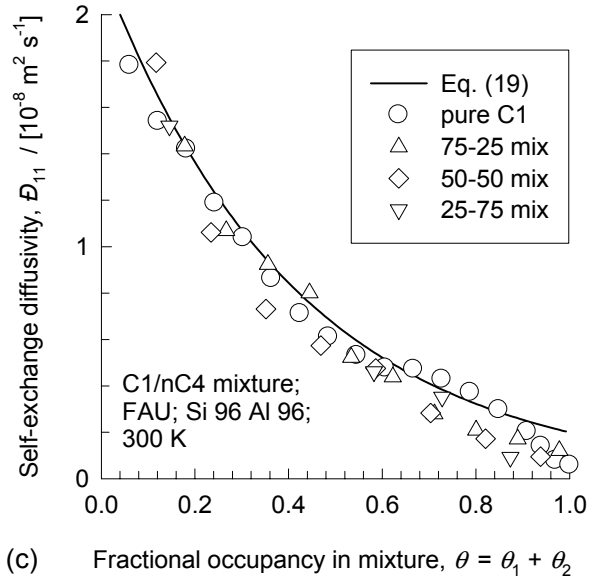

(c)

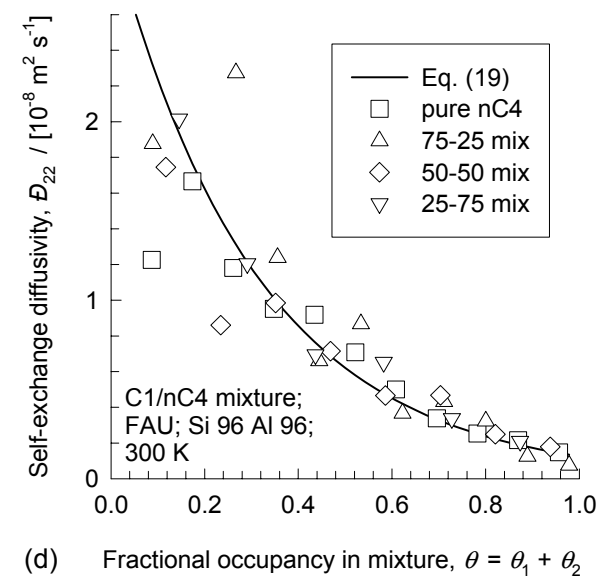

(d)

FAU; 300 K; C1/C2/C3 equimolar ternary; varying loadings

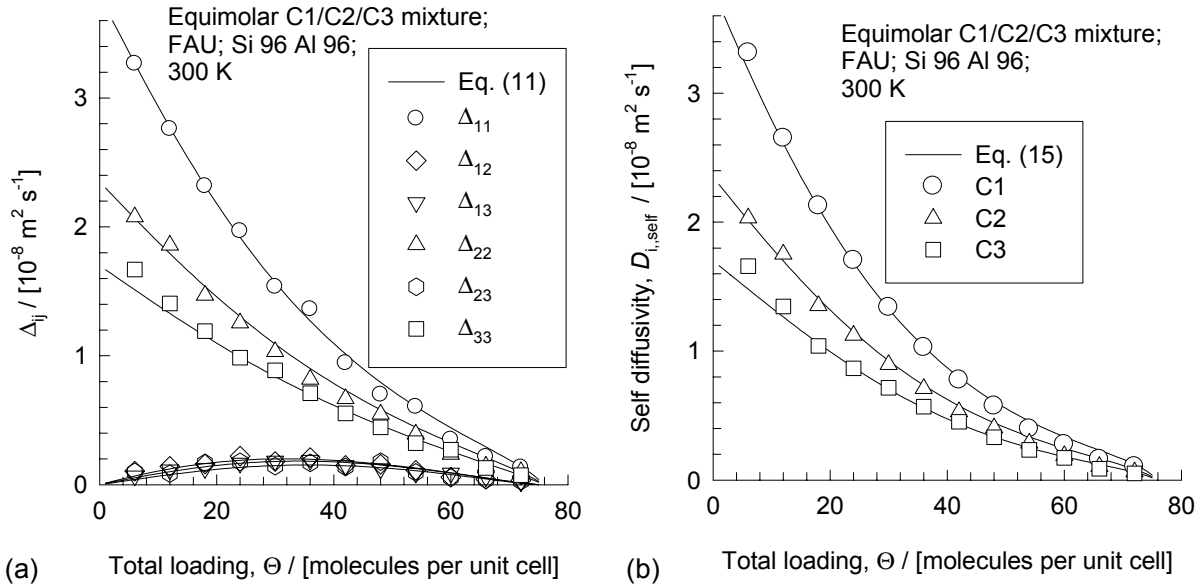

FAU; 300 K; C1/C2/C3 ternary; Θ = 48; varying compositions

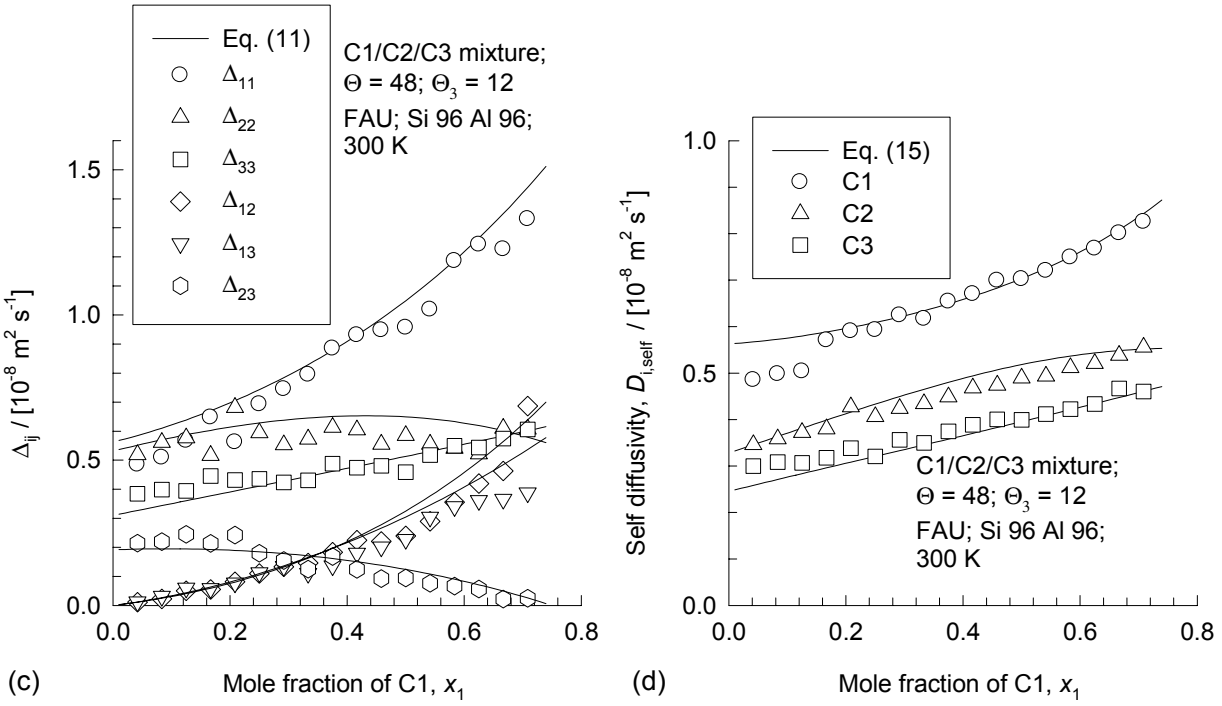

FAU; 300 K; pure, binary and ternary; C1, C2, C3
Data on $Đ_i$ and $Đ_{ii}$ backed out from all MD simulations

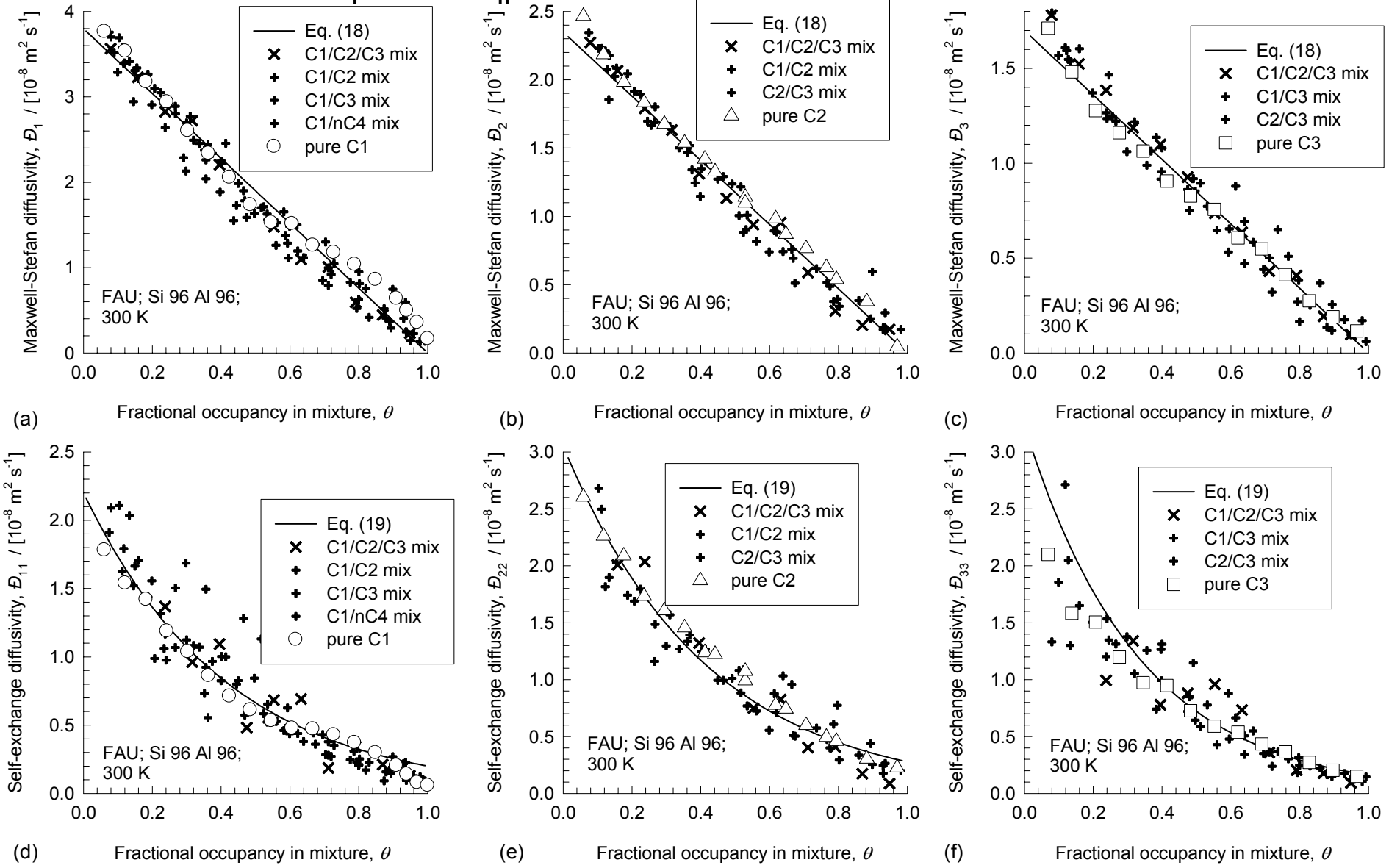

FAU; 300 K; nC4/iC4, 50-50 mix; varying loadings

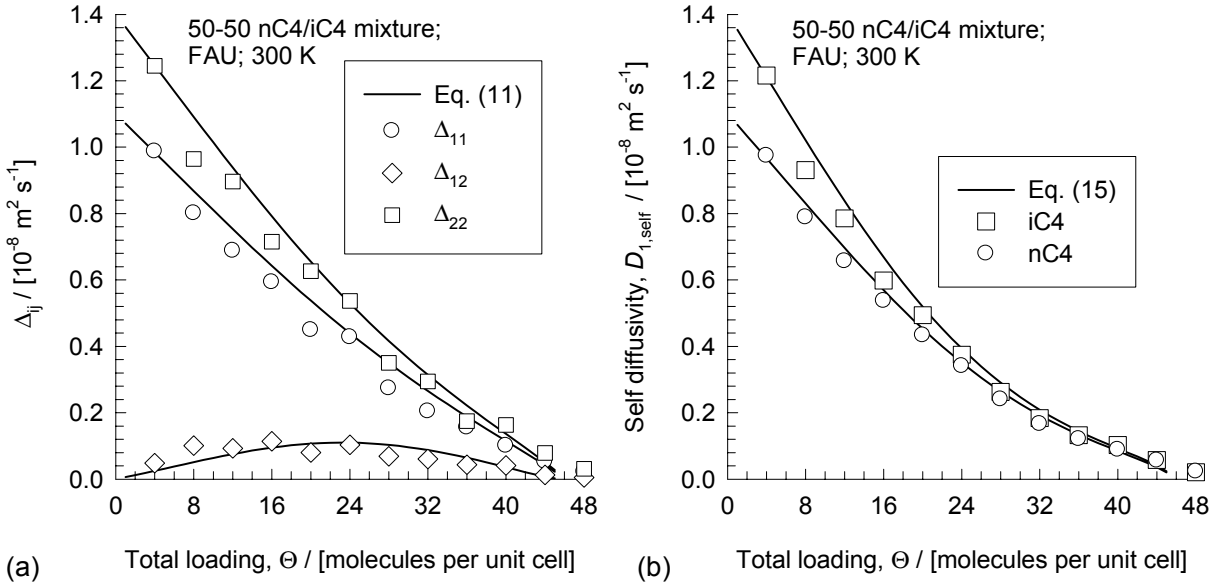

It is noteworthy that iC4 diffuses faster than nC4 In FAU

FAU; 300 K; nC4/iC4 50-50 binary mixture; Data on $Đ_i$ and $Đ_{ii}$ backed out from MD simulations

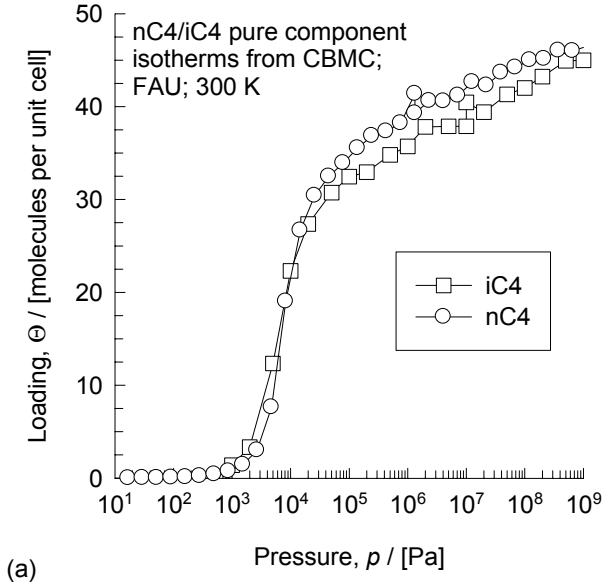

(a)

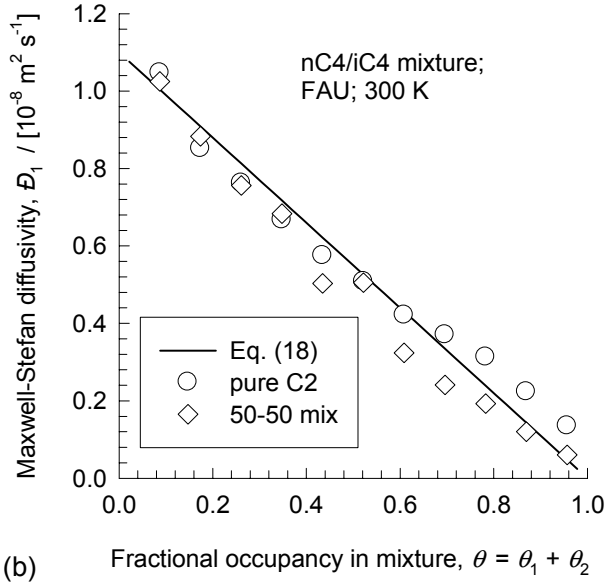

(b)

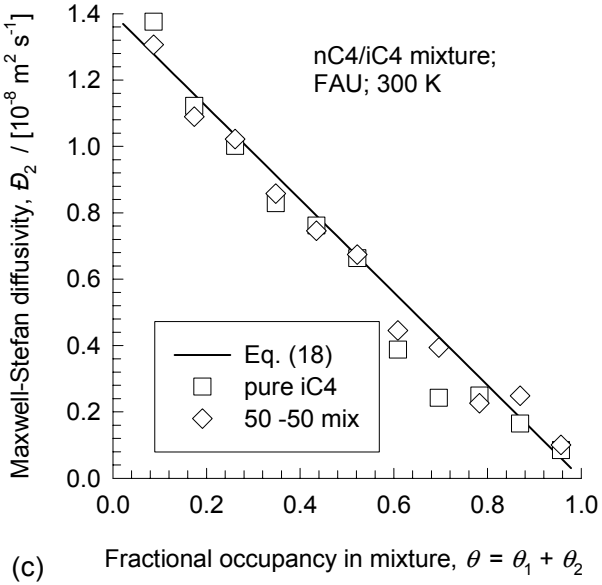

(c)

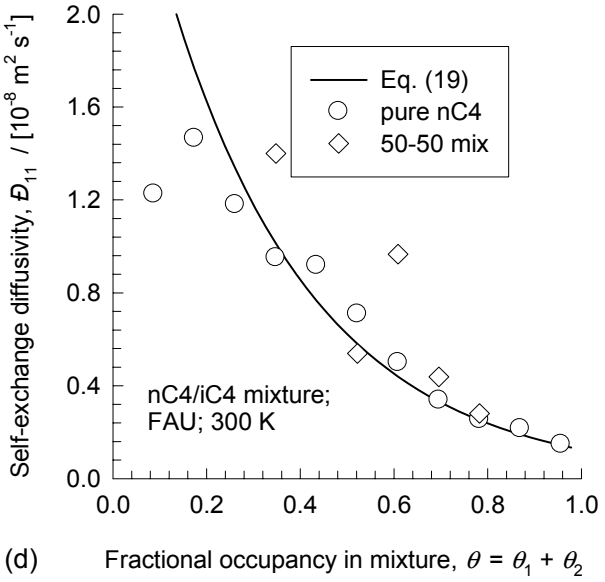

(d)

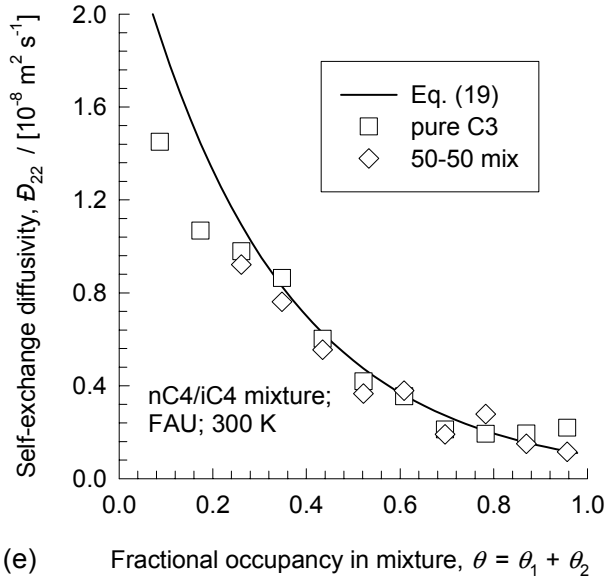

(e)

It is noteworthy that iC4 diffuses faster than nC4 In FAU

FAU; 300 K; C1/C2/C3/nC4 equimolar quaternary; varying loadings

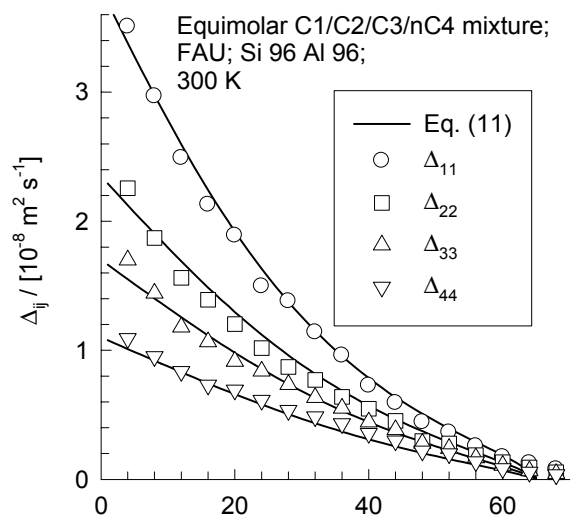

(a)

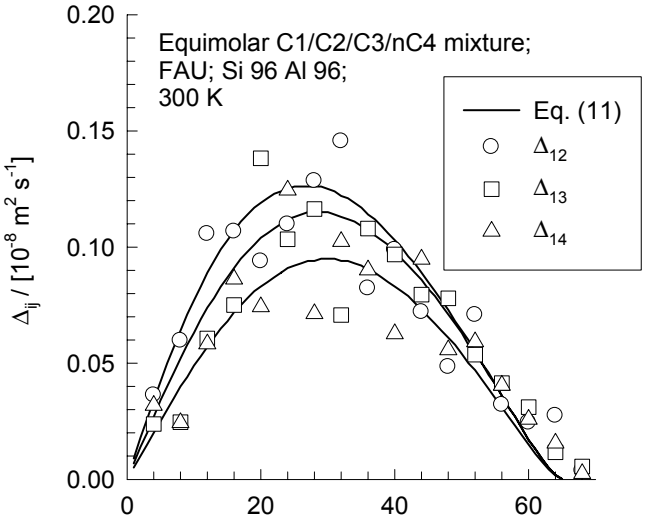

(b)

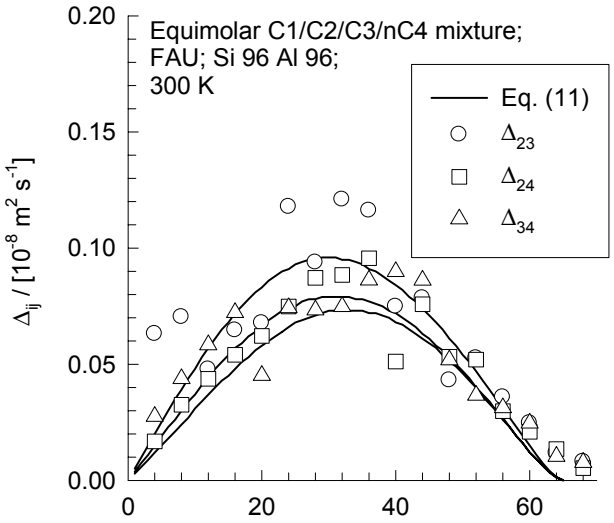

(c)

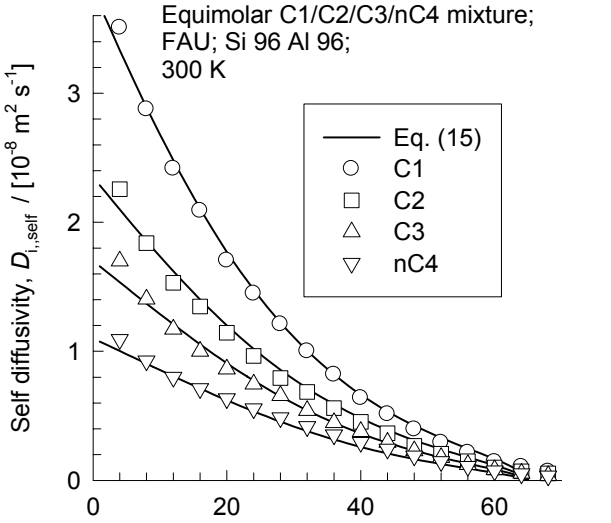

(d)

MFI; 300 K; pure component isotherms and diffusion data for C1, C2 and C3

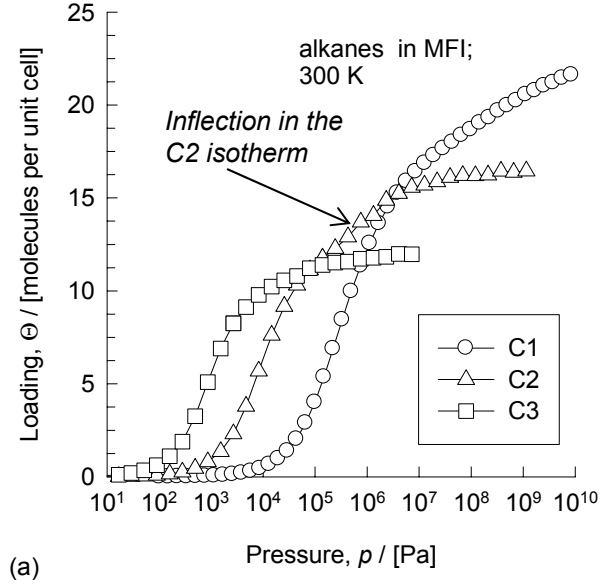

(a)

Note the inflection in the diffusion of C2

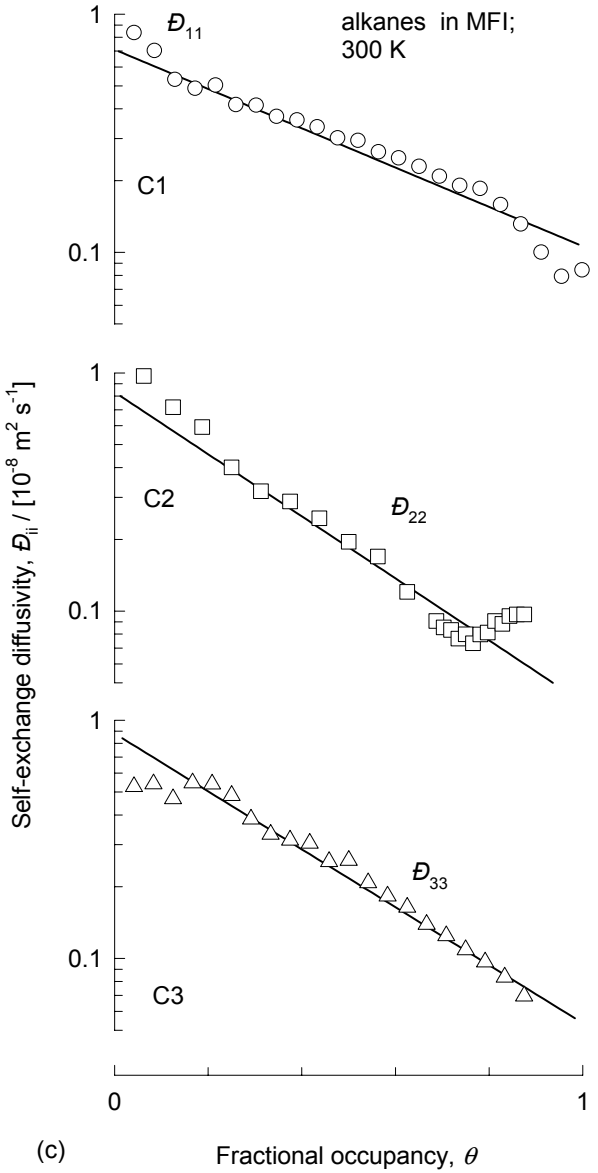

(c)

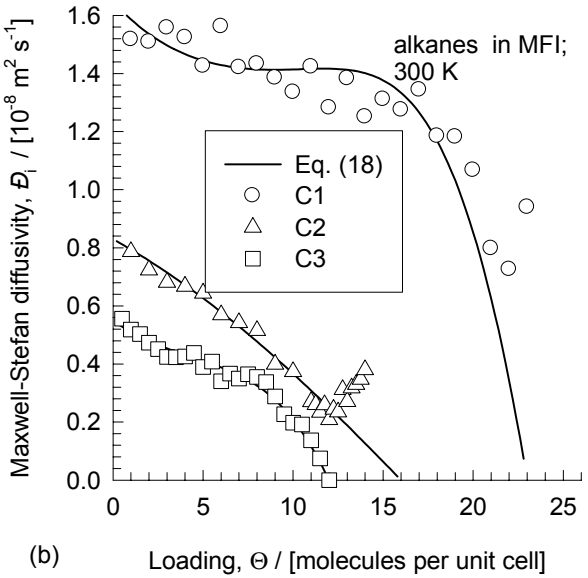

(b)

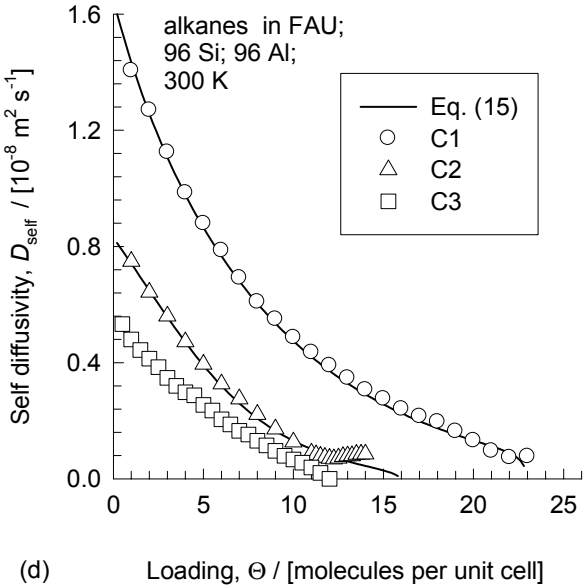

(d)

MFI; 300 K; C2/C3 75-25, 50-50, 25-75 mix; varying loadings

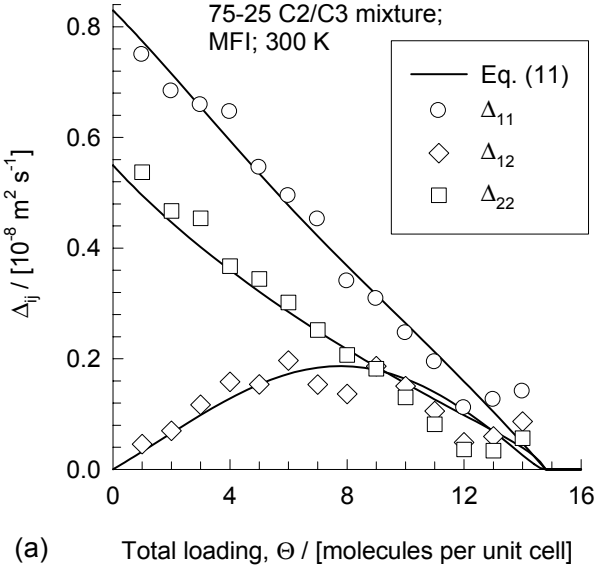

(a)

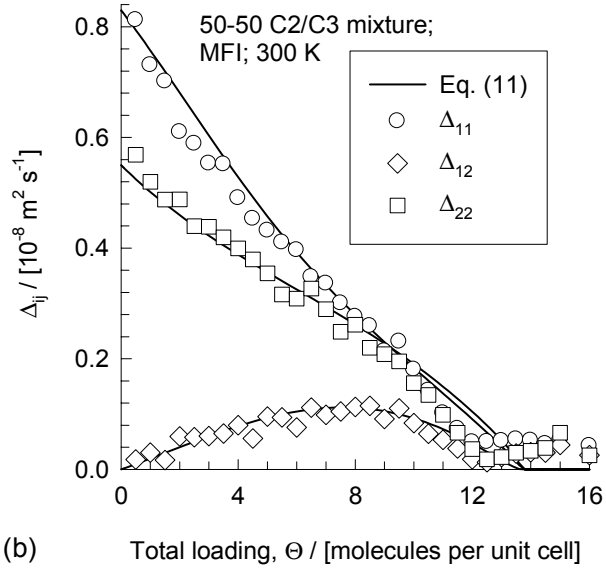

(b)

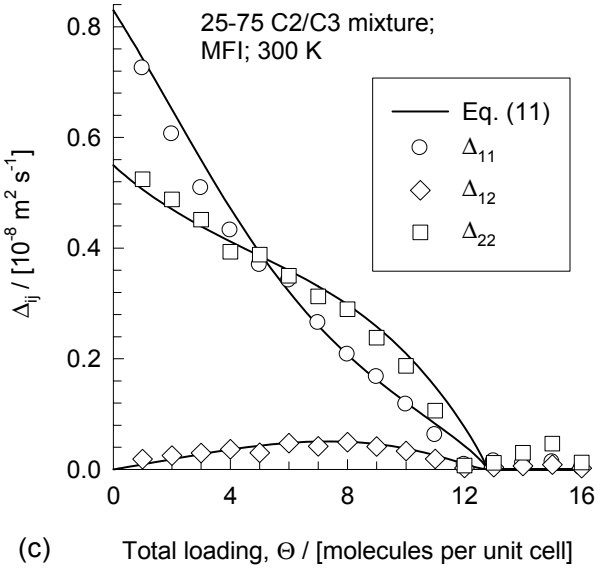

(c)

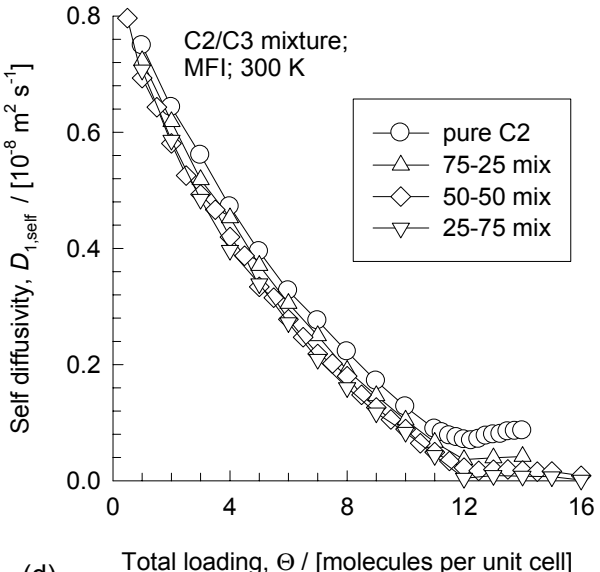

(d)

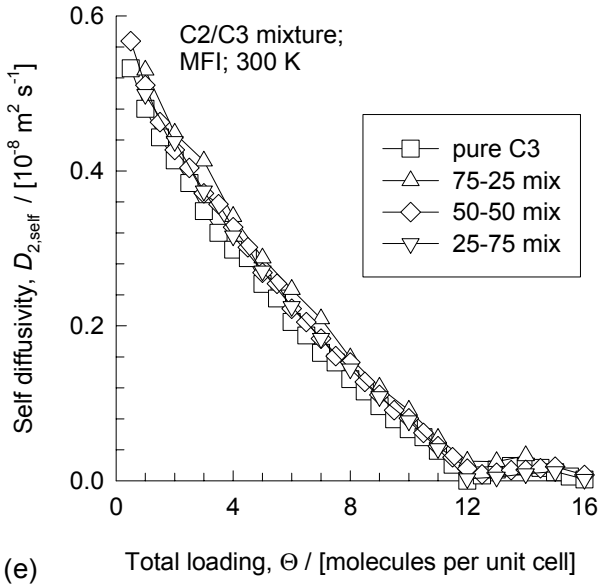

(e)

MFI; 300 K; C2/C3 binary; Θ = 8; varying compositions

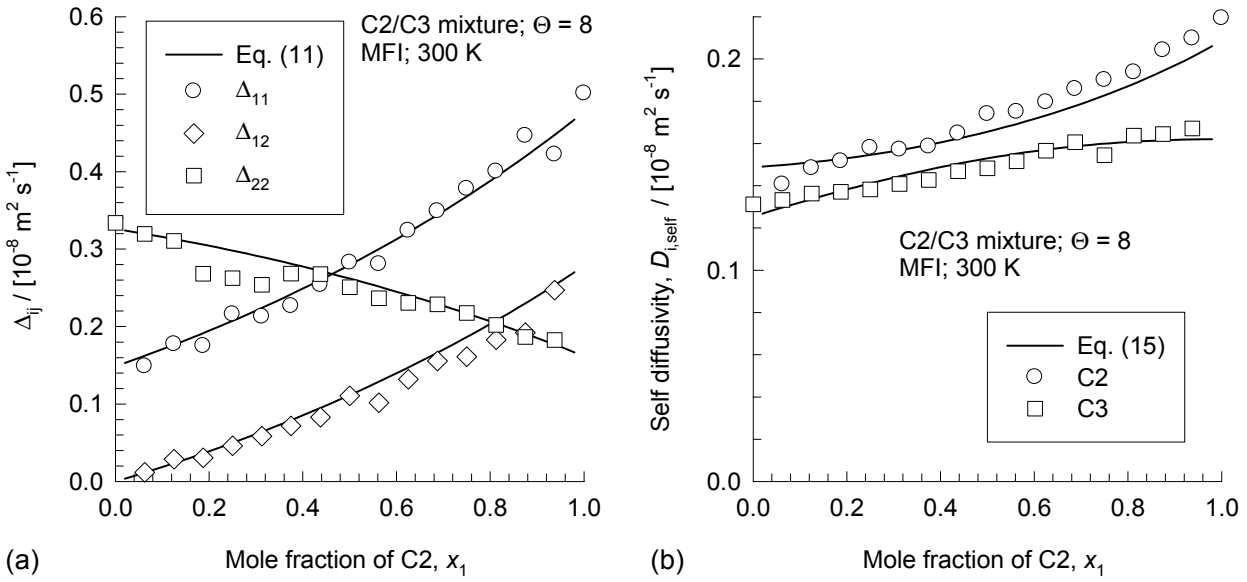

MFI; 300 K; C2/C3 75-25, 50-50, 25-75 binary mixtures; Data on $Đ_i$ and $Đ_{ii}$ backed out from MD simulations

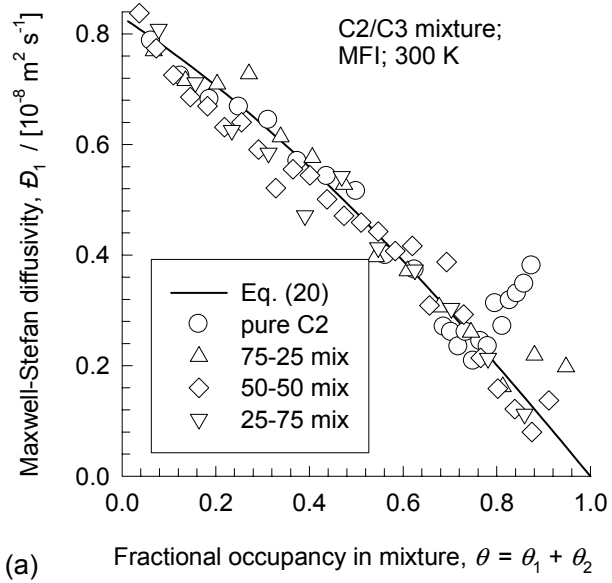

(a)

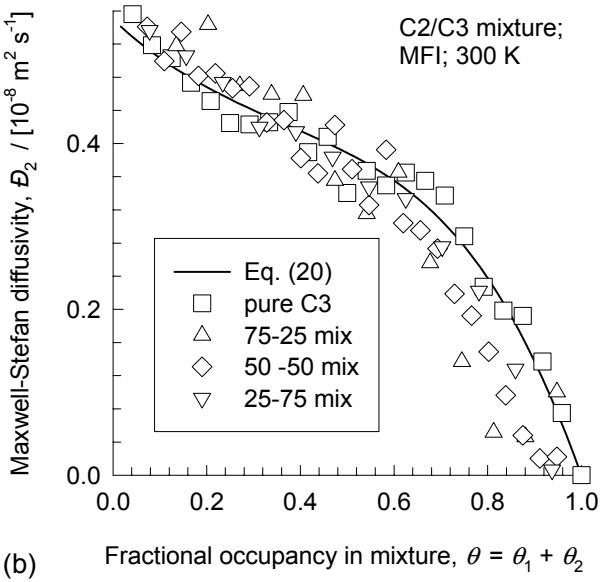

(b)

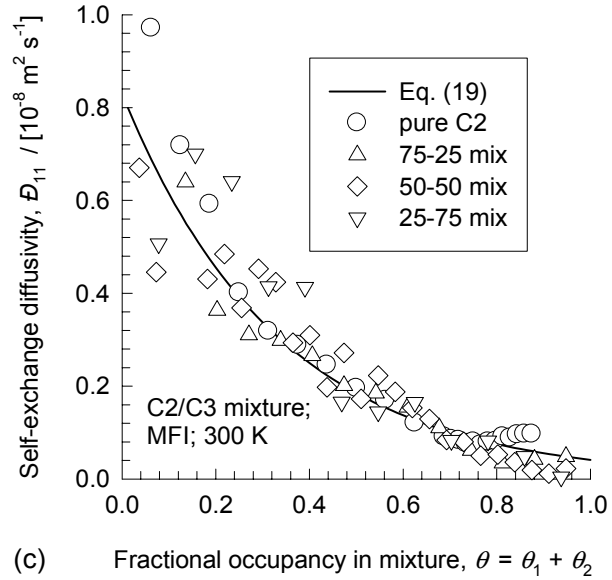

(c)

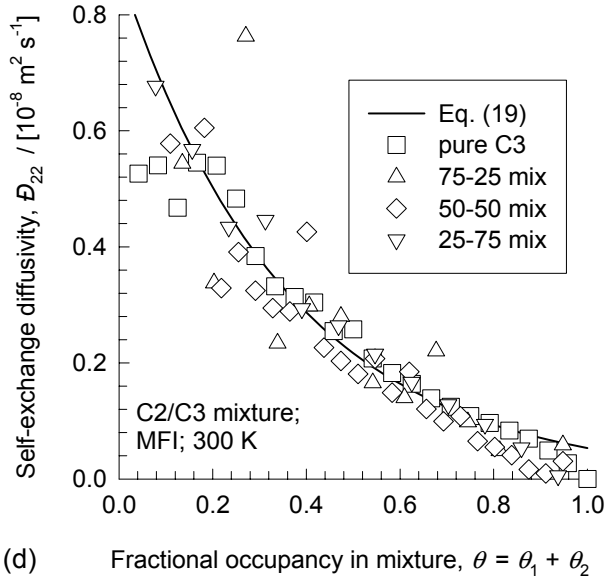

(d)

MFI; 300 K; C1/C2 75-25, 50-50, 25-75 mix; varying loadings

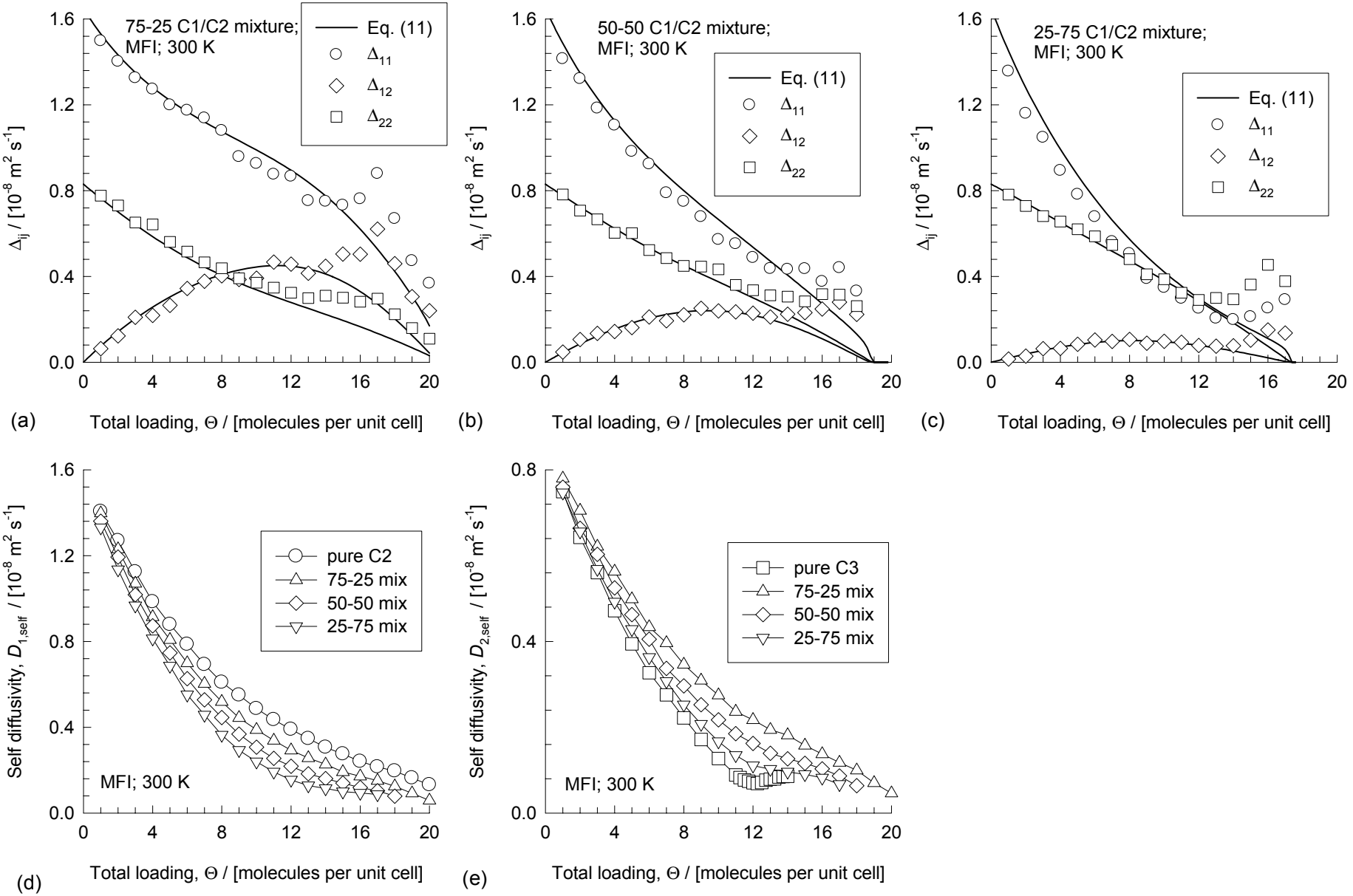

MFI; 300 K; C1/C2 binary; Θ = 8; varying compositions

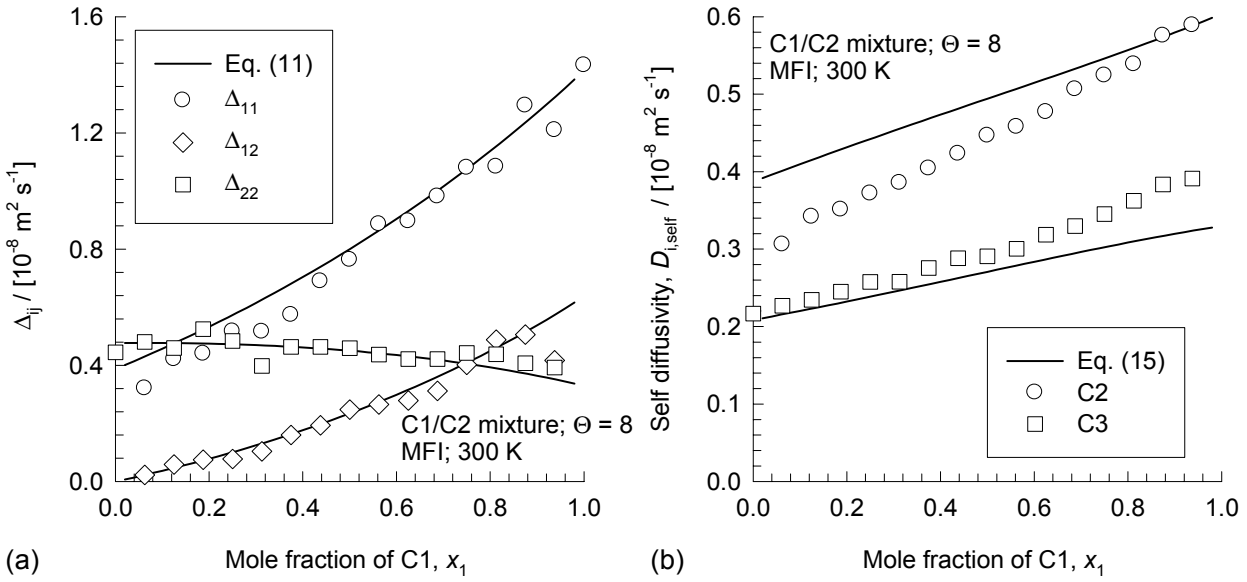

MFI; 300 K; C1/C2 75-25, 50-50, 25-75 binary mixtures; Data on $Đ_i$ and $Đ_{ii}$ backed out from MD simulations

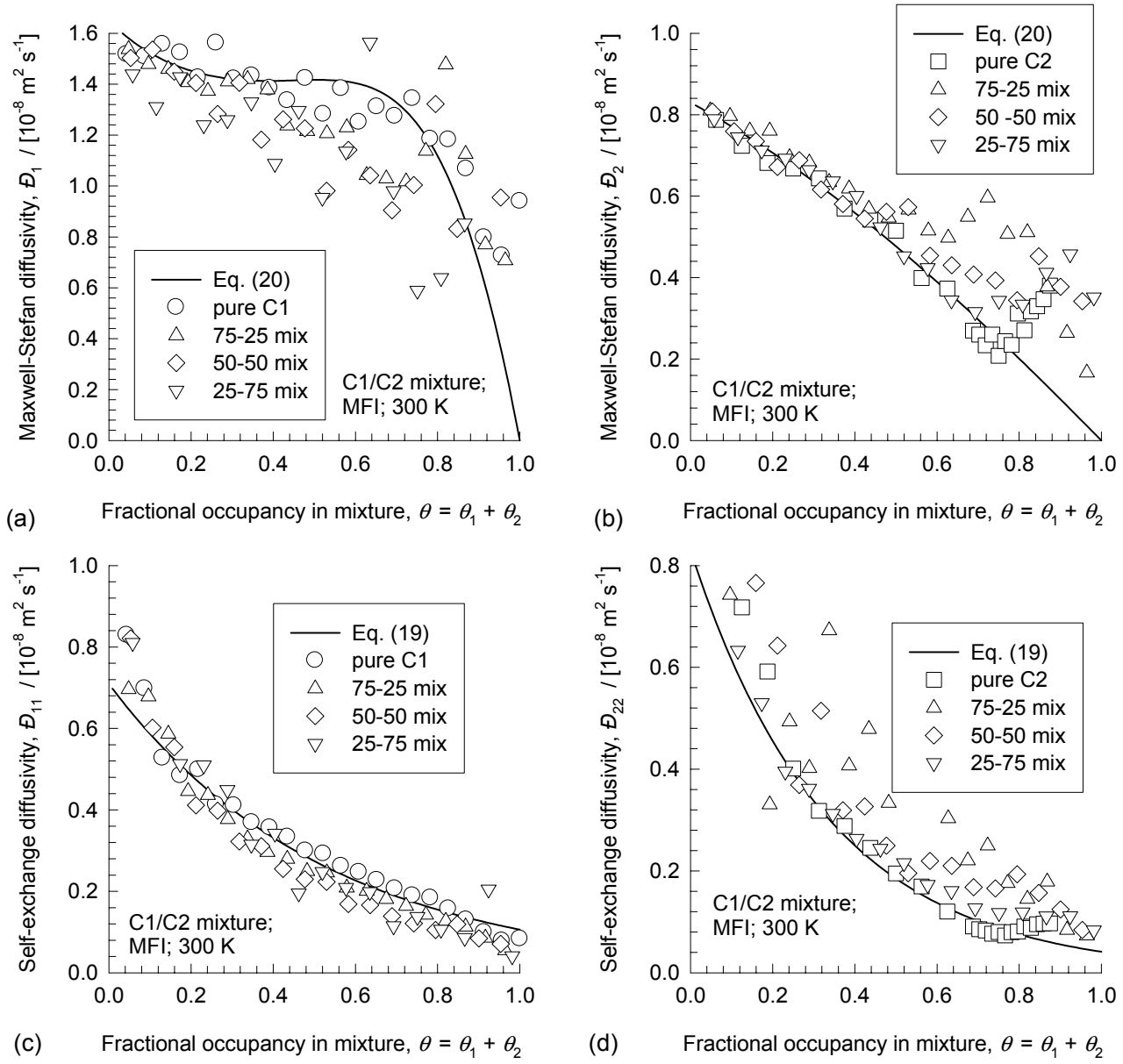

MFI; 300 K; C1/C3 75-25, 50-50, 25-75 mix; varying loadings

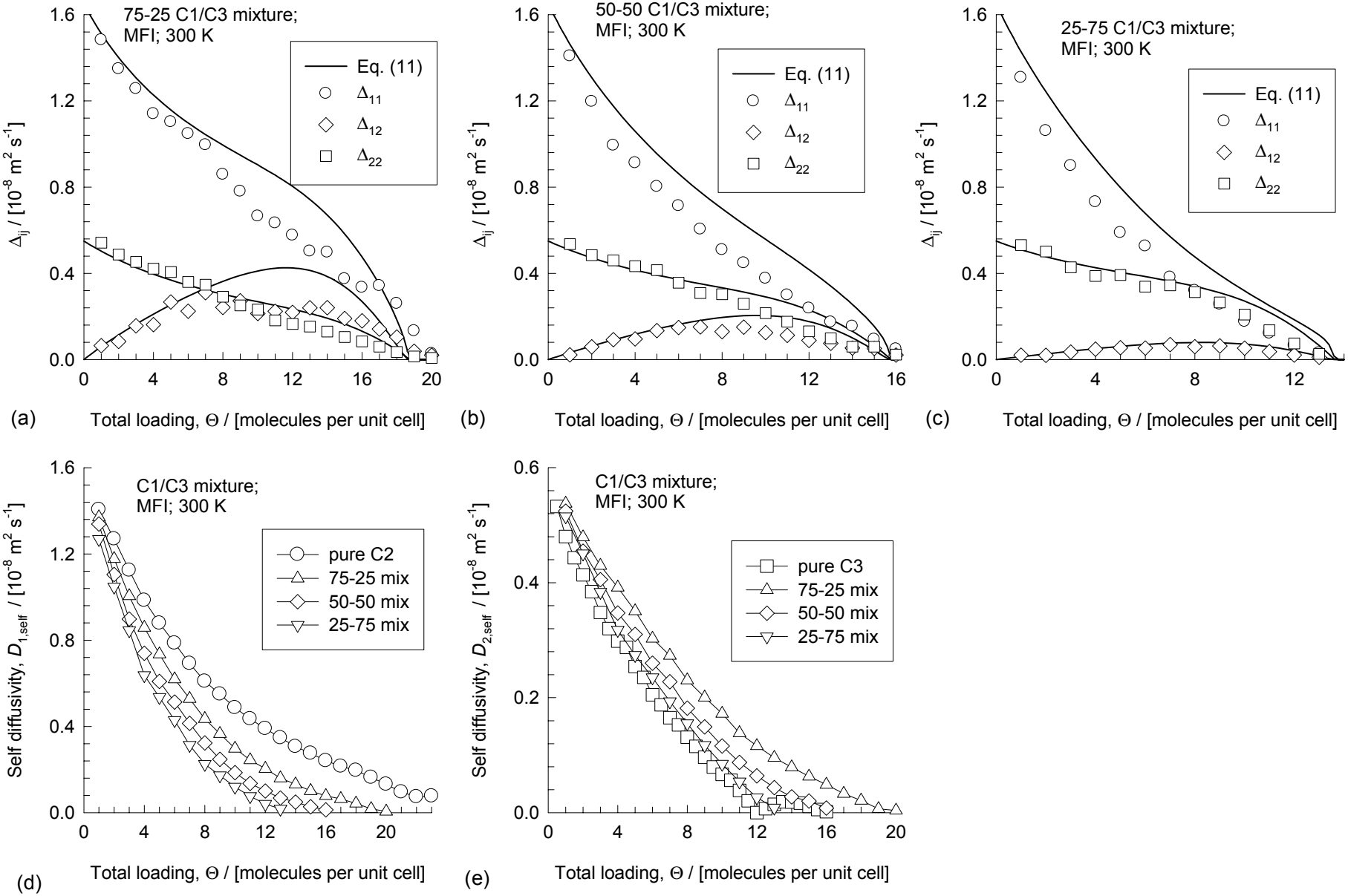

MFI; 300 K; C1/C3 binary; Θ = 8; varying compositions

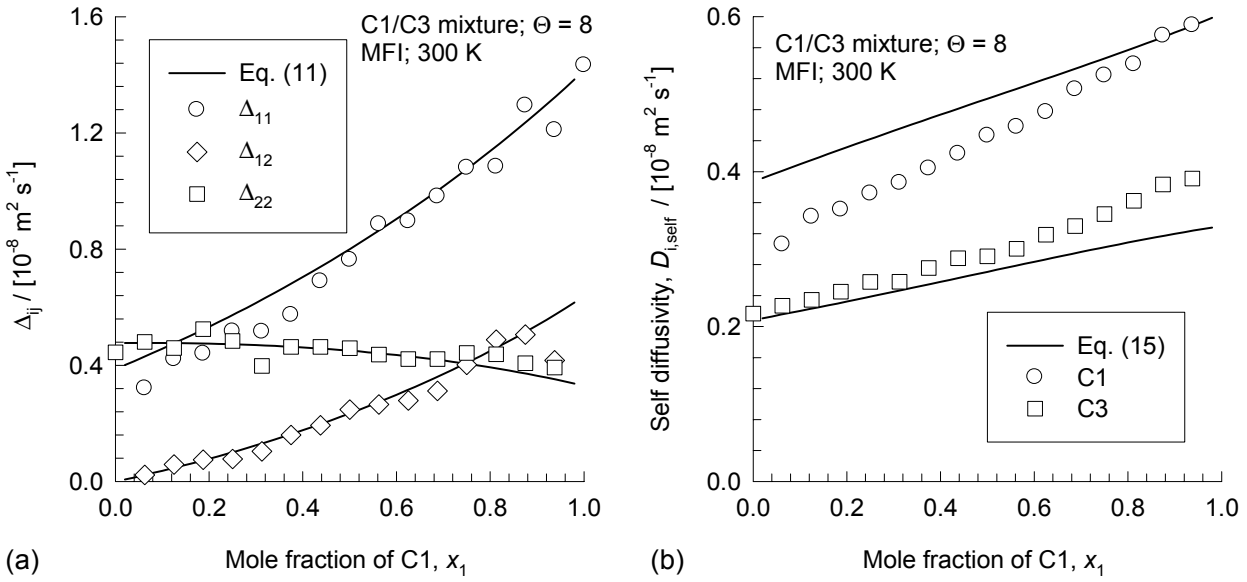

MFI; 300 K; C1/C3 75-25, 50-50, 25-75 binary mixtures; Data on $Đ_i$ and $Đ_{ii}$ backed out from MD simulations

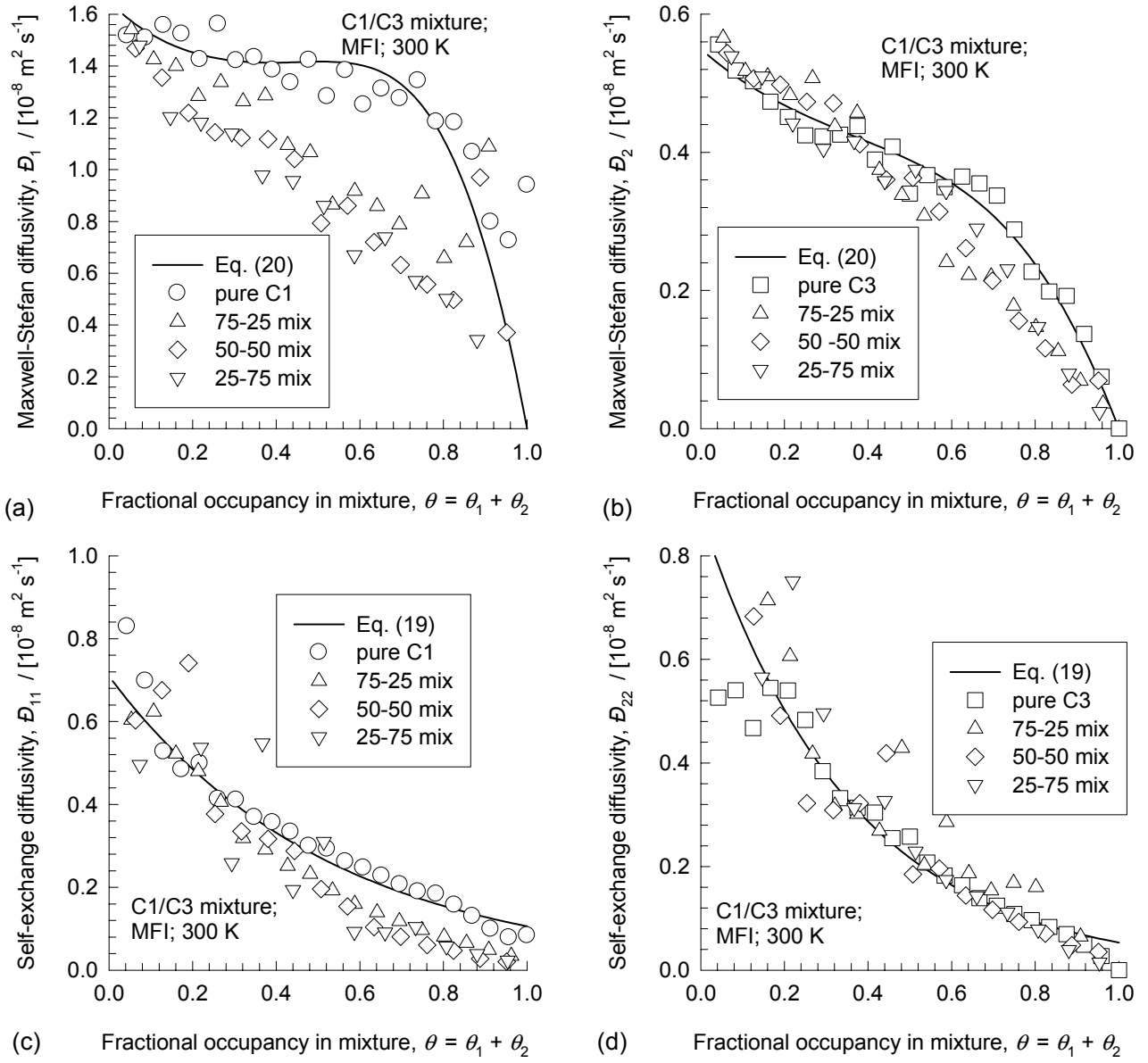

MFI; 300 K; C1/C2/C3 equimolar ternary mix; varying loadings

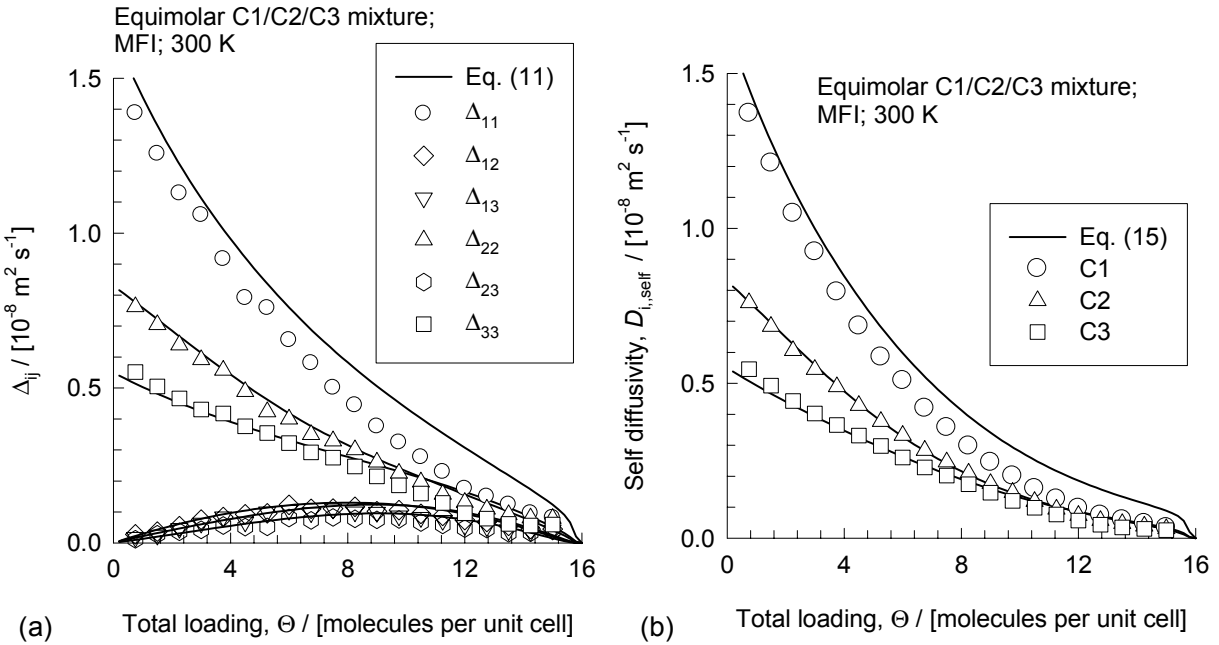

MFI; 373 K; C1/nC4 75-25, 50-50, 25-75 mix; varying loadings

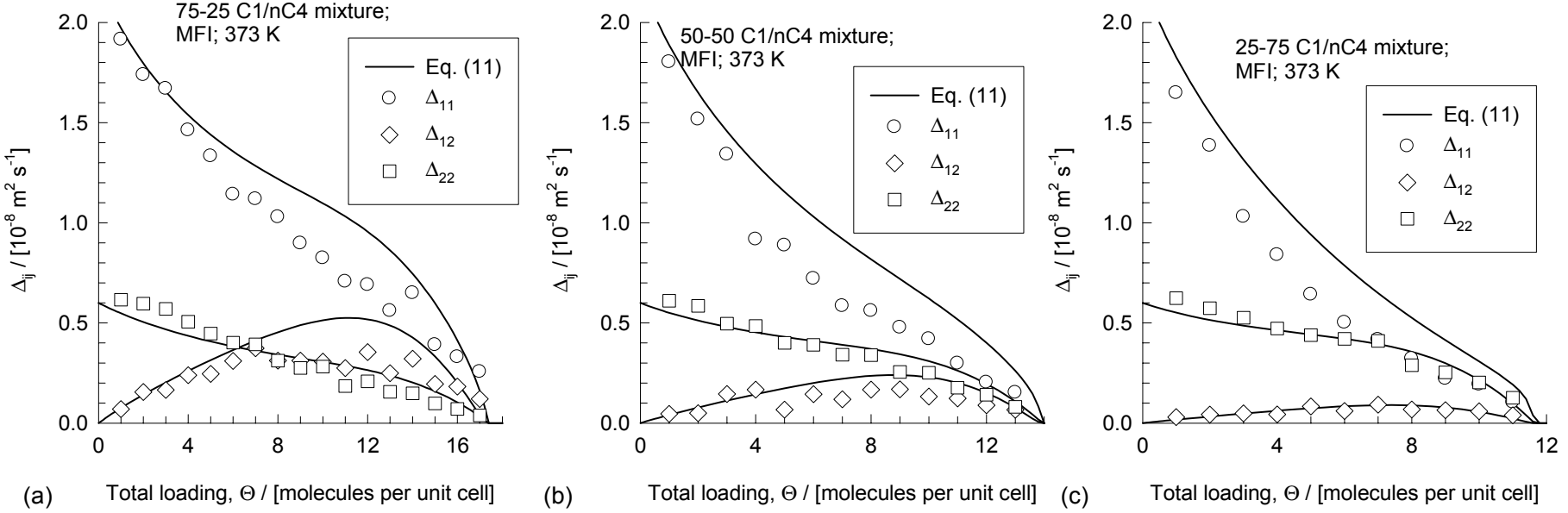

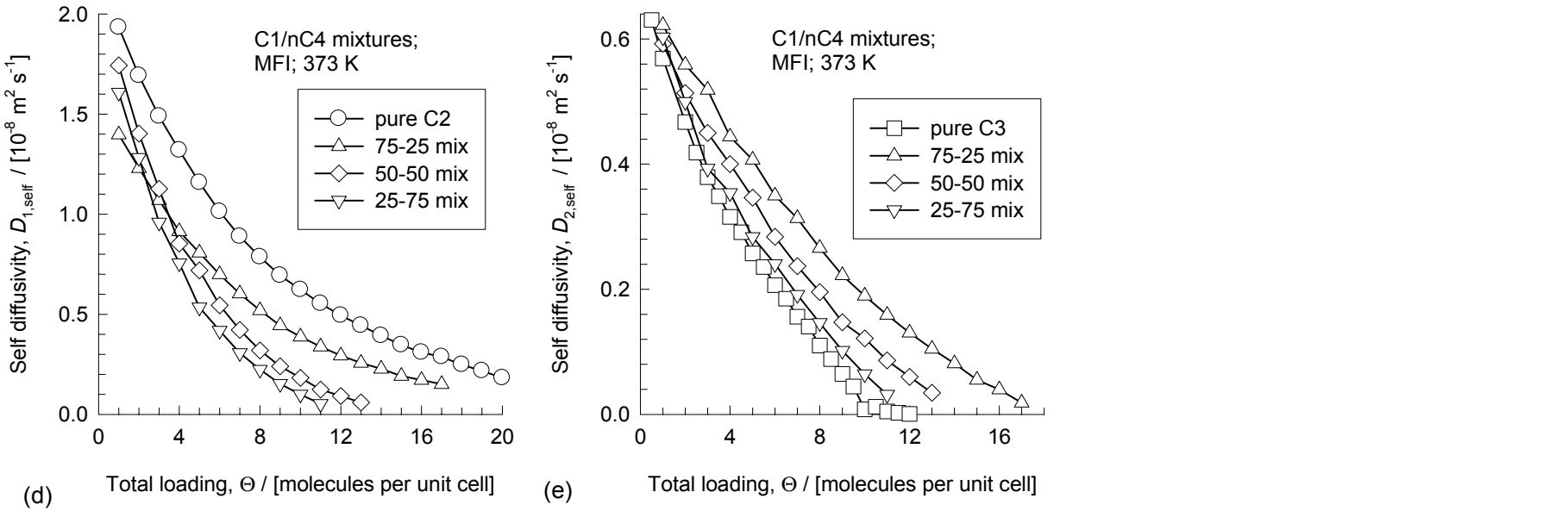

MFI; 373 K; C1/nC4 binary; Θ = 8; varying compositions

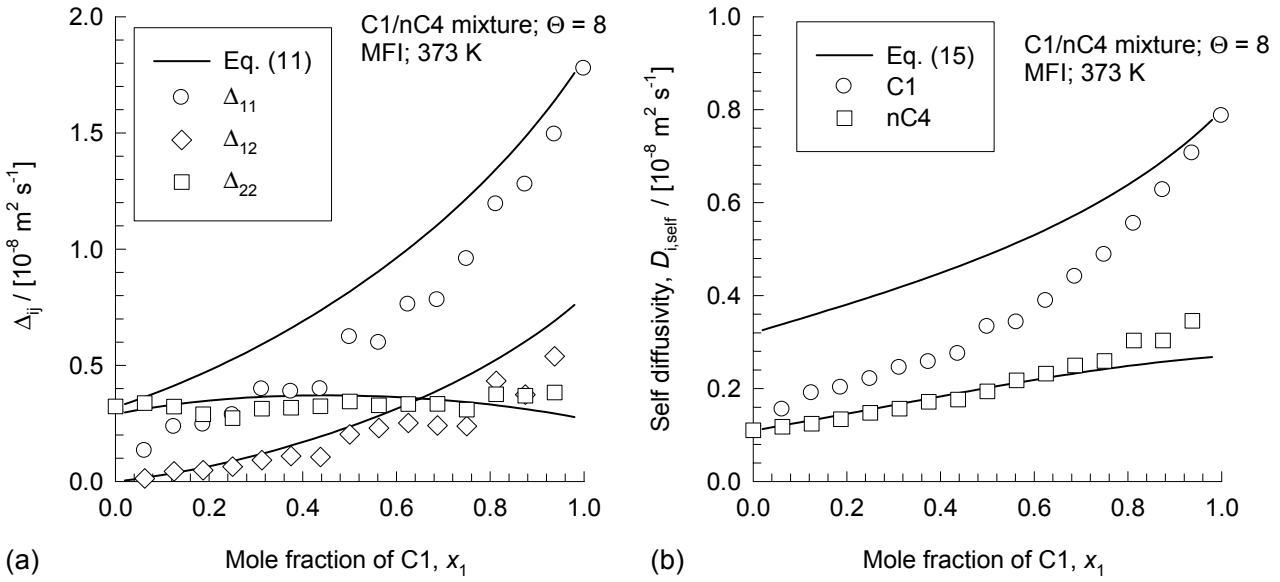

MFI; 373 K; C1/nC4 75-25, 50-50, 25-75 binary mixtures; Data on $Đ_i$ and $Đ_{ii}$ backed out from MD simulations

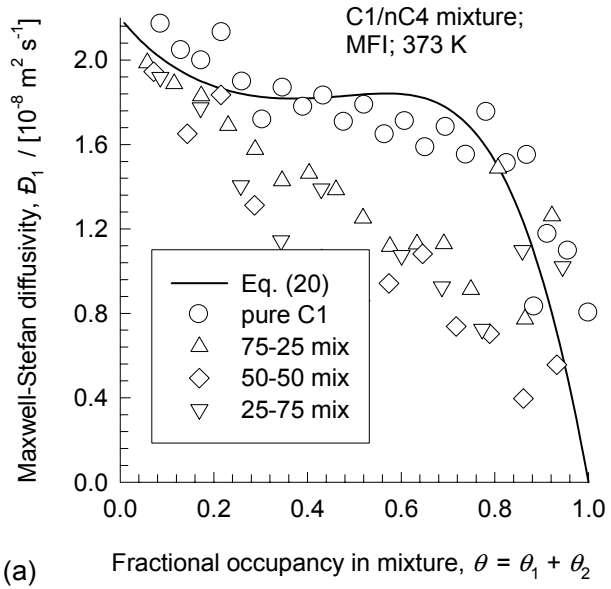

(a)

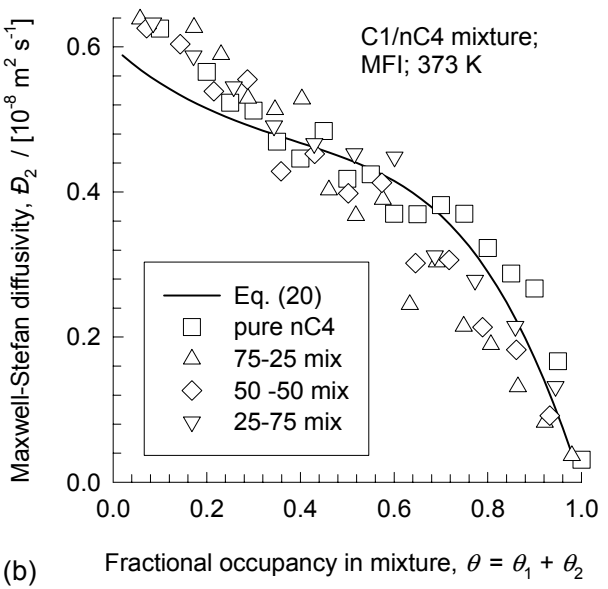

(b)

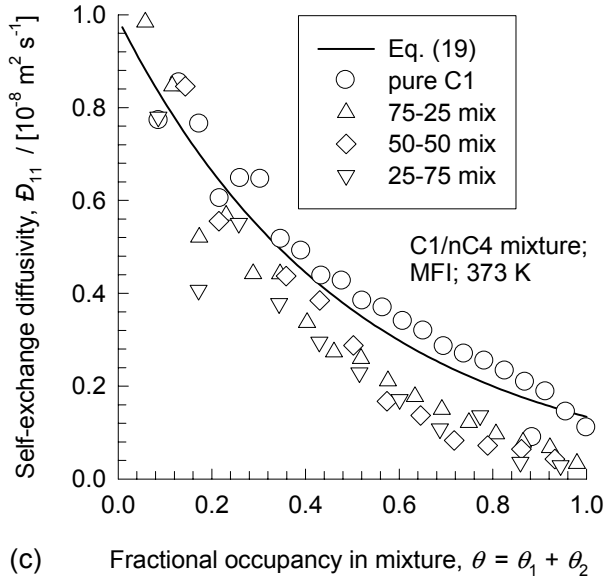

(c)

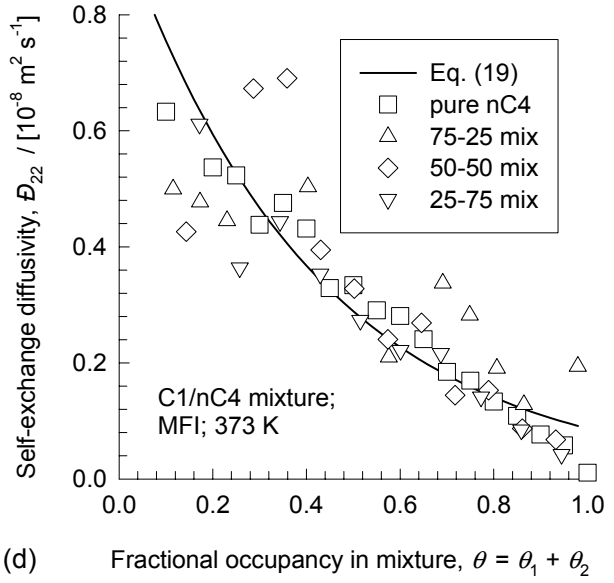

(d)

LTA; 750 K; C1/C2 75-25, 50-50, 25-75 mix; varying loadings

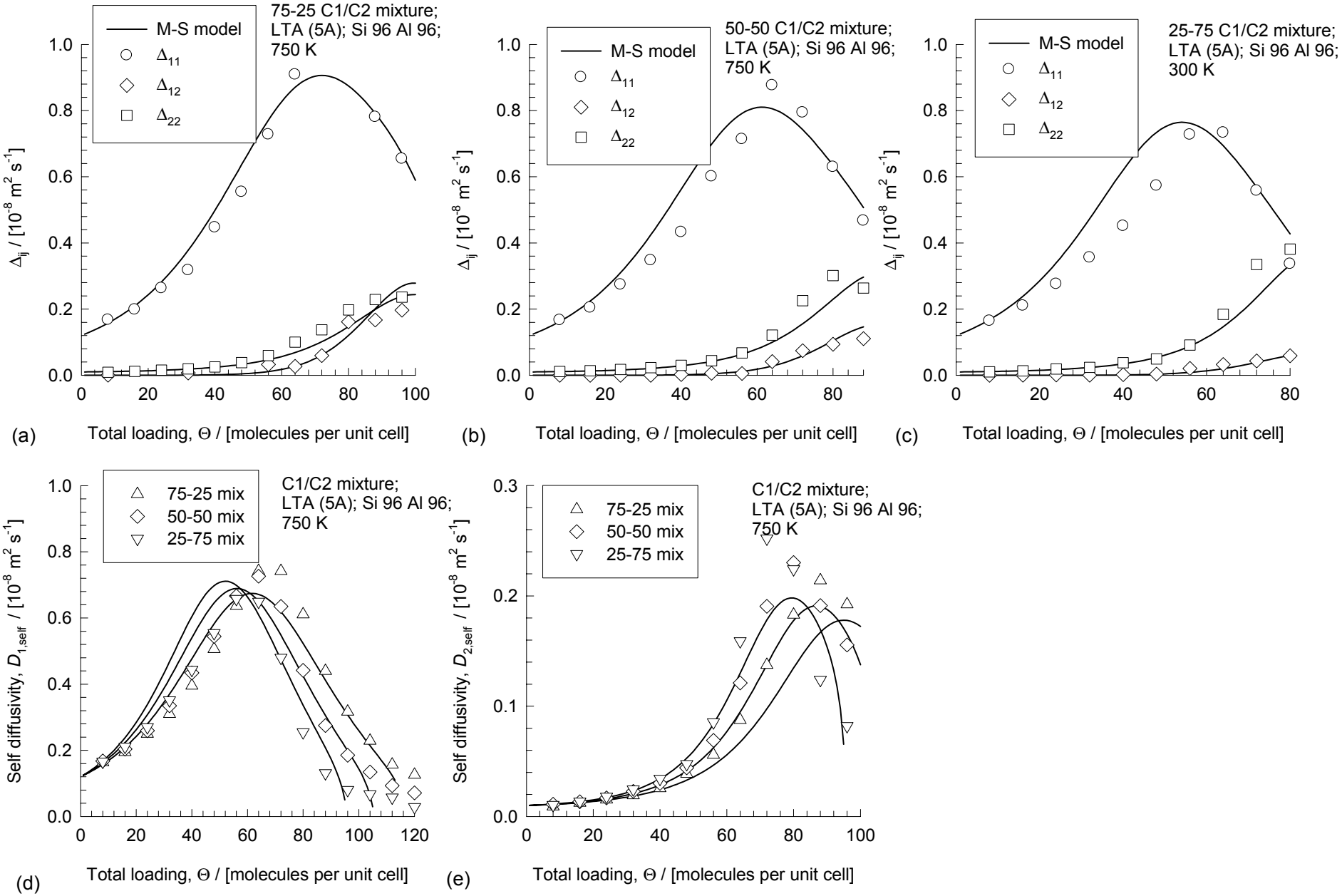

LTA; 750 K; C1/C2 binary; Θ = 72; varying compositions

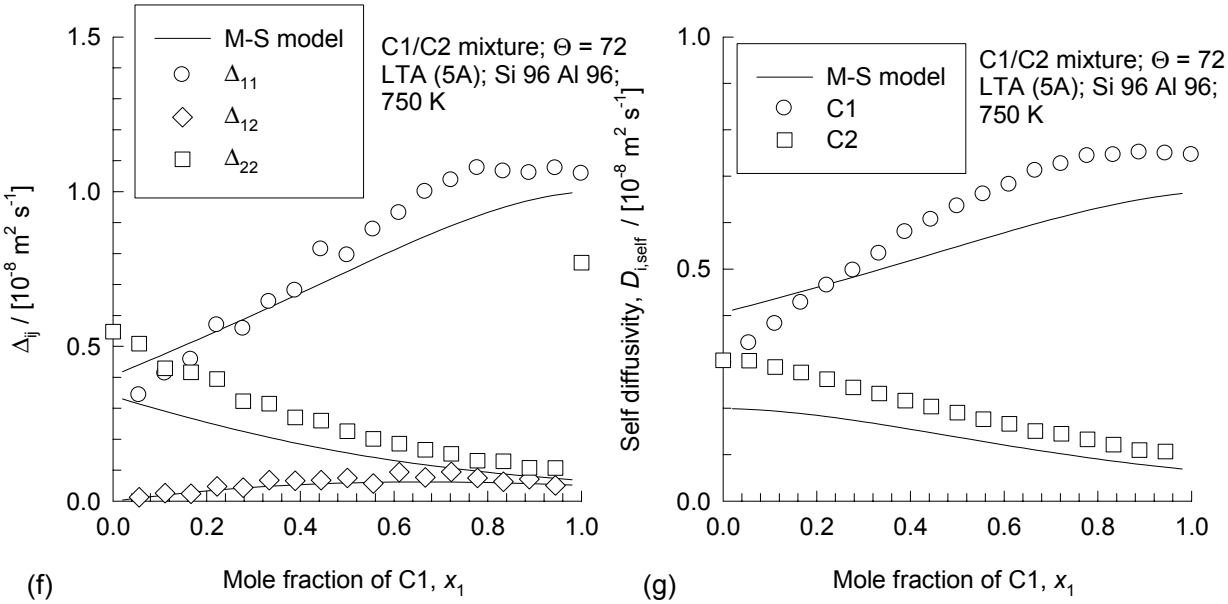

LTA; 750 K; C1/C2 75-25, 50-50, 25-75 binary mixtures; Data on $Đ_i$ backed out from MD simulations

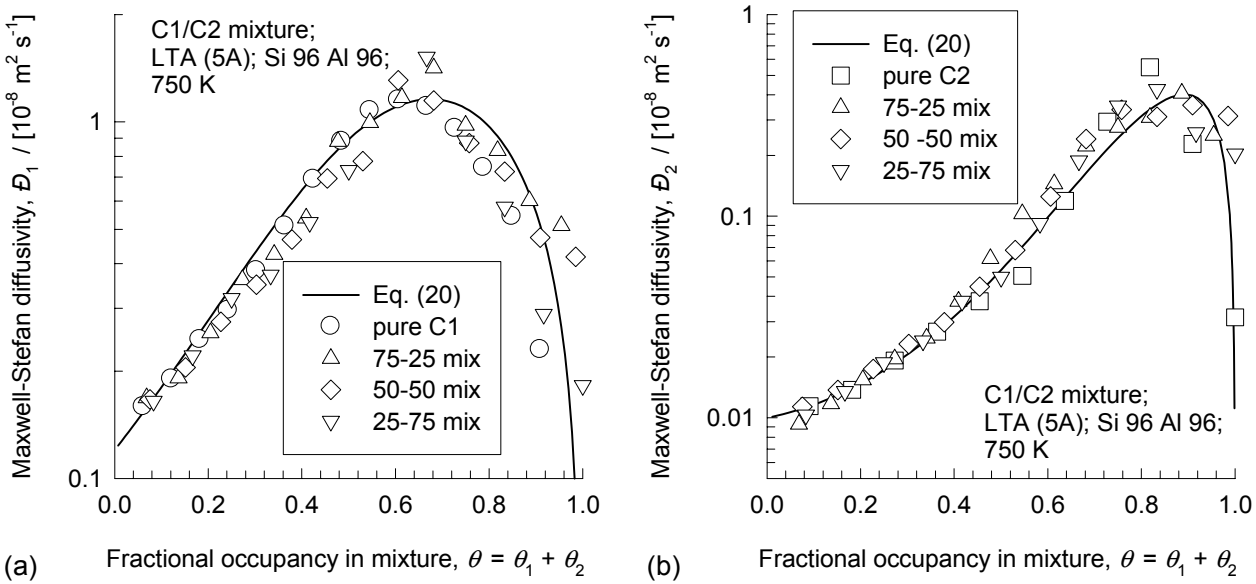

LTA; 750 K; C1/C2/C3 equimolar ternary mixtures; Data on $Đ_i$ backed out from MD simulations

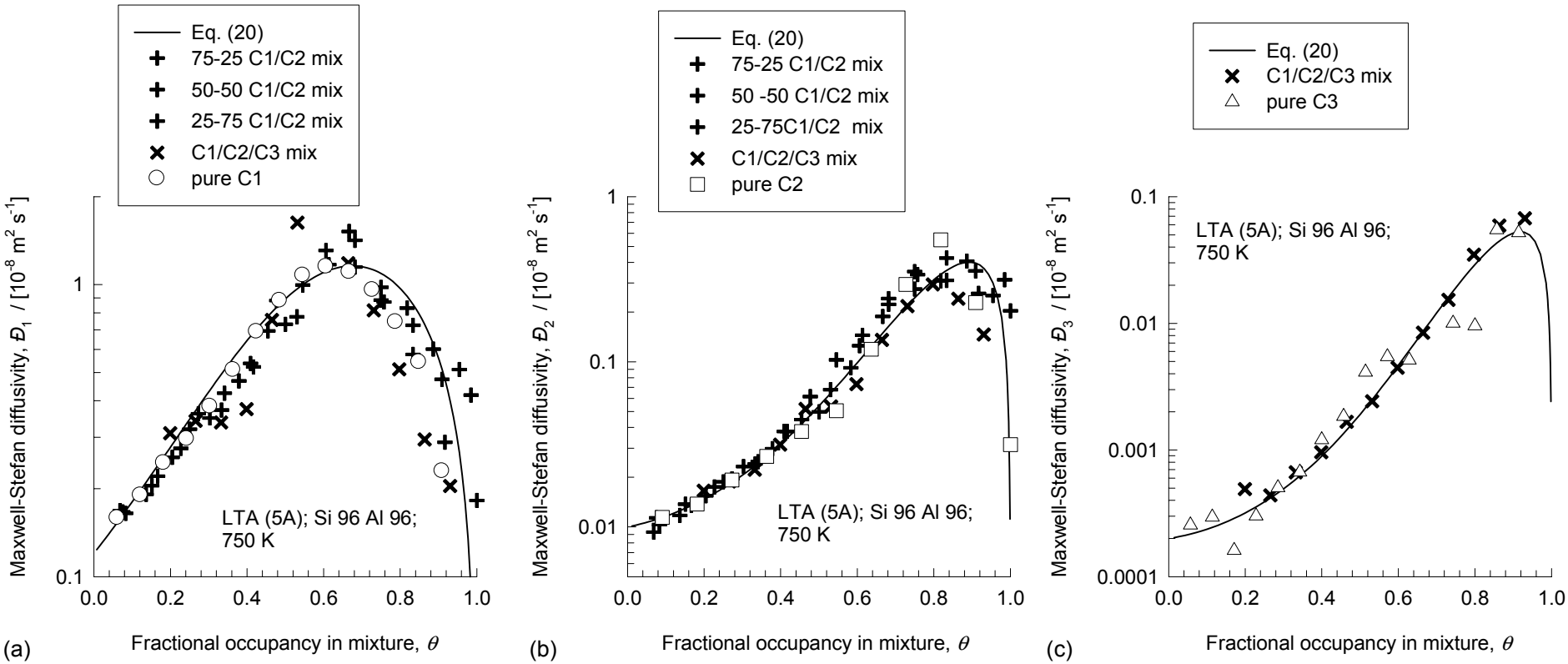

The plusses denote binary mixture data, the crosses denote equimolar ternary mixture data

Appendix B: M-S vs Onsager formulations

The Maxwell-Stefan (M-S) diffusion equations are[1-4]:

$$-\rho\frac{\theta_i}{k_BT}\nabla\mu_i=\sum_{\substack{j=1\\ j\neq i}}^{n}\frac{\Theta_j\mathbf{N}_i-\Theta_i\mathbf{N}_j}{\Theta_{i,sat}\Theta_{j,sat}Đ_{ij}}+\frac{\mathbf{N}_i}{\Theta_{i,sat}Đ_i};\quad i=1,...n \tag{1}$$

where $\mathbf{N}_i$ is the flux of species *i* expressed say in molecules per square meter per second, ρ is the zeolite density expressed as the number of unit cells per cubic meter, Θ_i is the loading in molecules per unit cell, $\Theta_{i,sat}$ represents the saturation loading of species *i*, *n* is the total number of diffusing species, μ_i is the chemical potential expressed in Joules per molecule and k_B is the Boltzmann constant. In Eq.(1) the fractional occupancies θ_i are defined by

$$\theta_i\equiv\Theta_i/\Theta_{i,sat}\quad i=1,2,...n \tag{2}$$

Equation (1) *defines* two types of M-S diffusivities: $Đ_i$ and $Đ_{ij}$. If we have only a single sorbed component, then only one $Đ_i$ is needed, and in this case $Đ_i$ is equivalent to the single component "corrected" diffusivity[5]. In the case of mixture diffusion, the $Đ_i$ depend, in general, on the loading of all sorbed species, so $Đ_i=Đ_i(\Theta_1,\Theta_2,....\Theta_n)$. The binary exchange coefficients $Đ_{ij}$ reflect *correlation* effects in mixture diffusion[6]. For mixture diffusion the $Đ_{ij}$ tends to slow down the more mobile species and speed up the relatively sluggish ones. A lower value of the exchange coefficient $Đ_{ij}$ implies a *stronger* correlation effect. When $Đ_{ij}\to\infty$, correlation effects vanish.

Equation (1) can be cast into *n*-dimensional matrix notation as

$$(\mathbf{N})=-\rho\,[B]^{-1}\,[\Gamma](\nabla\Theta) \tag{3}$$

with the following definitions of an *n*-dimensional square matrix [*B*] with elements

$$B_{ii} = \frac{1}{Đ_i} + \sum_{\substack{j=1 \\ j\neq i}}^{n} \frac{\theta_j}{Đ_{ij}}; \quad B_{ij} = -\frac{\Theta_{i,sat}}{\Theta_{j,sat}} \frac{\theta_i}{Đ_{ij}}; \quad i, j = 1,2....n \tag{4}$$

and the matrix of thermodynamic correction factors [Γ]

$$\frac{\Theta_i}{k_B T} \nabla \mu_i = \sum_{j=1}^{n} \Gamma_{ij} \nabla \Theta_j; \quad \Gamma_{ij} \equiv \frac{\Theta_i}{\Theta_j} \frac{\partial \ln f_i}{\partial \ln \Theta_j}; \quad i, j = 1,..n \tag{5}$$

where f_i represents the fugacity of component i in the bulk fluid phase. The Γ_{ij} can be calculated from knowledge of the multicomponent sorption isotherms.

It must be noted that in the paper by Kapteijn et al.[1] and Skoulidas et al.[3], an alternative, but consistent derivation is followed for the flux relation in the form

$$(\mathbf{N}) = -\rho[\Theta_{sat}][B^*]^{-1}[\Gamma^*](\nabla\theta) \tag{6}$$

with the following definitions:

$$B^*_{ii} = \frac{1}{Đ_i} + \sum_{\substack{j=1 \\ j\neq i}}^{n} \frac{\theta_j}{Đ_{ij}}; \quad B^*_{ij} = -\frac{\theta_i}{Đ_{ij}}; \quad i, j = 1,2....n \tag{7}$$

$$\frac{\theta_i}{k_B T} \nabla \mu_i = \sum_{j=1}^{n} \Gamma^*_{ij} \nabla \theta_j; \quad \Gamma^*_{ij} \equiv \left(\frac{\Theta_{j,sat}}{\Theta_{i,sat}} \right) \frac{\Theta_i}{f_i} \frac{\partial f_i}{\partial \Theta_j} \equiv \frac{\theta_i}{\theta_j} \frac{\partial \ln f_i}{\partial \ln \theta_j}; \quad i, j = 1,2 \ldots n \tag{8}$$

$$[\Theta_{sat}] \equiv \begin{bmatrix} \Theta_{1,sat} & 0 & 0 & 0 & 0 \\ 0 & \Theta_{2,sat} & 0 & 0 & 0 \\ 0 & 0 & \ddots & 0 & 0 \\ 0 & 0 & 0 & \ddots & 0 \\ 0 & 0 & 0 & 0 & \Theta_{n,sat} \end{bmatrix} \tag{9}$$

Using straightforward matrix algebra it is easy to show that Eqs (3) – (5) are entirely equivalent to Eqs (6) – (9). In the present paper it is more convenient to adopt the formulation given by Eqs (3) – (5).

More commonly in the literature MD simulations are used to determine the matrix of Onsager coefficients defined by

$$(\mathbf{N}) = -[L](\nabla\mu) \tag{10}$$

The units of L_{ij} $k_B T$ are molecules per meter per second. The elements of [L] are obtained from the MD simulations using

$$L_{ij} = \frac{1}{6Vk_BT}\lim_{\Delta t\to\infty}\frac{1}{\Delta t}\left\langle\left(\sum_{l=1}^{N_i}\left(\mathbf{r}_{l,i}(t+\Delta t)-\mathbf{r}_{l,i}(t)\right)\right)\bullet\left(\sum_{k=1}^{N_j}\left(\mathbf{r}_{k,j}(t+\Delta t)-\mathbf{r}_{k,j}(t)\right)\right)\right\rangle \tag{11}$$

In our paper we have defined the matrix [Δ]:

$$(\mathbf{N}) = -\rho\frac{[\Delta]}{k_BT}\begin{bmatrix}\Theta_1 & 0 & 0 & 0 & 0\\ 0 & \Theta_2 & 0 & 0 & 0\\ 0 & 0 & \ddots & 0 & 0\\ 0 & 0 & 0 & \ddots & 0\\ 0 & 0 & 0 & 0 & \Theta_n\end{bmatrix}(\nabla\mu) \tag{12}$$

and calculated this from MD simulations using

$$\Delta_{ij} = \frac{1}{6}\lim_{\Delta t\to\infty}\frac{1}{N_i}\frac{1}{\Delta t}\left\langle\left(\sum_{l=1}^{N_i}\left(\mathbf{r}_{l,i}(t+\Delta t)-\mathbf{r}_{l,i}(t)\right)\right)\bullet\left(\sum_{k=1}^{N_j}\left(\mathbf{r}_{k,j}(t+\Delta t)-\mathbf{r}_{k,j}(t)\right)\right)\right\rangle \tag{13}$$

where V is the volume of the simulation box.

The molecular loadings are

$$\Theta_i = \frac{N_i}{\rho V} \tag{14}$$

and so

$$\rho\Theta_i\Delta_{ij} = L_{ij}k_BT \tag{15}$$

The Onsager Reciprocal Relations $L_{ij} = L_{ji}$ imply

$$\Theta_i\Delta_{ij} = \Theta_j\Delta_{ji} \tag{16}$$

(1) Kapteijn, F.; Moulijn, J. A.; Krishna, R. *Chem. Eng. Sci.* **2000**, *55*, 2923.
(2) Krishna, R.; Baur, R. *Sep. Purif. Technol.* **2003**, *33*, 213.
(3) Skoulidas, A. I.; Sholl, D. S.; Krishna, R. *Langmuir* **2003**, *19*, 7977.

(4) Chempath, S.; Krishna, R.; Snurr, R. Q. *J. Phys. Chem. B* **2004**, *108*, 13481.
(5) Skoulidas, A. I.; Sholl, D. S. *J. Phys. Chem. B* **2001**, *105*, 3151.
(6) Kärger, J.; Vasenkov, S.; Auerbach, S. M. Diffusion in zeolites, Chapter 10. In *Handbook of Zeolite Science and Technology*; Auerbach, S. M., Carrado, K. A., Dutta, P. K., Eds.; Marcel Dekker: New York, 2003; pp 341.

Appendix C: Nomenclature

a_i	constants describing self-exchange, dimensionless
b_i	constants describing self-exchange, dimensionless
$[B]$	matrix of inverse Maxwell-Stefan coefficients, m^{-2} s
$[B^*]$	alternative definition of matrix of inverse Maxwell-Stefan coefficients, m^{-2} s
$[D]$	matrix of Fick diffusivities, m^2 s^-
$D_{i,self}$	self-diffusivity, m^2 s^{-1}
$Đ_i$	Maxwell-Stefan diffusivity of species *i* in zeolite, m^2/s
$Đ_i(0)$	zero-loading M-S diffusivity of species *i* in zeolite, m^2/s
$Đ_{ii}$	self-exchange diffusivity, m^2/s
$Đ_{ij}$	binary exchange diffusivity, m^2/s
f_i	Reed-Ehrlich parameter, dimensionless
k_B	Boltzmann constant, 1.38×10^{-23} J molecule^{-1} K^{-1}
$L_{ij}\,k_BT$	**(**modified) Onsager coefficients, molecule m^{-1} s^{-1}
$\mathbf{N}_i$	molecular flux of species *i*, molecules m^{-2} s^{-1}
N_i	number of molecules of species *i*, molecules
p_i	partial pressure of species *i*, Pa
t	time, s
T	absolute temperature, K
V	volume, m^3
x_i	mole fraction of species *i* in mixture, dimensionless
z	coordination number, dimensionless

Greek letters

β_i	Reed-Ehrlich parameter, dimensionless

$[\Delta]$	matrix of Maxwell-Stefan diffusivities, $m^2\ s^{-1}$
ε_i	Reed-Ehrlich parameter, dimensionless
$[\Gamma]$	matrix of thermodynamic factors, dimensionless
θ	total occupancy of mixture, dimensionless
θ_i	fractional occupancy of component *i*, dimensionless
Θ_i	molecular loading, molecules per unit cell
$\Theta_{i,sat}$	saturation loading, molecules per unit cell
μ_i	molar chemical potential, J $molecule^{-1}$
ρ	density, number of unit cells per m^3

Subscripts

sat	referring to saturation conditions
i,j	components in mixture

Superscripts

*	modified definitions of B_{ij} and Γ_{ij}

Vector and Matrix Notation

( )	vector
[ ]	square matrix